The short-term brain hypoxia affects long-term cardiac dysfunction in juvenile mild traumatic brain injury mouse model

Nitchawat Paiyabhroma

▶ **To cite this version:**

Nitchawat Paiyabhroma. The short-term brain hypoxia affects long-term cardiac dysfunction in juvenile mild traumatic brain injury mouse model. Human health and pathology. Université de Montpellier, 2022. English. ⟨NNT : 2022UMONT097⟩. ⟨tel-04931128⟩

HAL Id: tel-04931128

https://theses.hal.science/tel-04931128v1

Submitted on 5 Feb 2025

HAL is a multi-disciplinary open access archive for the deposit and dissemination of scientific research documents, whether they are published or not. The documents may come from teaching and research institutions in France or abroad, or from public or private research centers.

L'archive ouverte pluridisciplinaire **HAL**, est destinée au dépôt et à la diffusion de documents scientifiques de niveau recherche, publiés ou non, émanant des établissements d'enseignement et de recherche français ou étrangers, des laboratoires publics ou privés.

HAL Authorization

THÈSE POUR OBTENIR LE GRADE DE DOCTEUR DE L'UNIVERSITÉ DE MONTPELLIER

En Biologie Santé

École doctorale Sciences Chimiques et Biologiques pour la Santé (CBS2)

INSERM U1046 – CNRS UMR 9214

L'hypoxie cérébrale, suite à un choc traumatique léger du cerveau au stade juvénile, altère la fonction cardiaque au stade adulte : étude pré-clinique.

Présentée par Nitchawat PAIYABHROMA
Le 22 septembre 2022

Sous la direction de Sylvain RICHARD et Pierre SICARD

Devant le jury composé de

Jérome BADAUT, Directeur de Recherche CNRS, Bordeaux	Rapporteur
Mohamed CHAHINE, Professor, Université Laval, Canada	Rapporteur
Craig J. GOERGEN, Professor, Université Purdue, Etats-Unis	Examinateur
Sylvain RICHARD, Directeur de Recherche CNRS, Montpellier	Directeur de Thèse
Pierre SICARD, Ingénieur de Recherche, INSERM, Montpellier	Co-directeur de Thèse

UNIVERSITÉ DE MONTPELLIER

The short-term brain hypoxia affects long-term cardiac dysfunction in juvenile mild traumatic brain -injury mouse model

Acknowledgment

First and foremost, I would like to give my sincerely thankful to my thesis director Dr. Sylvain RICHARD and my co-thesis director Dr. Pierre SICARD, who have supported me throughout the length of the study with their attention, energy, patience, and kindness. Even the encountered obstacles from the COVID-19 situation since the start of my Ph.D. life. Throughout the tough times of my personal and thesis-processing period, they provided encouragement, mercy, and intense pushing forward to lead my way. I also would like to give special thanks to Dr. Nicola MARCHI and Dr. Jerome Baduat, who encouraged sound advice, and collaboration to contribute to the brain-heart study in my thesis. The powerful support of my supervisors pushes our work beyond by excellent collaboration of Dr. Craig J. Goergen's team, who play a part in the intensive data analysis. Dr. Mohamed CHAHINE, I want to thank you for your service at this trial. I appreciate your attention, your dedication, and your hard work. I also would like to give special thanks to all thesis jury members, and deeply grateful for their helpful comments.

I wish to acknowledge my colleagues and staff at the PhyMedExp and IGF for their encouragement and support. I would like to thank Emma ZUB, Anais BENOIT, and Alicia JANVIER who always help in experimental procedures. I am indebted to many of my friends, both the Thai community and PhyMedExp, for giving me many valuable suggestions and friendships.

Table of contents

List of the figures

List of the tables

Abbreviations

A'	:	Peak of late diastolic velocity
ACTH	:	Adrenocorticotropic hormone
AMPAR	:	α-amino-3-hydroxy-5-methyl-4-isoxazole propionate receptors
ANS	:	Autonomic nervous system
ATP	:	Adenosine triphosphate
BBB	:	Blood brain barrier
B-mode	:	Brightness mode
BNP	:	Brain natriuretic peptide
C5aR1	:	Component C5a Receptor1
Ca2+	:	Calcium ion
CCI	:	Controlled cortical impact model
CCL-2	:	C-C Motif chemokine ligand 2
CDC	:	Centers for disease control and prevention
CHI	:	Closed-head injury model
CHILD	:	Closed-head injury with long-term disorders
CINE		
CMR	:	Cinematographic CMR
ciné-IRM	:	Cardiaque et tagging en IRM
CK-MB	:	Creatine kinase MB
cm/s	:	Centimeter/second
CMR	:	Cardiac magnetic resonance imaging
CMRO2	:	Cerebral metabolic rate of oxygen
CO	:	Cardiac output
COX-2	:	Cyclooxygenase-2
CT	:	Computed tomography
CT-scan	:	Computed tomography scan
CXCL-1	:	C-X-C Motif chemokine ligand 1
D	:	Dimensional
DAI	:	Diffuse axonal injury
DAMPs	:	Damage-associated molecular patterns
DT	:	Deceleration time
E'	:	Peak of early diastolic velocity wave
ECG	:	Electrocardiogram
EDV	:	End-diastolic volume
EKV	:	ECG-gated kilohertz visualization
ESV	:	End-systolic volume
ET	:	Ejection time
FE	:	Fraction d'éjection
FiO2	:	Fraction of inspired oxygen
4US	:	Four-dimensional ultrasound
FPI	:	Fluid percussion injury model
fps	:	Frames per second

fUS	:	Functional ultrasound
GCS	:	Glasgow coma scale
G-CSF	:	Granulocyte colony-stimulating factor
GFAP	:	Glial fibrillary acidic protein
GLAST	:	Glutamate aspartate transporters
GLS	:	Global longitudinal strain
GLS	:	Global longitudinal strain
GLT-1	:	Glutamate transporter-1
GLUT4	:	Glucose transporter type 4
GRK2	:	G protein-coupled receptor kinase 2
h	:	Hour
HFABP	:	Heart-fatty acid binding protein
HFpEF	:	Heart failure with preserved ejection fraction
HMGB1	:	High mobility group protein B1
HR	:	Heart rate
HSP	:	Heat-shock proteins
ICP	:	Intracranial pressure
iGluR	:	Ionotropic-glutamate receptors
IL-12	:	Interleukin 12
IL-1ß	:	Interleukin 1 beta
IL-1α	:	Interleukin 1 alpha
IL-6	:	Interleukin 6
IP	:	Intraperitoneal
IRM	:	Imagerie par résonance magnétique
IVRT	:	Isovolumic relaxation time
IVRT	:	Augmentation du temps de relaxation
IVSd	:	LV interventricular septal thickness at diastole
jmTBI	:	Juvenile mild traumatic brain injury
LA	:	Left atrium
LOC	:	Loss of consciousness
LV	:	Left ventricle
LV mass	:	Left ventricular mass
LVDd	:	LV end-diastolic dimension
LVDs	:	LV end-systolic dimension
LVEF	:	Left ventricle ejection fraction
LVFS	:	Left ventricle fractional shortening
LVID	:	Left ventricular internal diameter
LVIDd	:	LV internal dimensions at diastole
LVPWd	:	LV posterior wall thickness at diastole
M	:	Month
m/s	:	Meter/second
MAPKs	:	Mitogen-activated protein kinases
MBP	:	Myelin basic protein
MCP-1	:	Monocyte chemoattractant protein 1

mGluR	:	Metabotropic-glutamate receptors
MHz	:	Megahertz
mm	:	Millimeter
mm s^{-1}	:	Milimeter/second
M-mode	:	Motion-mode
MMP9	:	Matrix metallopeptidase 9
MPI	:	Myocardial performance index
mPTP	:	Mitochondrial permeability transition pores
MRI	:	Magnetic resonance imaging
ms	:	Milisecond
mTBI	:	Mild traumatic brain injury
MV	:	Mitral valve
MVO2	:	Myocardial O2 consumption
NE	:	Norepinephrine
NIRS	:	Near-infrared spectroscopy
NLC	:	Non-linear contrast
NMDAR	:	N-methyl-d-aspartate receptors
NO	:	Nitric oxide
NOX-2	:	NADPH oxidase 2
NPs	:	Nanoparticles
NSM	:	Neurogenic stunned myocardium
P	:	Post-natal
PACT	:	Photoacoustic computed tomography
PAI	:	Photoacoustic imaging
PAI	:	Photoacoustique
PANs	:	Photoacoustic nano-transducers
PaO2	:	Arterial oxygen pressure
PCA	:	Analyse en composantes principales
PCA	:	Principal component analysis
PECARN	:	Pediatric emergency care applies research network
PET	:	Positron emission tomography
PRRs	:	Pattern recognition receptors
PSAX	:	Parasternal short axis
PSH	:	Paroxysmal sympathetic hyperactivity
PSLAX	:	Parasternal long axis
PSV	:	Peak systolic velocity
PTA	:	Post-traumatic amnesia
PW Doppler-mode	:	Pulsed-wave Doppler mode
rLSR	:	Regional longitudinal strain rate
ROS	:	Reactive oxygen species
RWMA	:	Regional wall motion abnormalities
s	:	Peak of systole

s^{-1}	**:**	Per second
SIHI	**:**	Stroke-induced heart injury
SIRS	**:**	Systemic inflammatory response syndrome
SNS	**:**	Sympathetic nervous system
sO2	**:**	Oxygen saturation
SOD	**:**	Super oxide dismutase
SRC	**:**	Sports-related concussions
ßAR	**:**	ß-adrenergic receptor
STE	**:**	Speckle-tracking echocardiography
SV	**:**	Stroke volume
TBARS	**:**	Thiobarbituric acid reactive substance
TBI	**:**	Traumatic brain injury
TC	**:**	Traumatisme crânien
TCL	**:**	TC léger
TDI	**:**	Tissue Doppler Imaging
TLR	**:**	toll-like receptors
TNF-α	**:**	Tumor necrosis factor alpha
TNT	**:**	Trinitrotoluene
TSPO	**:**	18 -kDa translocator protein
TTC	**:**	Takotsubo cardiomyopathy
US	**:**	Ultrasound
US	**:**	Ultrasons haute résolution
WDI	**:**	Weight-drop injury model

Résumé exhaustif en Français

Le traumatisme crânien (TC) représente un enjeu clinique important (Ouellet M-C, 2015; Dewan MC, 2018). Au-delà des lésions cérébrales locales et des activations neuro-inflammatoires (van Vliet EA, 2022), le TC pourrait être associé à des adaptations physiopathologiques d'organes périphériques, avec des implications d'inflammation systémique et de dérégulation du système nerveux autonome (McDonald SJ, 2020). Les effets du TC sur le système cardiovasculaire font leur apparition dans des études cliniques utilisant l'examen échocardiographique (Hasanin A, 2016). Le TC s'est avéré associé à un risque plus élevé de comorbidités cardiovasculaires chroniques chez les patients adultes (Izzy S, 2022). Ces études cliniques se sont concentrées sur les traumatismes crâniens, modérés à sévères, dans la population adulte âgée ; cependant, environ 80 % de toutes les visites aux urgences liées à un TC sont dues à des cas bénins, avec des données non structurées avec des évolutions pathologiques potentielles pour les enfants de moins de 18 ans (Delage C, 2021). Le TC léger (TCL), ou la commotion cérébrale telle qu'elle se produit dans les sports de contact (Owens TS, 2021), est généralement défini comme la conséquence de l'impact de forces biomécaniques traumatiques au niveau du cerveau. Celles-ci n'entraînent pas nécessairement une perte de conscience et ne montrent que peu ou pas de signes de dommages structurels par imagerie CT-scan (Lumba-Brown A, 2018). Le manque de connaissances actuelles appelle des études précliniques pour étudier systématiquement les évolutions physiopathologiques fonctionnelles des TC juvéniles aux niveaux cérébral et cardiaque, et identifier les associations temporelles à l'âge adulte (Krishnamoorthy V, 2015).

Pour résoudre ce problème, nous avons étudié expérimentalement les adaptations cardiaques à long terme survenant après un TCL juvénile. Nous avons corrélé rétrospectivement une mal-adaptation cardiaque avec une hypo-oxygénation cérébrovasculaire, survenant immédiatement après le TCL (Ichkova A, 2020). Nous avons utilisé l'imagerie

photoacoustique (PAI), qui combine des impulsions laser et des ultrasons haute résolution (US), pour créer des images à contrastes multiples des structures cardiaques et cérébrales (Wang LV, 2012). Cette approche non invasive permet une surveillance sans précédent des fonctions cardiaque et cérébrale chez les mêmes animaux et ceci de manière répétée sur de longues périodes. Bien que les modalités d'imagerie telles que l'IRM permettent d'évaluer la fonction ventriculaire gauche, l'acquisition est souvent longue et coûteuse (Saeed M, 2015). L'émergence de nouvelles technologies basées sur l'échographie permet une évaluation *in vivo* des modifications cérébrovasculaires et cardiaques avec une grande spécificité (Ichkova A, 2020). De plus, nous avons utilisé l'échographie quadridimensionnelle à haute fréquence (4DUS), une technique comparable à ciné-IRM, pour évaluer la progression de la maladie cardiaque dans le temps avec une résolution spatio-temporelle élevée (Damen FW, 2017). Nous montrons des corrélations quantitatives entre la baisse initiale de l'oxygénation cérébrovasculaire et la dysfonction diastolique cardiaque observée à long terme chez le même animal et au fil du temps, et s'étendant aux adaptations négatives lors d'un sollicitation cardiaque extra-physiologique. Nous rapportons des changements comportementaux à long terme, spécifiques à la souris, et en corrélation croisée avec les données de PAI. Collectivement, ces données établissent un lien direct entre l'hypoxie cérébrovasculaire précoce après un TCL chez les souris juvéniles et les maladaptations cardiaques qui persistent à l'âge adulte.

Nos données font écho à des études cliniques suggérant une interrelation cerveau-cœur chez les sujets TC. Des effets cardiovasculaires, endocriniens et neurologiques chroniques ont été rapportés à la suite de lésions cérébrales tant chez des patients et que dans des modèles de rongeurs (Bailes JE, 2014). Nos résultats démontrent l'implication de l'axe cœur-cerveau dans le TCL et introduisent la surveillance cardiaque comme modalité possible de marqueur non invasif dans ce contexte pathologique.

Association du TCL à la dysfonction cardiaque à l'âge adulte

Des symptômes de dysfonctionnement cardiovasculaire ont été rapportés à court terme chez des patients adultes présentant un TC léger à sévère, en évaluant les caractéristiques cliniques telles que la pression artérielle, la fraction d'éjection et les modifications morphologiques sur les électrocardiogrammes (Gregory T, 2012; Izzy S, 2022). En combinant expérimentalement le 2DUS et le 4DUS, nous révélons un dysfonctionnement cardiaque subclinique persistant à l'âge adulte après un TL juvénile. Aucun changement dans la morphométrie cardiaque du ventricule gauche ou de la fonction systolique globale (fraction d'éjection) n'a été identifié dans le groupe TCL. Cependant, la fonction systolique diminue dans les TC modérés à sévères dans les études cliniques (Krishnamoorthy V, 2015). Fait intéressant, nous avons constaté que le groupe TCL présentait des changements du volume de l'oreillette gauche, une augmentation du temps de relaxation (IVRT) et une vitesse de déformation diastolique diminuée jusqu'à 190 jours après le TCL. Ces résultats indiquent un dysfonctionnement diastolique cardiaque (Schnelle M, 2018). Ces résultats sont en accord avec ceux de Cuisinier et al., ne montrant pas de modification de la fonction systolique, mais mettant en évidence une dysfonction diastolique subclinique avec un allongement significatif de l'IVRT chez les patients TC (Cuisinier A, 2016). De plus, les études de cohorte prospectives de Krishnamoorthy et al. ont montré une dysfonction cardiaque à court terme après un TBI avec un retour à la valeur initiale en une semaine (Krishnamoorthy V, 2020); cependant, notre étude indique plutôt que ces effets persistent à long terme. Les tests d'effort à la dobutamine, qui augmentent la demande et la consommation d'O2 (Sturgill MG, 2011), ont mis en évidence une dysfonction cardiaque sous-jacente en cas d'insuffisance cardiaque à fraction d'éjection (FE) préservée (AbouEzzeddine OF, 2019). De même, notre modèle de dysfonctionnement diastolique induit par mTBI avec FE préservée a montré qu'une réponse au stress est corrélée avec la désaturation initiale en oxygène après le TCL. De plus, l'absence d'une diminution

significative de la sO2 cardiaque dans le groupe mTBI suggère une réduction de l'apport d'oxygène myocardique qui a été associée à des réponses de stress anormales (van Empel VPM, 2014). Ainsi, il existe une interrelation potentielle entre le TCL, les réponses au stress cardiaque et l'apport d'oxygène au myocarde. En résumé, notre étude élargit la compréhension des effets cardiaques du TC où la dysfonction diastolique subclinique et la dysfonction induite par le stress sont observées des mois après une blessure légère en utilisant des techniques non invasives de pointe, la PAI et 4DUS. La manière dont la dysfonction diastolique avec fraction d'éjection préservée peut être liée à la prise en charge clinique à long terme des jeunes patients TCL mérite une enquête plus approfondie.

Imagerie moléculaire et biomarqueurs fonctionnels myocardiques après mTBI

Les outils de diagnostic utilisés après le TC comprennent la tomodensitométrie et l'imagerie par résonance magnétique. Cependant, la plupart des TCL ne montrent aucun marqueur d'imagerie (Bigler ED, Abildskov TJ, 2016). Pour cette raison, les patients reçoivent fréquemment un traitement inadéquat, en particulier les enfants (Amyot F, 2015; Bigler ED, 2016). Nos résultats indiquent que l'imagerie PAI et US peut être utilisée pour évaluer les effets cérébrovasculaires et cardiovasculaires du TCL, générant des biomarqueurs utilisables sur le long terme. La PAI cérébrale montre que l'oxygénation du sang de l'hémisphère gauche dans le groupe TCL a été significativement diminuée. Ces résultats concordent avec les travaux d'Ichkova et al., dans lesquels une hypoxie cérébrovasculaire immédiate post-TCL a été observée (Ichkova A, 2020). De plus, l'hémoglobine totale dans le groupe TCL était plus élevée que dans le groupe sham après 4 heures, avec une influence possible du saignement pétéchial au site de la lésion (Kurland D, 2012; Jolliffe IT, 2016; Barud M, 2021).

Ici, une analyse en composantes principales (PCA) a été utilisée comme un outil pour réduire la dimensionnalité des ensembles de données multivariées et identifier les modèles sous-jacents

(Ljubicic ML, 2021). Nos résultats montrent que la combinaison de treize mesures physiologiques de la lésion cérébrale initiale et du test de stress à la dobutamine permet de différencier avec succès les animaux sham des animaux TCL. Le taux d'hémoglobine au niveau de la lésion était un contributeur important à la différenciation entre les groupes ; cependant, les mesures de dysfonctionnement cardiaque ont eu une plus grande influence sur l'analyse que la saturation en oxygène. Ces résultats s'alignent sur des travaux antérieurs où le PCA a été utilisée pour discriminer entre des groupes cliniquement stratifiés (Andkhoie M, 2018) et ainsi identifier les facteurs dpris en compte pour le traitement (Danna-Dos-Santos A, 2018). Ainsi, le PCA peut faire la distinction entre les groupes et identifier les variables sous-jacentes qui peuvent être importantes dans la prise en charge clinique des patients atteints de TC.

Les résultats neurologiques sont corrélés à la lésion cérébrale initiale et au dysfonctionnement cardiaque à long terme

Les effets à long terme du TCL sur le cerveau et la fonction cognitive ont été largement étudiés dans des études précliniques et cliniques (Dean PJA, 2013). Les déficits cognitifs peuvent apparaître des mois ou des années après la lésion initiale (El-Menyar A, 2019). Nos résultats montrent que la distance parcourue par les souris et l'indice de discrimination des nouveaux objets, qui mesurent respectivement l'activité locomotrice et la mémoire, ont diminué dans le groupe TCL. Nous montrons que les mesures neurologiques à long terme sont en corrélation avec l'hypoxie et l'hémorragie cérébrovasculaire évaluées quatre heures après le TCL. Ainsi, les mesures physiopathologiques de la phase aiguë peuvent offrir des informations prédictives sur le comportement à long terme de l'adulte. Ces biomarqueurs d'imagerie (So2 ; hemoglobine…) peuvent alors être utilisés pour adapter à la fois le traitement initial et à long terme. Une corrélation entre la mauvaise adaptation de la mémoire à long terme et le dysfonctionnement cardiaque ($r = -0,547$, $p = 0,043$) montre de nouvelles interactions

bidirectionnelles potentielles au sein de l'axe cœur-cerveau. Les résultats de cette étude offrent un aperçu des interventions cliniques et thérapeutiques potentielles. Par exemple, l'utilisation de la PAI chez les patients pédiatriques TC pourrait permettre aux médecins d'évaluer la saturation en oxygène cérébral, de manière non invasive, immédiatement après le traumatisme et de déterminer des mesures préventives pour éviter les complications. En phase aiguë, l'évaluation des taux de troponine I cardiaque (cTnI) pourrait représenter une stratégie complémentaire, car l'augmentation de la cTnI est associée à une altération légère et transitoire de la fonction ventriculaire gauche (Nguembu S, 2021). Les agents pharmacologiques tels que les bêta-bloquants ont montré des effets cardioprotecteurs et sont utilisés chez les patients souffrant de TC modéré à sévère (Bretzin AC, 2018). L'échocardiographie, pourrait alors être utilisée comme un outil non invasif post-TC pour évaluer les effets à long terme tels que la fonction ventriculaire gauche et la réponse cardiaque à un stress.

Limites

La biomécanique sous-jacente au TC humain (civils, sport ou guerre) est hétérogène par rapport aux modèles précliniques. Cependant, l'utilisation d'un modèle de TC sans contrainte où la tête est libre de ses mouvements lors du choc, peut reproduire certains aspects de l'imprévisibilité du TBI chez l'homme. Nous avons signalé une variabilité des niveaux de sO2 immédiatement après le TCL, ce qui suggère que tous les animaux n'ont pas subi la même lésion mécanique. Dans notre étude, cela représente un avantage et une variable que nous avons entièrement contrôlée et stratifiée à l'aide de la PAI. Nous avons également inclus une population représentative de souris mâles et femelles, car des études cliniques suggèrent que les jeunes athlètes féminines subissent un TCL avec une incidence plus élevée que pour les hommes (Zhang YP, 2014). Nous notons également que bien que la batterie de tests comportementaux ait été assez limitée, les tests inclus sont classiques chez les rongeurs et

informatifs (Rodriguez-Grande B, 2018). Enfin, notre étude ne fournit pas d'indices mécanistiques ou de voies de signalisation candidates pour déchiffrer les modifications cœur-cerveau survenant après le TC. Cette question sera étudiée dans le cadre de la progression de notre programme de recherche.

CONCLUSION

En résumé, nous montrons que les empreintes pathologiques du TCL s'étendent au-delà du cerveau pour englober les fonctions cardiaques, avec des corrélations directes se déroulant dans le temps et de manière spécifique à l'animal, de l'adolescence à l'âge adulte. L'hypoxie cérébrovasculaire post-TBI précoce pourrait représenter un marqueur prédictif pour évaluer le risque de maladaptation cœur-cerveau. Nos résultats encouragent l'utilisation de modalités non invasives pour identifier et suivre les impacts systémiques du TCL et des interactions cœur-cerveau, conduisant éventuellement à des améliorations des résultats pour les patients.

Introduction

1. Definition, Prevalence, Incidence and of Traumatic Brain injury

Traumatic brain injury (TBI) is defined as damage or disruption of brain functions by the application of direct or indirect external brutal contacts, such as a fall, sports injury, motor vehicle collisions, abuse, acceleration-deceleration, or blast impact (Menon DK, 2010). TBI can impair physical and cognitive faculties, and behavior changes, resulting globally in temporary or permanent brain dysfunction (Reis C, 2015). Otherwise, the non-TBI can also damage the brain, such as tumors, infection, and ischemic conditions (stroke) (**Table 1**).

TBI contributes significantly to death or disability. It generates visits of about 70 million people worldwide to the emergency department each year, with an incidence rate of 939 per 100,000 people (Dewan MC, 2018). TBI is a frequent cause of morbidity and mortality in people under 45 years old (Taylor CA, 2017; Langlois JA, 2006). TBI is called "silent-epidemic" due to the high impact on being-life, and the progression of the symptoms is difficult to define by appearance (Rusnak M, 2013). To make matters worse, TBI is also affecting more than 3 million children worldwide every year (Dewan MC, 2018). Indeed, children have a higher risk of TBI than adults for physiological reasons during growth development. These reasons include a larger head, flexible skull, weaker supporting neck muscles, brain water content, and higher brain activity (Morrison G, 2013). Thus, the previous study reported that the adolescents and young adults reflect a high incidence rate of TBI, followed by long-term effects such as post-concussion syndrome and even not severe injury (McKinlay A, 2008; Barlow KM, 2015). Additionally, these population are at higher risk of TBI than children due to their activity and behaviors (Lowry R, 2021). Many cases could not be taken care of and were unclear diagnosed (Emery CA, 2016). These problems could have intensive effects when remaining long-term and show up with physiological, psychological, and socioeconomic burdens.

Table 1. The difference between traumatic brain injury and non-traumatic brain injury (Modified from Najem D, 2018)

Brain injury	**Traumatic brain injury**		**Non-traumatic brain injury**				
Definition	**Damage to the brain caused by external force**		**Damage to the brain caused by infection, brain tumors, ischemia or stroke**				
Type	Penetrating head injury	Closed-head injury	Ischemia	Stroke	Toxicity	Infection	Tumors
Description	Open head injury that the object penetrates into skull	Closed-head injury that the skull no significantly damaged, but the brain is injury	Anoxic injury, which the brain could not receive adequate oxygen supply	Hypoxic injury, which the blood supply is blockaded	Expose with toxic substance that affect to brain	microbes harm to the brain (virus, bacteria)	Malignant tumor by spreading, or benign tumor, which could induce brain injury
Examples	Gunshot, Abuse by sharp object	Accelerating force (vehicle crashes), Fall, Blast force, Abuse by blunt force	Post-cardiac arrest	Ischemic stroke, Hemorrhage stroke, Emboli	Leads, Arsenic, Pesticide	Meningitis, Encephalitis	Brain cysts, Glioma

2. Classification of TBI

2.1 Classifying of TBI by severity/symptoms

It is possible to classify traumatic brain injury from consciousness, and eye, verbal, and motor responses using the Glasgow Coma Scale (GCS). The GCS discriminates the severity into three categories, following 13-15 scores from the total score. Which represents the following mild TBI (mTBI: comprising about 80% of total TBIs), 9-12 scores represent moderate TBI (approximately 10% of total TBIs), and ≥8 scores represent severe TBI (accounting for about 10% of total TBIs) (Kraus JF, 1988; Gardner AJ, 2016). The Centers for Disease Control and Prevention (CDC) proposed a guideline for discriminating the severity of traumatic brain injury by using the GCS, the duration of loss of consciousness (LOC), and the duration of post-traumatic amnesia (PTA) (CDC, 2003). The Mayo Clinic added the clinical symptoms and adapted with CDC criteria to classify the severity of TBI (**Table 2**) (Fraunberger

E, 2019). The mild traumatic injury is accounted chiefly for severity (~80%), the one subset called "concussion," which came from the Latin verb '*concutere* — shake violently' (Gardner AJ, 2016; Kazl C, 2019). However, the term concussion is confused with definition and symptoms, suggesting replacement by mild traumatic brain injury (Sharp DJ, 2015).

Table 2. Classification severity of TBI following Mayo Clinic adapted with CDC guideline (Fraunberger E, 2019)

Severity	Clinical Criteria	GCS
Symptomatic (Possible)	- Blurred vision - Confusion - Dazed - Dizziness - Focal neurological symptoms - Headache - Nausea	**Mild: 13-15**
Mild (Probable)	- LOC < 30 min - Post-traumatic anterograde amnesia < 24h - Depressed, Basilar, or Linear skull fracture (dura intact)	
Moderate-Severe (Definite)	- LOC > 30 min - PTA ≥ 24h - GCS < 13 - One or more of intracranial hemorrhage, subdural/epidural hematoma, cerebral contusion, hemorrhagic contusion, penetrating TBI, subarachnoid hemorrhage, brain stem injury	**Moderate: 9-12** **Severe: 3-8**

2.2 Classify TBI by pathoanatomic changes

TBI can be classified by the location of the injury, which divides focal and diffuse injuries depending on focal lesion evidence. Focal and diffuse injuries contribute to characteristic appearance (Mckee AC, 2015). The focal injury is usually caused by impact, and diffuse injuries are found in acceleration-deceleration (Mckee AC, 2015). This pathoanatomic classification could be summarized in **Table 3**.

Focal injury	Diffuse injury
Skull fracture	Axonal injury
Contusion	Hypoxic-ischemic injury
Epidural hemorrhage	Microvascular injury
Subdural hemorrhage	
Subarachnoid hemorrhage (SAH)	
Intraparenchymal hemorrhage	

Table 3. Pathoanatomic classification of TBI (Modified from Hawryluk GWJ, 2015)

3. The differences between adult TBI vs pediatric TBI

The effects of pediatric TBI are different from adult TBI because of the processes involved in brain development. The main factors are the brain physiological differences in children consisting of greater brain water content, lower elastic brain parenchyma, higher demand for oxygen consumption, and cerebral blood flow. Furthermore, the anatomical body differences such as a larger head compared to body size and lower stability in the center of gravity increase vulnerability and severity after TBI (Fraunberger E, 2019) (**Figure 1**). Pediatric TBI has a worse outcome when compared to motor and cognitive function in adults (Brickler T, 2017). Moreover, pediatric TBI affects long-term behavioral outcomes and interrupts the white matter maturation and development in adolescents (Brickler T, 2017). Pediatrics can also affect childhood in the short-term while growth development is processed simultaneously, which also impacts persistent injury in the long term of TBI.

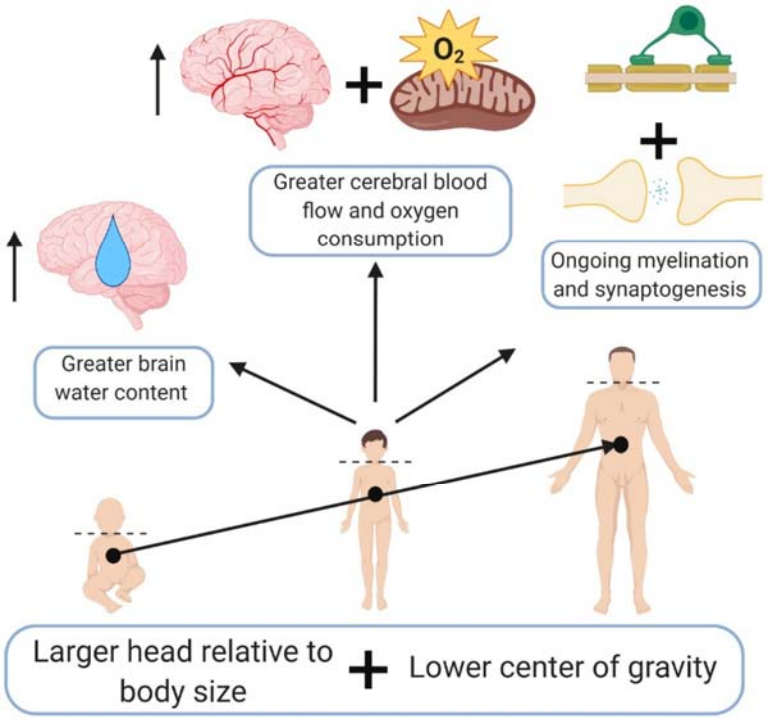

Figure 1. The graphic demonstrates anatomical and physiological differences between children and adults, which could affect outcomes of TBI (Fraunberger E, 2019)

Neuroimaging is an important step in the management of a patient with predominantly severe or moderate TBI. However, different studies have questioned the relevance of performing a brain scan for minor head trauma.

Generally, computed tomography (CT) is performed for scanning on the first day of head injury to ensure rapid broad-spectrum detection (Bigler ED, Abildskov TJ, 2016). However, the limitation of ionizing radiation needs to be cautious in the pediatric population. Magnetic resonance imaging (MRI) has been used to follow up on the chronic phase of TBI. CT scanning usually relates to TBI severity, while almost mTBI was found with minor abnormalities. The positive-CT images in mTBI typically demonstrated skull fracture, small hemorrhages, and contusion (Bigler ED, Abildskov TJ, 2016). Two main factors have been considered in CT scanning on the day of head injury in mTBI. Firstly, the abnormalities found in mTBI were considered complicated mTBI. Secondary, positive CT images on the day of head injury were used as a baseline, which might be transient abnormalities and not detected in

MRI follow-up. The frequency of positive-neuroimaging detection in mTBI is low in cohort studies of mTBI in sports-related concussions (SRC). The pediatric emergency care applies research network (PECARN) study showed that only 130(4%) of 3,289 patients who visited the emergency department exhibited positive CT scanning evaluation. The 151 SRC patients aged 19 or below were more investigated. Only 36 met the criteria for neuroimaging follow-up, and only 2 of 36 showed positive results with CT and MRI (Ellis MJ, 2015). Similarly, in the study, 23 of 52 pediatric mTBI patients met the criteria, and only one showed abnormality with CT and MRI (Morgan CD, 2015). The pediatric mTBI is a prospective study assessed in children 8 to 15 years old with criteria GCS ≥ 13 (Lee LK, 2014). The 251 pediatric mTBI patients were included by CT imaging and compared with the children who visited ED with orthopedic injury as control images (Lee LK, 2014). Then, after six months, this study was a follow-up by MRI imaging: only 25 (9.9%) of 251 pediatric mTBI had abnormalities identified using neuroimaging (Stanley RM, 2014).

The mTBI in the pediatric population confronts the difficulty determined with the neuroimaging because more than 90% of them could not find significant pathology. Moreover, the growth process in pediatrics could affect mTBI, thus resulting in poor outcomes in the future.

4. Pre-clinical TBI model

To better understand the molecular physiopathology process involved during and after TBI, pre-clinical studies are mandatory. In this way, rodents are the most useful model. (DeWitt DS, 2018; Smith DH, 2021) The four methods usually performed in TBI rodent models consist of weight drop, fluid percussion injury, controlled cortical impact, and closed head injury models (Wiegand TLT, 2021).

4.1 Weight-drop injury model (WDI)

The weight-drop models could create brain injury by using free falling objects onto the head of the animal with or without the craniotomy (Morales DM, 2005). The severity could be optimized by adjusting the height and mass of the weight; the metal disk was used to prevent skull fracture when the weight dropped (Marmarou A, 1994). The unstrained head procedure was used to represent the TBI in the human, which affected diffuse axonal injury, skull fracture, edema, or hemorrhage (Kane MJ, 2012; Xiong Y, 2013).

4.2 Fluid percussion injury model (FPI)

The percussion injury is achieved by the use of a pendulum force to press the fluid pressure pulse into the brain with craniotomy (McIntosh TK, 1989). The strength of the pressure pulse is the factor that indicates the severity of TBI (McIntosh TK, 1989; Xiong Y, 2013). However, the inconsistency of the force to create reproducible brain damage remains a problem (Xiong Y, 2013; Bruce ED, 2015). The fluid percussion is closer to the realistic brain injury in the human without skull fracture, which demonstrated brain swelling, intracranial hemorrhage, and loss of gray matter (Borg J, 2004; Koerte IK, 2016).

4.3 Controlled cortical impact model (CCI)

The CCI is widely used to generate TBI. The pneumatic or electromatic impactor is used directly into cortical tissue with the piston after craniectomy. The CCI model could define and control the depth, velocity, dwell time, and specific location of impact (Dixon CE, 1991; Romine J, 2014) The location of the injury is about 2-2.5 mm anterior or posterior to the bregma, which is the area where the impact could damage the primary motor cortex above the hippocampus (Paxinos G, 2019; Chou A, 2016). The repetitive CCI models could be performed for mimicking experiences in humans such as military personnel, and athletes (Huang L, 2016; Thomsen GM, 2017). However, the damage from CCI models is focal in nature and induces almost contusions (non-mild TBI) because of craniectomy (Bruce ED, 2015; Osier ND, 2016).

4.4 Closed head injury model (CHI)

The CHI model is also performed by using pneumatic or electromatic impactors like the CCI but without the craniectomy (Yang Z, 2016). This non-invasive model allows free head movement and the use of blunt silicon cap-piston gives the possibility to generate the TBI in all ranges of severity (mild, moderate, severe), which is similar to humans in case of no skull fracture (Namjoshi DR, 2014; Rodriguez-Grande B, 2018).

The TBI models could brief summarize in the table that described below:

Table 4. The models of TBI (Modified from Siebold L, 2018)

Model	Injury type	Strengths	Weaknesses	Major pathological features
weight drop injury (WDI)	diffuse and focal subtypes	1) injury mechanism closely resembles human TBI injury biomechanics 2) low technical skill needed for implementation	1) low reproducibility 2) high mortality rate	concussion, traumatic axonal injury (moderate-severe)
fluid percussion injury (FPI)	mixed	1) highly reproducible	1) requires craniotomy which may reduce ICP pathology 2) high mortality rate 3) requires surgical skilled technician 4) no immediate post-injury neuro scoring	contusion (moderate-severe) *less in mild
controlled cortical impact (CCI)	mainly focal	1) highly reproducible 2) low mortality rate	1) requires craniotomy which may reduce ICP 2) requires surgical skilled technician 3) no immediate post-injury neuro scoring	contusion, hemorrhage (mild-severe)
closed head injury (CHI) *subtype of CCI	mainly focal	1) high reproducible 2) low mortality rate 3) freely head (no stereotaxis frame) 4) mimic human injury with no-penetration 5) immediately brain assessment after procedure	1) might not precise in case focus specific part of the brain	contusion, hemorrhage (mild-severe)
Blast Injury Models	diffused	1) average reproducible 2) Mimics real-world blast scenarios	1) Complex and expensive setup 2) Species differences in brain response to blast 3) Limited representation of secondary/tertiary injuries	Diffuse axonal injury

*ICP = intracranial pressure

In humans, we could classify the severity of TBI by using the criteria which consist of GCS, PTA period, and imaging techniques. However, pre-clinical studies used different criteria for relating severity and symptoms in TBI. which will describe the next section.

5. Classifying TBI severity in pre-clinical models: Pediatric vs Adult

Traumatic brain injury is a significant public health concern, with severe consequences for individuals and their families. While the field has made progress in understanding the pathophysiology of TBI, there remains a need for robust predictive models to guide clinical decision-making and improve patient outcomes (Courville E, 2023). Animal models have played a crucial role in advancing our understanding of TBI, providing insights into the complex interplay of biomechanical, cellular, and neurophysiological changes that occur following injury.

One key aspect of TBI research is the distinction between pediatric and adult populations, as the developing brain may respond differently to traumatic insults. Increased awareness of the unique vulnerabilities of the pediatric brain has led to a growing emphasis on age-appropriate pre-clinical models to better understand the complex trajectory of recovery and long-term sequelae (Blackwell LS, 2016). The diverse array of TBI models, ranging from focal to diffuse injury, has been the subject of extensive research and debate.

Classifying the severity of traumatic brain injury is a significant challenge, particularly when comparing pediatric and adult populations. Pediatric brains are more susceptible to traumatic insults due to their ongoing development, which can lead to different pathophysiological responses compared to mature adult brains (Delage C, 2021) **(Figure 2)**. For example, the pediatric brain exhibits higher plasticity and neuroinflammatory responses, which can influence the trajectory of recovery and long-term outcomes. Consequently, the diverse array of TBI animal model have been instrumental in advancing our understanding of TBI, there is an ongoing challenge in accurately recapitulating the complexity and

heterogeneity of human TBI. Specifically, the classification of injury severity in pre-clinical models, such as "mild" "moderate" or "severe", may not accurately reflect the clinical presentation and functional impairments observed in human patients.

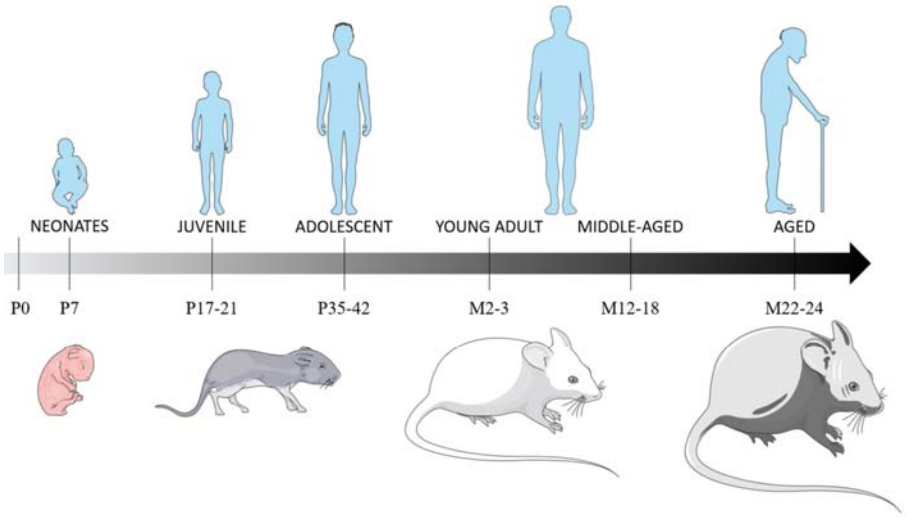

Figure 2. The comparison graphic of age between rodents and human.

(P: post-natal, M: month) (Delage C, 2021)

In response to this challenge, researchers have emphasized the importance of a multifaceted approach to classifying TBI severity in animal models. This may involve integrating biomechanical measures, neurological assessments, and advanced neuroimaging and biochemical biomarkers. Utilizing a comprehensive set of outcome measures enables researchers to gain a more nuanced understanding of the underlying pathophysiology of TBI and identify potential therapeutic interventions to help address its consequences. (Xiong Y, 2013; Petersen A, 2021; Smith DH, 2021)

5.1 Inducing TBI techniques of pediatric and adult in pre-clinical models

A variety of techniques have been used to induce traumatic brain injury in animal models, including fluid percussion injury, controlled cortical impact, blast-induced TBI, and

weight-drop approaches. Selecting the appropriate model is critical, as it must accurately recapitulate the specific biomechanical and pathological features observed in human TBI.

The developing brain in pediatric traumatic brain injury exhibits unique vulnerabilities and responses to traumatic insults. To account for these age-specific differences, researchers have developed specialized pediatric TBI models, such as using immature animals or models that mimic the biomechanical forces and injury patterns observed in pediatric patients. For instance, fluid percussion injury models have been adapted for use in juvenile rodents, enabling researchers to investigate the impact of TBI on the developing brain and explore the potential for neuroplasticity and functional recovery. In contrast, adult TBI models have been more extensively studied and utilized, reflecting the larger body of clinical data available for this population. These models have been instrumental in elucidating the complex pathophysiological processes that contribute to TBI-induced neurodegeneration and impaired neurological function. The classification methods for inducing TBI severity in pre-clinical models, whether in pediatric or adult populations is shown in **Table 5**.

Severity	Pediatric TBI Models (17-28 PND)	Adult TBI Models (6wk-5m)
Mild	CCI: Low impact velocity (3-4 m/s) small tip diameter (3 mm) brief impact duration (100-200 ms) FPI: Low fluid pressure pulse (1-1.5 atm) short duration (10-20 ms) Weight Drop: Light weight (10-20 g) short drop distance (10-20 cm) CHI: Impact velocity (2-3 m/s) Impact depth (1-3 mm) Dwell time (0.1 s)	CCI: Similar to pediatric, but with potentially slightly higher impact parameters Weight Drop: Similar to pediatric, but with potentially slightly higher weight and/or drop distance CHI: Less severe impact, controlled parameters (e.g., using a pneumatic piston)
Moderate	CCI: Moderate impact velocity (4-6 m/s) larger tip diameter (4-5 mm) longer impact duration (200-300 ms) FPI: Moderate fluid pressure pulse (1.5-2.5 atm) longer duration (20-30 ms) Weight Drop: Moderate weight (30-50 g) moderate drop distance (30-50 cm)	CCI: Moderate impact velocity (5-7 m/s) larger tip diameter (5-6 mm) CHI: More severe impact, adjusted parameters for increased injury Weight Drop: Moderate weight (50-100 g) moderate drop distance (50-80 cm)
Severe	CCI: High impact velocity (>6 m/s) large tip diameter (>5 mm) prolonged impact duration (>300 ms) FPI: High fluid pressure pulse (>2.5 atm) prolonged duration (>30 ms) Weight Drop: Heavy weight (>50 g) long drop distance (>50 cm) Consider additional factors: Hypoxia, hypothermia, repeated mild injuries	CCI: High impact velocity (>7 m/s) large tip diameter (>6 mm) prolonged impact duration(>400 ms) CHI: Severe impact, potentially with rotational component Weight Drop: Heavy weight (100 g) long drop distance (>80 cm) Blast Injury: High blast overpressure (>200 kPa) longer duration
References	Pediatric and Adult TBI: (Marklund N, 2012) (Xiong, 2013) (O'Connor C, 2016) (Smith DH, 2021) Pediatric TBI: (Tong W,2004) (Pullela R, 2011) (Pirns ML, 2013) (Rodriguez-Grande B, 2018) Adult TBI: (Dixon CE, 1991) (Marmarou A, 1994)	

Table 5. Classifying TBI severity in pre-clinical models

5.2 Assessment of TBI severities in pre-clinical models

Accurately assessing TBI severity in pre-clinical models is crucial for translating research findings to the clinical setting. As highlighted in the sources, a key challenge is the mismatch between how injury severity is characterized in animal models versus the clinical presentation observed in human TBI patients (Smith DH, 2021). To address this, researchers have utilized a range of experimental approaches, such as detailed neurological assessments, quantitative analysis of lesion volume, and advanced neuroimaging techniques. This multifaceted approach enables researchers to gain a more nuanced understanding of the

underlying pathophysiology and identify potential therapeutic interventions to address the complex consequences of TBI.

5.2.1 Behavioral assessment of TBI severity

To evaluate the functional consequences of TBI in pre-clinical models, researchers have developed a comprehensive suite of behavioral tests, including the rotarod, Morris's water maze, and novel object recognition tasks. These assessments provide insights into the extent of motor, cognitive, and memory deficits resulting from the injury, allowing for a more accurate classification of injury severity. (Smith DH, 2021; Xiong Y, 2013)

5.2.2 Neuroanatomical assessment of TBI severity

Beyond behavioral measures, researchers have leveraged advanced neuroimaging techniques, such as magnetic resonance imaging and positron emission tomography, to quantify the structural and metabolic changes within the brain following traumatic brain injury. MRI allows for the detailed characterization of lesion volume and white matter integrity, offering insights into the anatomical consequences of the injury (Smith DH, 2019; Freeman-Jones E, 2023). PET scanning, on the other hand, can provide information about regional changes in neural activity and metabolic function, which can further inform the assessment of injury severity (Nencka AS, 2018; Zhao T, 2019). Together, these advanced neuroimaging modalities enable a more objective and comprehensive evaluation of the pathological changes in the brain following TBI.

5.2.3 Physiological assessment of TBI severity

Physiological measurements to further characterize the pathophysiological consequences of traumatic brain injury in pre-clinical models (Gao N, 2020; Lee YL, 2020). For example, monitoring intracranial pressure and cerebral blood flow can provide insights into the disruption of normal cerebrovascular regulation following TBI (Smith DH, 2018; Freeman-

Jones E, 2023). Additionally, analyzing biochemical markers such as neurotransmitters, inflammatory mediators, and oxidative stress indicators can shed light on the dysregulated neurochemical signaling that occurs in the injured brain (Thompson S, 2021). By incorporating these comprehensive physiological evaluations, researchers can gain a more nuanced understanding of injury severity and identify potential therapeutic targets to address the multifaceted effects of TBI.

5.2.4 Histological assessment of TBI severity

Histological analyses of the injured brain tissue can provide invaluable insights into the cellular and molecular pathological changes that occur in response to traumatic brain injury (Smith DH, 2021). These detailed histological assessments complement the information gained from behavioral, neuroimaging, and physiological evaluations, offering a comprehensive understanding of the pathological mechanisms underlying TBI. By examining the injured brain tissue at the cellular and molecular level, researchers can identify specific pathological hallmarks, such as neuronal death, glial activation, axonal damage, and disruption of the blood-brain barrier (Perez G, 2021). Furthermore, histological techniques enable the quantification of these pathological changes, allowing for a more objective classification of injury severity. Additionally, advanced histological methods, including immunohistochemistry and electron microscopy, can reveal the spatial and temporal patterns of these cellular and molecular alterations, providing critical insights into the complex, dynamic pathophysiology of traumatic brain injury.

In summary, by employing a multifaceted research approach that integrates behavioral, neuroimaging, physiological, and histological evaluations, researchers can achieve a more comprehensive characterization of traumatic brain injury severity in pre-clinical models.

6. Consequences of TBI severity in pediatric and adult

Traumatic brain injury is a critical public health issue, presenting substantial challenges and long-lasting impacts for individuals, families, and the broader community. While the effects of TBI can manifest across the lifespan, the specific consequences and trajectories of recovery often vary between pediatric and adult populations. (Maria NSS, 2019) Elucidating the distinct neuropathological mechanisms and neurodevelopmental processes that underlie the response to TBI in the immature brain is essential for developing targeted interventions and optimizing long-term prognosis (Girgis F, 2016; Maria NSS, 2019; Blackwell LS, 2016; Anderson V, 2005).

Mild TBI, often referred to as concussion, is the most common form of TBI and is responsible for the majority of cases. However, even in the absence of overt morphological defects, victims of mild TBI frequently suffer lasting cognitive deficits, memory difficulties, and behavioral disturbances. Emerging evidence suggests that these persistent symptoms are related to subtle physiological changes that occur in the hippocampus and other vulnerable brain regions (Girgis F, 2016). The consequences of repeated mild TBIs, as seen in contact sports and military service, can be particularly insidious, with potentially lifelong behavioral and neuropathological consequences. (Mouzon BC, 2017)

In contrast, moderate to severe TBIs are associated with more profound and widespread structural and functional changes, impacting numerous neurological domains. In the pediatric population, the vulnerability of the developing brain confers even greater susceptibility to the devastating effects of TBI, with the potential for long-lasting impairments and altered developmental trajectories (Maria NSS, 2019). A review of the literature highlights the acute and chronic sequelae of pediatric TBI, including deficits in cognitive, behavioral, and psychosocial functioning, as well as the impact on health-related quality of life (Blackwell LS, 2016).

The distinct developmental stage at which pediatric TBI occurs requires a comprehensive understanding of the processes involved in both the short and long-term sequelae. Delineating the complex interplay between the evolving neurobiology of the immature brain and the pathophysiological cascades triggered by TBI is crucial for guiding clinical management, informing prognostic indicators, and developing targeted interventions that leverage the adaptive capacity of the young brain while mitigating the deleterious effects of injury.

6.1 Pre-clinical TBI

Advances in neuroimaging and experimental models have shed light on the complex pathophysiological processes underlying TBI, including excitotoxicity, oxidative stress, neuroinflammation, and axonal injury. These molecular and cellular changes, occurring in the acute and chronic phases, can disrupt neural networks and connectivity, leading to lasting cognitive, emotional, and behavioral deficits. Importantly, the specific manifestations of these neuropathological processes can vary substantially between the developing and mature brain, underscoring the need for a developmental perspective. (Maria NSS, 2019)

Experimental animal models of mild, moderate, and severe TBI have been invaluable for elucidating the distinct neurobiological responses to injury across the severity spectrum.

6.1.1 Pre-clinical pediatric TBI short-term effects and TBI long-term effects

Preclinical studies in juvenile animal models have demonstrated the unique vulnerability of the developing brain to the deleterious effects of TBI, as well as its potential for adaptive plasticity and functional recovery (Freeman-Jones E, 2023; Smith DH, 2021). Compared to adults, young animals exhibit more pronounced neuroinflammation, excitotoxicity, and cell death in the acute phase following TBI, as well as more profound and persistent white matter and connectivity disruptions (Johnson LW, 2022; Miller HA, 2019;

Lumba-Brown A, 2018; Williams HC, 2022). These pathological processes can lead to deficits in cognitive, motor, and social functioning that may persist into adulthood.

In contrast, the immature brain also displays greater neuroplastic potential, driven by ongoing developmental processes such as synaptogenesis, myelination, and neurogenesis (Park MK, 2020; Chen X., 2021). This adaptive capacity may facilitate functional compensation and reorganization, offering a potential avenue for therapeutic intervention (Smith DH, 2022; Lee YL., 2020).

6.1.2 Pre-clinical adult TBI short-term effects and TBI long-term effects

Preclinical studies in adult animal models have demonstrated that the acute response of the mature brain to traumatic brain injury is characterized by a cascade of pathological processes, including heightened neuroinflammation, excitotoxicity, and oxidative stress (Smith DH, 2021; Freeman-Jones E, 2023). These secondary injury mechanisms contribute to extensive neural damage, disruption of neural networks, and impairments in cognitive, motor, and emotional functioning (Lumba-Brown A, 2018; Nguyen T, 2023).

In contrast to the developing brain, however, the adult brain exhibits a more limited capacity for structural and functional reorganization following TBI (Park MK, 2020; Wang KK, 2018). This reduced neuroplasticity may result in a more linear and predictable recovery trajectory, with a clearer distinction between the short-term and long-term consequences of the injury (Gao N, 2020). While the cognitive and behavioral deficits observed in adult TBI survivors can be severe, the stable nature of the mature brain's response may facilitate more reliable prognostic indicators and the development of targeted interventions.

6.2 Clinical TBI

Clinical studies have elucidated the distinct consequences of traumatic brain injury across pediatric and adult populations. These investigations have illuminated both the commonalities and divergences in impairment patterns observed across the age spectrum. (Xiong Y, 2013; Girgis F, 2016; Anderson V, 2005; Maria NSS, 2019) Understanding the unique developmental context and neurobiological determinants shaping the response to TBI is essential for informing effective clinical management and intervention strategies.

6.2.1 Clinical pediatric TBI short-term effects and long-term effects

The clinical studies demonstrate that traumatic brain injury is a leading cause of mortality and morbidity in pediatric populations, with the severity of the initial insult strongly predictive of long-term prognosis. (Maria NSS, 2019; Blackwell LS, 2016) In the acute stage, severe pediatric TBI is associated with profound neurological deficits, including compromised consciousness, cognitive impairments, and behavioral dysregulation. These impairments may persist and evolve as the disruption of critical developmental processes catalyzes cascading effects on cognitive, social, and emotional functioning. Furthermore, pediatric TBI has been linked to an elevated risk of neurodegenerative disorders later in life, underscoring the need for comprehensive long-term monitoring and supportive interventions.

Conversely, even mild traumatic brain injuries in children, often perceived as less severe, can have lasting consequences. The study indicates that seemingly mild injuries can disrupt the delicate balance of the developing brain, leading to difficulties in academic, social, and behavioral domains.

6.2.2 Clinical Adult TBI short-term effects and long-term effects

Existing clinical literature on adult traumatic brain injury populations has consistently documented associations between the severity of the initial injury and the nature

and persistence of resulting impairments (Smith DH 2021; Freeman-Jones E, 2023). In the acute phase following severe TBI, individuals often exhibit a spectrum of neurological deficits, including altered consciousness, cognitive dysfunction, and emotional dysregulation (Miller HA, 2019). However, due to the more stabilized developmental trajectories and reduced neuroplastic capacity of the mature brain, the recovery process in adult TBI cases tends to be more linear and predictable, in contrast to the complex, evolving sequelae observed in pediatric TBI (Giza & Difiori, 2011; Wilde EA, 2012).While the long-term consequences of adult TBI can be highly debilitating, including persistent cognitive, executive, and psychosocial impairments (Thompson WH, 2016; Karr JE., 2014), the recovery trajectory is typically more well-defined, allowing for clearer prognostic indicators and greater opportunities for targeted intervention (Steyerberg EW, 2019).

In conclusion, the consequences of traumatic brain injury severity vary significantly between pediatric and adult populations, highlighting the critical importance of a developmental perspective. Preclinical and clinical studies have revealed distinct patterns in the short-term and long-term effects of TBI, reflecting the unique vulnerabilities and adaptive capacities of the developing versus mature brain. While both age groups can experience profound neurological, cognitive, and behavioral deficits following severe TBI, the evolving nature of the pediatric brain's response and its heightened neuroplasticity can lead to more complex and unpredictable recovery trajectories. In contrast, adult TBI survivors tend to exhibit a more linear and predictable recovery process, facilitating clearer prognostic indicators and targeted interventions. Collectively, these findings underscore the need for tailored clinical management and rehabilitation strategies that account for the distinct developmental contexts shaping the consequences of TBI across the age spectrum.

The TBI consequences not only affect the brain but also implicate other organs. The autonomic nervous systems and systemic inflammation via blood circulation are the bridges for expanding the injury post-TBI. The next section describes the interaction between the brain and peripheral organs in terms of TBI.

7. The brain-peripheral organ's interactions after TBI

The consequences after TBI could prolong processes that affect other organs by two main mechanisms, which are autonomic dysregulation and/or systemic inflammatory response. The previous studies suggested that TBI could alter physio-pathological trajectories of the heart, lung, gut, liver, and musculoskeletal, which could worsen impact outcomes (McDonald SJ, 2020).

7.1 Autonomic dysregulation

The autonomic nervous system (ANS) regulates homeostasis across peripheral organs via sympathetic and parasympathetic pathways, performing a function with the neuroendocrine system. TBI disrupts the regulation of ANS by the hypothalamic-pituitary-adrenal axis (McDonald SJ, 2020). The Paroxysmal Sympathetic Hyperactivity (PSH) or sympathetic storm is the main cause that plays a role in about 80% of TBI, which is dysregulation of the sympathetic system and disruption of cortical inhibitory brain areas (Meyfroidt G, 2017; Jafari AA, 2022). Even, the pathophysiology of PSH in TBI is not well-defined and still warrants a description of the mechanisms involved.

7.1.1 Excitatory/Inhibitory ratio imbalance

This mechanism could simplify the two-stage pathological process. TBI causes destruction and interruption in the inhibition centers and failure response of the positive-feedback loop, which could produce sympathetic overactivity to other organs (Jafari AA, 2022).

7.1.2 Disconnection of controlled sympathetic brain areas

The damage of TBI could interrupt the sympathetic tone in the spinal cord, hypothalamus, and brainstem without alteration in cortical structures (Fernandez-Ortega JF, 2017). These alterations could lead to uncontrolled sympathetic outflow from downstream (Jafari AA, 2022).

7.1.3 Interruption of neuroendocrine regulation

PSH causes impaired descending inhibition (unchecking) that could increase sympathetic output, stimulating the massive secretion of catecholamines, dopamine, and adrenocorticotropic hormone (ACTH) during PSH. The norepinephrine (NE) and dopamine decline during intermittent periods because these elevate depend on excitation of the central sympathetic nervous system. While epinephrine is almost releases from the adrenal medulla. The excessive catecholamines increase about 200-300% from normal levels and about 40% in ACTH. These changes during PSH could play an important role in abnormal function in peripheral organs (Fernandez-Ortega JF, 2017; Jafari AA, 2022).

7.2 Systemic inflammatory response

One of the post-TBI consequences is neuroinflammation. The immune responses after TBI lead to pro-inflammatory cytokines release and recruitment of leukocytes. These local responses still affect other organs, called the systemic inflammatory response.

As previously described in the acute phase after TBI, microglia are the local site-immune cells that respond to neuroinflammation. In the same period, the injured cells and adjacent cells such as neurons and astrocytes release pro-inflammatory cytokines (IL-1ß, IL-6, IL-12, TNF-α, etc.), chemokines, and ROS (**Figure 3**). These factors could cross to blood circulation due to BBB disruption, which causes increased attraction and proliferation of peripheral leukocytes from lymphoid organs (Tobin RP, 2014; Simon DW, 2017). The

dysregulated inflammation affects leukocyte interactions in peripheral organs from the acute to the chronic phase of TBI.

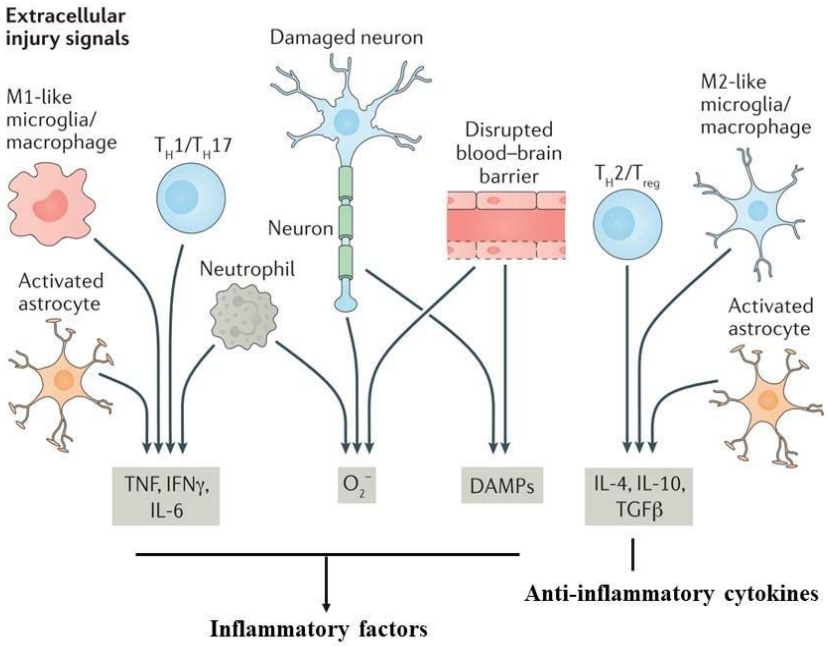

Figure 3. The inflammatory factors release to blood circulation, which induce systemic inflammatory response after TBI (Modified from Simon DW, 2017)

Complications after TBI occur from two main mechanisms consisting of autonomic dysregulation and systemic inflammatory response. All TBI severity (mild, moderate, and severe) can induce pathophysiological effects in peripheral organs such as the heart, lung, guts, liver, spleen, kidney, and bone as demonstrated in **Figure 4** (McDonald SJ, 2020; Sabet N, 2021).

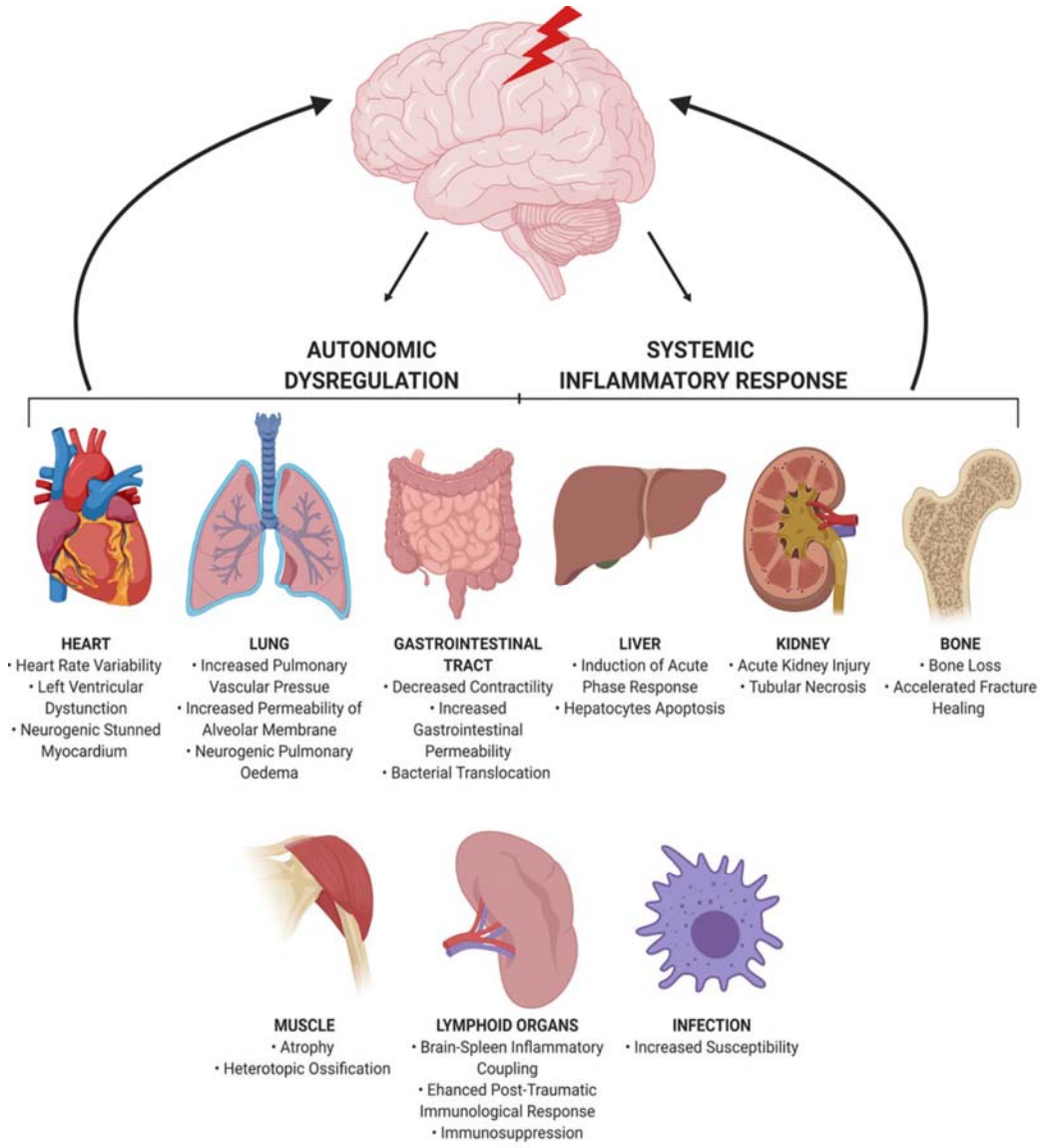

Figure 4. The linkage between brain and peripheral organs after TBI (McDonald SJ, 2020)

Based on a previous study, Ichkova et al investigated the juvenile mTBI (jmTBI) in a mice model (P17) in the acute phase. They showed brain hypoxia at 6-24 h post-TBI and found evidence of cerebrovascular damage but no anatomical changes, with a later modification of cortical blood vessels during 1-3 days post-TBI. Then, behavior results showed long-term neurological defects at 30 days post-TBI (Ichkova A, 2020). However, the chronic phase of jmTBI with systemic complications remains to be investigated. In our work, we focused on the systemic complications of the interaction between the brain and heart, which describe in the next section.

8 Brain-Heart interaction after TBI

The link, interaction, and communication between the brain and heart have been known for centuries. This can be illustrated simply by the control of the heart rhythm exerted by the sympathetic and parasympathetic systems (Coote JH, 2007). The homeostasis of the processing is related to the autonomic nervous system and endocrine system synchronized with the central nervous system (Samuels MA, 2007). Then, some clinical studies and observations demonstrated that various neurological disorders could regulate both cardiac morphology and physiology (Palma J-A, 2014).

The cerebrovascular disease or brain injury showed shreds of evidence involving cardiac injury (Oppenheimer SM, 1994; Ay H, 2006). The clinical and pre-clinical studies made a great effort to understand the underlying relationship between the brain-heart, both normal conditions, and disease (Samuels MA, 2007). This 'invisible' link which starts in the brain and ends with cardiac dysfunction, has been demonstrated in many conditions such as thermal injuries, septic shock, subarachnoid hemorrhage, stroke, and TBI (Krishnamoorthy V, 2016).

8.1 Brain hypoxia, neuroinflammation and implication to cardiac dysfunction in TBI

Normal brains in adults need oxygen to maintain body function at the normal range for oxygen saturation (sO2), i.e between 95-98%, and the normal range of arterial oxygen pressure (PaO2) is between 11.0-14.4 kPa (Williams AJ, 1998). The insufficiency of oxygen or 'hypoxia' is when the cells and tissues cannot receive adequate oxygen for metabolic-energetic demands. The term hypoxemia is used to define the low concentration of oxygen that transfers from air into the blood, and tissue hypoxia is used to define the inadequate concentration of oxygen in tissue perfusion (Roffe C, 2008). The brain consumes about 20% of the total oxygen of the body, and it has no reserve for oxygen or glucose, which is the source of energy for maintaining function (Hoiland RL, 2016). Therefore, the partial blockage of cerebral blood

flow or injured vessels causes tissue hypoxia, and it worsens when completely disrupted in brain injuries, such as TBI and stroke, resulting in anoxia (no oxygen), hypoglycemic condition, and ultimately ending in cell death (**Figure 5**) (Ferdinand P, 2016). The neurons attempt to maintain brain activity during tissue hypoxic conditions and release the excitatory neurotransmitter such as glutamate, which leads to activation of multiple receptors (e.g. NMDA receptors) and massive calcium (Ca^{2+}) influx into the cells. Hypoxia causes the lacking of ATP to eliminate Ca^{2+} overload, resulting in stimulating the multiple cascades that ultimately lead to mitochondria dysfunction and cell death (Guo M-F, 2011; Nathaniel TI, 2015; Simon DW, 2017). The only possibility to rescue and/or limit neuronal cell death is to restore blood flow in the ischemic area. However, the reperfusion phase induces the production of reactive oxygen species, which expands the injury (Won SJ, 2015).

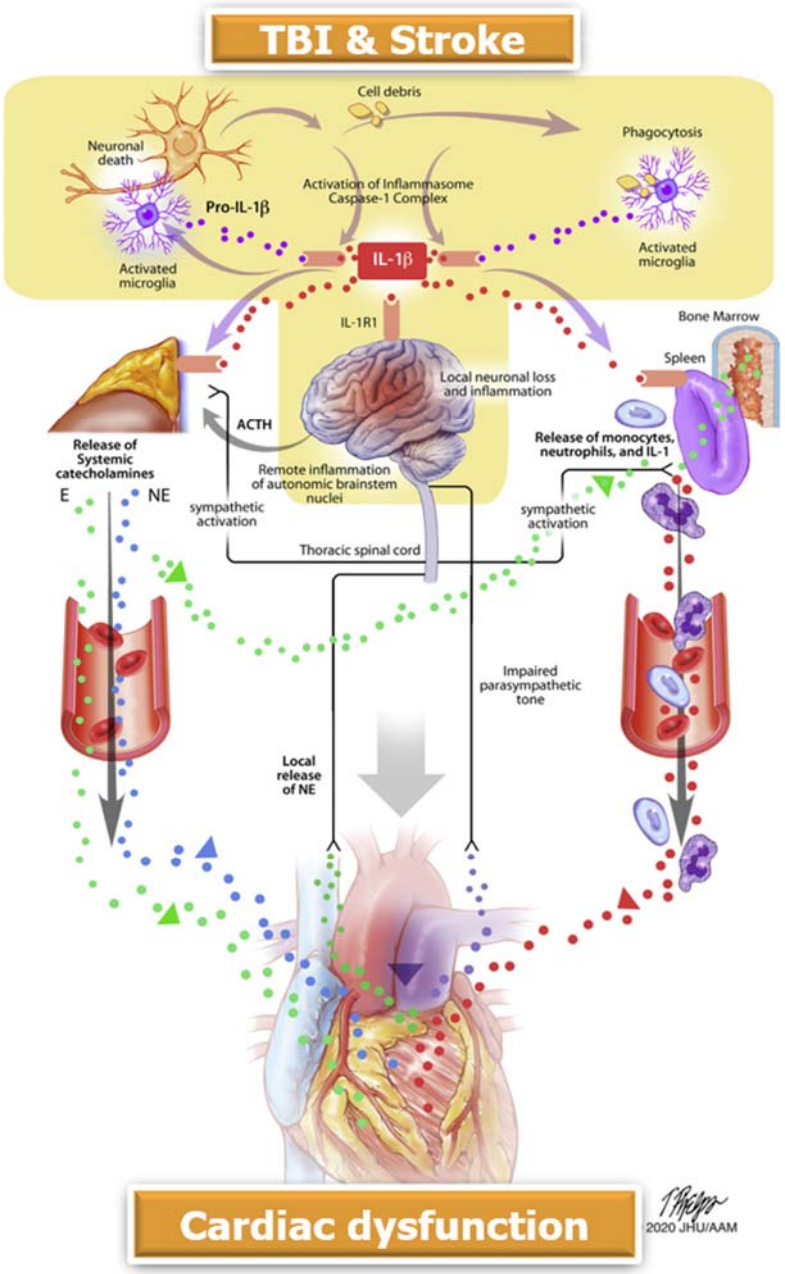

Figure 5. The illustration of systemic mechanisms in TBI and stroke-induced cardiac dysfunction. After brain injuries caused by injured and dead neurons, hypoxia and neuroinflammation stimulate the activation of microglia, releasing chemokines and pro-inflammatory cytokines. The inflammasome activates main pro-inflammatory cytokines such as pro-IL-1into IL-1. IL-1 and remote brain area stimulate the sympathetic system in the adrenal gland, resulting in catecholamine surges. The bone marrow and spleen respond by releasing the leukocytes consisting of neutrophils, macrophages, and pro-inflammatory cytokines. The ANS massively secrete catecholamines causing amplifying severity and chronic inflammation. (Modified from Sposato LA, 2020.)

8.2 Neurogenic Stunned Myocardium

The neurogenic stunned myocardium (NSM) is a term to explain neurogenic injury-induced cardiac dysfunction, which is characterized by left ventricle (LV) dysfunction, ECG changes, arrhythmias, and cardiac biomarker elevation (Nguyen H, 2009). Additionally, other terms attempt to explain the same phenomenon such as catecholamines, autonomic, and sympathetic storms, catecholamines surges, and PSH, all describing the over-function of the sympathetic nervous system (SNS) after brain injury (Meyfroidt G, 2017; Sposato LA, 2020). The previous studies demonstrated the role of SNS and secretion of catecholamines caused the cardiac biomarkers elevation and histological changes in myocardial injury (Masuda T, 2002; Lambert E, 2002). The excess of catecholamines plays a major role in the development of cardiac pathophysiology within NSM. Krishnamoorthy proposed three key factors involving NSM on the brain side: the location of the injury, intracranial pressure elevation, and activation of underlying neuroendocrine pathways in the hypothalamus, which are related to the amount of released catecholamines (Krishnamoorthy V, 2016). The insular cortex acts to control cardiovascular function and regulate the autonomic nervous system see **Figure 6** (Oppenheimer SM, 1990; Hrishi PA, 2019). The subcortical and insular regions are damaged in subarachnoid hemorrhage, stroke, and TBI, which increased sympathoadrenal tone, catecholamine release, neuroinflammation, and autonomic dysfunction (Nguyen H, 2009; Sposato LA, 2020; Mele C, 2021). As previously described, which showed that PSH caused massive secretion of catecholamines after TBI that could be affected in NSM. Although the effect of NSM on TBI is not fully described, this phenomenon has already been reviewed in the stroke that might be explained to TBI. The adrenocorticotropic hormone transient elevation could regulate the release of adrenaline and noradrenaline at adrenal glands, ganglionic sympathetic nerves, and adrenal medulla by sympathetic activation (Sposato LA, 2020). The splenic nerves consist of sympathetic nerve fibers about 98% as well in the inflammatory cells such as monocytes,

macrophages, neutrophils, and lymphocytes could respond with sympathetic receptors from pro-inflammatory cytokines and catecholamine surges post-stroke (Sanders VM, 2002; Scanzano A, 2015). The local SIHI relies on the response of catecholamines at sympathetic nerves ending and cardiomyocytes, which is increased by the regulation of ß2-adrenergic receptors that express nerve growth factors caused by sympathetic nerves spouting in the myocardium (Franzoso M, 2016). Additionally, the activation of cardiac fibroblast into myofibroblast and macrophages could release nerve growth factors for stimulating nerve sprouting (Franzoso M, 2016). The excess of catecholamines is toxic to the myocardium due to over-action of ß-adrenergic receptors following contractile dysfunction, apoptosis, and contraction necrosis band (White M, 1995; Nguyen H, 2009; Gregory T, 2012). The noradrenaline could cause impairment of endothelium function, which is a risk for plaques in acute and chronic phases (van Tassell BW, 2013). The leukocytes amplify injury by releasing the pro-inflammatory cytokines and recruiting more immune cells (van Tassell BW, 2013) see **Figure 7**. The points of view in the SIHI mechanisms originate from main two factors, which are the role of catecholamines in over-stimulating SNS and the other systemic inflammation regulating the release of pro-inflammatory cytokines and leukocytes recruitment. Interestingly, most stroke mortality comes from heart disease, and one in three stroke patients is prone to coronary stenosis, and about 3% end up with myocardial infarction (Gunnoo T, 2016). The consequences after stroke apart from a cardiac injury such as arrhythmias, LV dysfunction, and acute coronary events could affect in the long-term by promoting the risk for heart failure by about 10-24% (Kim W, 2018). These notices show that the complications in the short term between the brain and heart could make it worsen in the long term. The TBI-affected cardiac dysfunction and shared events such as systemic inflammation (at heart), arrhythmia, and cardiac dysfunction that occurred in stroke, are reviewed in the next section (TBI and cardiac dysfunction).

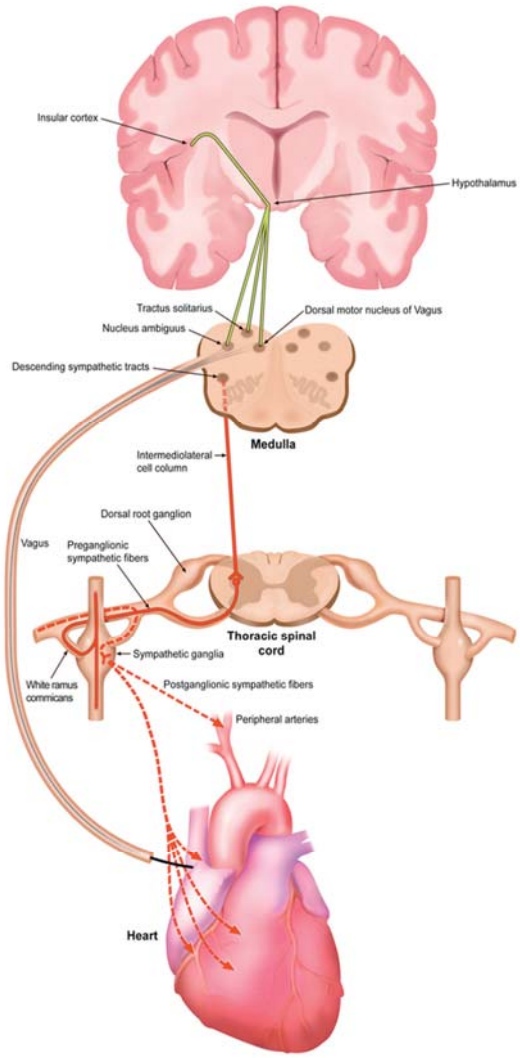

Figure 6. Sympathetic and parasympathetic regulation from the brain to the heart (Dombrowski K, 2014)

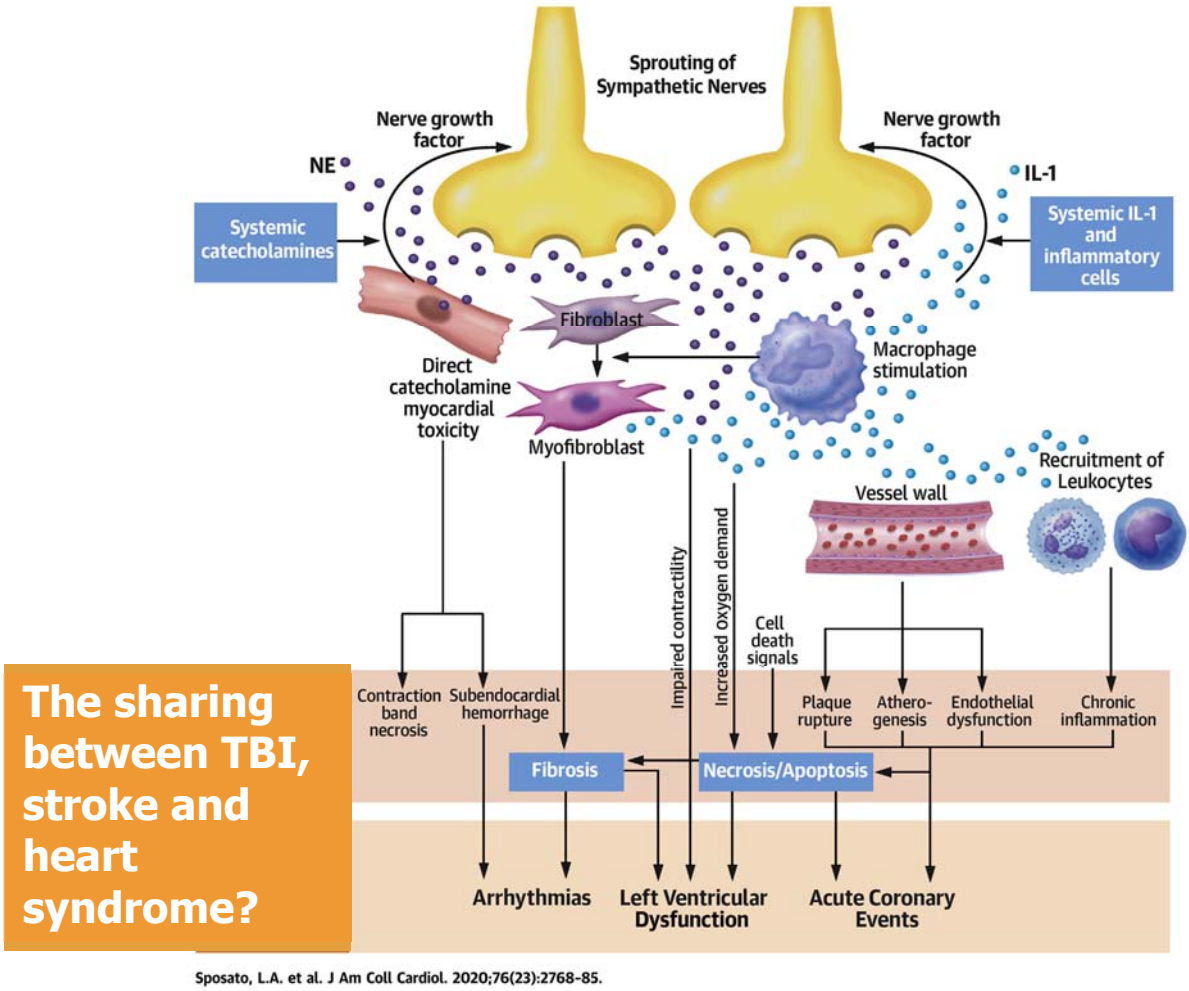

Figure 7. The illustration of local mechanisms in SIHI and TBI sharing the heart events. The catecholamines surge (Noradrenaline) in the bloodstream and sympathetic nerves cause cardiomyocytes prone to contraction band necrosis, risk for subendocardial hemorrhage, and activation of fibroblast to myofibroblast. The inflammatory cells and cytokines such as IL-1 further activate macrophages and fibroblasts causing chronic inflammation, endothelial impairment, and fibrosis. The vicious cycle progresses with increased spouting of sympathetic nerves. The heart could end up with arrhythmias, LV dysfunction, and acute coronary syndromes (Modified from Sposato LA, 2020)

8.3 TBI and cardiac dysfunction

The previous section described mechanisms that could be at the origin of cardiac dysfunction after TBI. Then, in this section, we review and summarize the results from previous studies, which are both on the clinical (13 publications) and pre-clinical (9 publications) sides, as shown in the tables below (**Table 6 & Table 7**).

8.3.1 TBI and cardiac dysfunction in clinical studies

The clinical studies in TBI focus mainly on the severity at moderate to severe stages. The age of patients is mainly adult to elderly (about 16-60 years). Only two works focused on the pediatric population with a follow-up for a maximum period of approximately two weeks (Krishnamoorthy V, 2015; Lele AV, 2020). The main findings in the short term (within 24 to 72 hours after TBI) showed arrhythmogenesis, systolic-diastolic dysfunction with defects in the global longitudinal strain (GLS), regional wall motion abnormalities (RWMA), and high level of cardiac biomarkers (CK-MB, Troponin I and BNP) (**Table 7**). On the other hand, the long-term finding for 1-2 weeks post-injury remains that cardiac dysfunction and biomarkers exist. Interestingly, the moderate-severe TBI met the clinical criteria of systemic inflammatory response syndrome (SIRS) (Chaikittisilpa N, 2018).

8.3.2 TBI and cardiac dysfunction in pre-clinical studies

Animal models were used in the experimental setting, which consisted of rodents, porcine, and canines attempting to mimic human TBI **(Table 7)**. The pre-clinical studies integrate and investigate the interaction between TBI and cardiac dysfunction by using the cardiac function measurements (echocardiography and ECG recording) combined with cardiac biomarkers, gene and protein expression, and myocardium structure. The short-term finding showed arrhythmogenesis (Najafipour H, 2014) and systolic-diastolic dysfunction as found in clinical studies (Larson BE, 2012; Qian R, 2015; Zhao Q, 2019; Lee YL, 2020; Qian Y, 2020). Moreover, evidence for local and systemic inflammation was found with the pro-inflammatory

cytokines released in heart tissue and circulation (Lackner I, 2021), increased cardiac biomarkers (Armstead WM, 2019; Lee YL, 2020), and structural modification (Ozisik K, 2004). The long-term finding demonstrated the progression of TBI from week to month with the development of cardiac dysfunction, morphology changes, fibrosis, and specific cardiac biomarkers (Zhao Q, 2019; Armstead WM, 2019; Lee YL, 2020; Qian Y, 2020). Thus, the clinical and pre-clinical studies provided important information that TBI not only affects the heart in the short term but also promotes the progression of cardiac dysfunction. Systemic inflammation is one of the mechanisms raised to describe the interaction between TBI and cardiac dysfunction.

However, from the point of view that both clinical and pre-clinical studies focus on moderate-severe TBI, we pointed out in the first part (Classification of TBI) that more than 80% of TBI is mTBI, which is careless both in a real-world setting and experimental setting. One of the reasons might be that the brain structure, brain imaging, or clinical signs show no significance. The studies already showed that TBI could affect cardiac dysfunction in the long term. The; mTBI might also be silent-epidemic. The other fact is that the pediatric population is in the same situation as mTBI, mainly in adult-elderly studies. The previous section (*The differences between adult TBI vs pediatric TBI*) described that TBI affects neurological defects during growth development in children experienced with TBI in the long term. In a scenario of jmTBI, which combines two unnoticed factors (pediatric and mild TBI), we hypothesize that jmTBI could affect cardiac dysfunction in the long term as well as other TBI severity.

Table 6. The brain-heart interaction of TBI and cardiac dysfunction in clinical studies

Model of TBI	Severity	Severity Grading/ parameters	*N*	Species	Sex	Age	Short-term finding	Long-term finding	Reference
Clinical studies									
human TBI	mild to severe (49%/15,5%/35,5%)	GCS	335	human	male/female	adult (32±10 y)	(Within 24 hours after TBI) electrophysiology abnormal depending on severity; ST-T changes, sinus tachycardia, QT dispersion prolongation	-	Fan X, 2012
	mild to severe (36,7%/7,2%/56,1%)	GCS	139	human	male/female	adult (58±20 y)	-	(2 weeks after TBI) systolic dysfunction; ↓LVEF, RWMA and ↑cardiac enzymes; CK-MB, Troponin I, BNP	Prathep S, 2014
	mild to severe (39%/8,5%/52,5%)	GCS	59	human	male/female	adult (63±2 y)	(Within 24 to 72 hours after TBI) electrophysiology abnormal; sinus tachycardia, QT prolongation	-	Krishnamoorthy V, 2014
	severe	**GCS**	**32**	**human**	**male/female**	**pediatric (1-16 y)**	**(*1-13 days after TBI) systolic dysfunction; ↓ LVEF, RWMA**		**Krishnamoorthy V, 2015**
	severe	GCS	40	human	male/female	adult (~40 y)	(Within 24 hours after TBI) diastolic dysfunction; ↓IVRT, apical peak strain and basal rotation	-	Cuisinier A, 2016
	moderate and severe (16%/84%)	GCS	49	human	male/female	adult (16-81 y)	(*8-189 hours after TBI) No evidence of cardiac dysfunction, cardiac enzymes; CK-MB, Troponin I		Serri K, 2016

	severe	GCS	50	human	male/female	adult (30±12 y)	(Within 24 to 72 hours after TBI) electrophysiology abnormal; sinus tachycardia and bradycardia, QT prolongation, systolic dysfunction: ↓GLS, RWMA	-	Hasanin A, 2016
	mild, moderate-severe (50%/50%)	GCS	64	human	male/female	adult (~36 y)	(Within 24 hours after TBI) Systolic dysfunction; ↓LVFS, ↑LV area, mitral valve velocity(S') only moderate-severe TBI	(1 week after TBI) Reversible LVFS	Krishnamoorthy V, 2017
	moderate and severe (19,6%/80,4%)	GCS	46	human	male/female	adult (~44,7 y)	(Within 48 hours after TBI) systolic dysfunction; ↓ LVEF	-	Venkata C, 2018
	moderate and severe (12%/88%)	GCS	32	human	male/female	adult (~37 y)	(Within 24 to 48 hours after TBI) found SIRS systolic dysfunction; ↓LVFS, diastolic dysfunction; Mitral in-flow (E wave), mitral annular velocity(e') only in SIRS	(1 week after TBI) Reversible LVFS, SIRS	Chaikittisilpa N, 2018
	mild to severe (50%/10,7%/39,3%)	**GCS**	**28**	**human**	**male/female**	**pediatric (0-18 y)**	**(Within 24 hours after TBI) ↑cardiac enzymes; Troponin I, systolic tachycardia and hypotension**	**-**	**Lele AV, 2020**
	moderate and severe	GCS	30	human	male/female	adult (43±13,5 y)	(Within 24 hours after TBI) alteration of systolic parameter: ↓LV volume(s) diastolic parameters: ↑Mitral in-flow (A wave), lateral mitral annular velocity (a') systolic dysfunction: ↓GLS, RWMA (base and mid of LV)	(1 week after TBI) systolic dysfunction: ↓GLS, RWMA (base and mid of LV)	Krishnamoorthy V, 2020

	mild to severe (20,54%/17,86%/56,25%)	GCS	272	human	male/female	adult (46-58 y)	(Within 24 to 48 hours after TBI) cardiac dysfunction, but *no-show results, ↑cardiac enzymes; Troponin I, BNP	-	Zhang Y, 2021

Table 7. The brain-heart interaction of TBI and cardiac dysfunction in pre-clinical studies

Model of TBI	Severity	Severity Grading/ parameters	*N*	Species	Sex	Age	Short-term finding	Long-term finding	Reference
Pre-clinical studies									
WDI TBI	-	weight 140 g, height 10 cm (craniectomy)	40	Wistar rat	male	adult	(2 to 24 hours after TBI) ↑Heart ultrastructural score (nucleus, mitochondria, sarcoplasmic reticulum of myocardium), ↑ oxidative stress (TBARS)	-	Ozisik K, 2004
FPI TBI	moderate	pressure 1 atm, duration 19-23 ms (craniectomy)	NA	Sprague–Dawley rat	male	adult	(48 hours after TBI) systolic dysfunction; ↓ LVEF, ↑ oxidative stress (SOD)	-	Larson BE, 2012
WDI TBI	severe	weight 450 g, height 2 m	32	Wistar rat	male	adult	(24 hours after TBI) electrophysiology abnormal; ↑P duration and PR-interval	-	Najafipour H, 2014
Blast TBI	-	TNT 1g, range 10 mm	20	Mongrel dog	male/female	adult	(6 to 72 hours after TBI) cardiac dysfunction; ↓ S, E and peak but *no show abnormal segmental strain analysis	-	Qian R, 2015

CCI TBI	moderate to severe	velocity 6 m/s, depth 1,5 mm (craniectomy)	60	C57BL/6J mouse	male	adult (8-10 weeks)	(72 hours after TBI) systolic dysfunction; ↓ LVEF, LVFS, ↑inflammation response by releasing chemokines (MCP-1), oxidative stress (NOX2) and recruiting immune cells, ↑apoptosis, splenectomy could improve cardiac function	(1 month after TBI) Systolic dysfunction; ↓ LVEF, LVFS, fibrosis and hypertrophy, exist of ↑inflammation response and apoptosis *splenectomy improve cardiac function but not neurological defects	Zhao Q, 2019
FPI TBI	**moderate**	**pressure 1,9-2,3 atm, duration 19-23 ms**	**40**	**Yorkshire pig**	**male/female**	**pediatric (1-5 days)**	**(1-4 hours after TBI) ↑cardiac enzymes; CK-MB, Troponin I**	**(1 week after TBI) ↑cardiac enzymes; Troponin I**	**Armstead WM, 2019**
FPI TBI	moderate to severe	pressure 2,4 atm, duration 25 ms (craniectomy)	156	Sprague–Dawley rat	male	adult	(24 to 72 hours after TBI) systolic dysfunction; ↓ LVEF, LVFS	(2 weeks after TBI) ↑cardiac enzymes; Troponin I	Lee YL, 2020
CCI TBI	moderate to severe	velocity 6 m/s, depth 1,5 mm (craniectomy)	20	C57BL/6J mouse	male	adult (10-12 weeks)	(36 hours after TBI) systolic dysfunction; ↓ LVEF, LVFS	(1 month after TBI) systolic dysfunction; ↓ LVEF, LVFS and ↑ LV volume (s, d), LVID (s, d), ↑apoptosis, fibrosis	Qian Y, 2020
CCI TBI	moderate to severe	velocity 4 m/s, depth 2 mm (craniectomy)	48	C57BL/6J mouse	male	adult (10-12 weeks)	(6 and 24 hours after TBI) ↑inflammatory cytokine (G-CSF) and ↓Troponin I, HFABP expression in plasma, ↑CSaR1, GLUT4 in heart tissue	-	Lackner I, 2021

Abbreviations; LVEF: left ventricular ejection fraction, LVFS: left ventricular fraction shortening, RWMA: regional wall motion abnormalities, CK-MB: creatine kinase-myoglobin binding, GLS: global longitudinal strain, BNP: Brain Natriuretic Peptide, TNT: Trinitrotoluene, SOD: super oxide dismutase, TBARS: thiobarbituric acid reactive substance, SIRS: systemic inflammation response syndrome, MCP-1: *monocyte chemoattractant protein-1*, NOX2: NADPH oxidase 2, LVID: left ventricular internal diameter, G-CSF: granulocyte colony-stimulating factor, HFABP: heart-fatty acid binding protein, C5aR1: complement component C5a Receptor1, GLUT4: glucose transporter type 4

8.3.3 Takotsubo cardiomyopathy and TBI

The well-known heart consequence of severe stress in the brain is called *broken heart syndrome* or *Takotsubo cardiomyopathy* (TTC). Sato et al first described that emotional or physical stress can induce or mimic the consequences of the acute coronary syndrome and changes the appearance of heart morphology like an octopus trap pot (Akashi YJ, 2008). The catecholamine surge and sympathetic activation can induce temporary and reversible regional wall motion abnormalities, decreased LVEF or changes of ECG, and/or elevation of cardiac biomarkers without evidence of previous heart problems (Prasad A, 2008). TTC is commonly found in the elderly (about ±50 years) population especially in post-menopausal women, suggesting that the cardioprotective effect of estrogen was reduced, when against catecholamines (Schneider B, 2014; Matta A, 2022). Amid controversy, the patterns of TTC are various abnormal heart appearances from apex to basal, but mainly basal hyperkinesis, apical ballooning, and hypokinesis of the apical and mid ventricle (Matta A, 2022). The pathophysiology of TTC results from the massive catecholamine response in cardiomyocytes via a ß-adrenergic receptor (ßAR), which promotes intracellular calcium overload and increases the expression of genes causing myocardial hypercontractility. Additionally, the catecholamines stimulate multi-vessels epicardial spasms and induce microcirculatory dysfunction (Matta A, 2022). TTC stimulates ßAR by increasing the expression of G protein-coupled receptor kinase 2 (GRK2) and ß-arestin2, which cause increased ROS production and altered contractility (Nakano T, 2018). However, excessive catecholamines could increase the expression of ßAR genes (b1AR&b2AR), but not found variants that are specific in TTC (Onrat ST, 2021). The cardiac dysfunction in TTC can be reversed by two mechanisms. The first is feedback from catecholamine stimulation, which works via switching G-coupling protein from *Gs* to *Gi* for restricting contractility. The second is the activation of the AKT survival pathway (Matta A, 2022). A recent review study about TBI and TTC showed that it is the most severe

TBI (GCS: 3-11) with various age periods (pediatric to elderly), which found both preserved and decreased LVEF and various patterns of TTC characteristics (Gruhl SL, 2022). This confirmed that severe TBI is a short-term cause of autonomic dysregulation in the brain involving massive catecholamine release and originating from TTC in the heart. However, the correlation between TBI and TTC still needs more investigation due to other mechanisms occurring in TBI.

Based on the information available at this point, TBI and cardiac dysfunction demonstrate the key role of brain-heart interactions during disease progression. Current diagnostic and monitoring tools are imaging techniques used separately in the brain and heart. The following section describes imaging modalities used to assess brain and heart function that could be the tools to understand the likelihood of disease better.

9 Imaging techniques for assessing brain and cardiac function

9.1 Magnetic resonance imaging (MRI)

The general principle of MRI is the detection of protons or neutrons (hydrogen mainly from water and fat molecules), which are positive charges moving (spin) around the nucleus of atoms and using the static dipolar magnetic field to increase the spinning (Stoffey RD, 2012). Then the increased energy level causes radio frequency energy in the magnetic field, which is amplified into free-induction decay and apply to the Fourier transformation process (Stoffey RD, 2012). The spinning physical principle could provide biochemical information (**Figure 8**). The MRI with horizontal and high magnetic fields has been performed on the small animals at 4.7, 7, 9.4 11.7, or 21.1 Tesla depending on the categories of the studies (Leftin A, 2015).

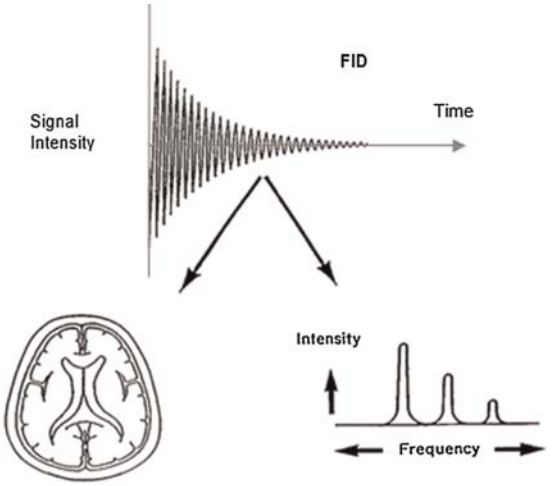

Figure 8. The schematic diagram constructs the image from free induction decay and Fourier transformation (Leftin A, 2015)

9.1.1 MRI in neurological study

The brain MRI could be accessed by the properties of the water molecules (hydrogen) in the brain and the difference between the signal and the brain structure (Aggarwal M, 2012). The goal of the brain MRI is to achieve the evaluation or monitoring of anatomical and physiological changes from brain disorders (Aggarwal M, 2012). A recent study showed that MRI with diffusion-weighted imaging could monitor and detect (*ex vivo*) the changes in white matter structures that close injury sites in the 6-month pediatric TBI model (Zamani A, 2021). A previous study showed the T2-weighted MRI assessed and monitored brain injury volume in the long-term severe TBI in the mouse model. The scanning of the whole brain was performed using more than 40 minutes per animal (Tatara Y, 2021).

9.1.2 MRI in cardiovascular study

Cardiac measurement by using MRI or Cardiac magnetic resonance imaging (CMR) was proven to be the gold standard with high accuracy in clinics (Dewey M, 2006). The properties of CMR are high contrast for dividing between myocardium and blood, high temporal and spatial resolution, and freely slice orientation (Zuo Z, 2017). These might

be covering the limitations of 2D ultrasound in the geometric and volumetric calculation. The previous study showed the IntraGate cinematographic (CINE) in CMR technique, which could access to measure cardiac function such as EF, EDV, ESV, SV, and LV mass in the healthy mouse model by using a total scan time of about 30 minutes per animal (Zuo Z, 2017). The CINE CMR was used to evaluate both morphology and function during dobutamine stress in muscular dystrophy mouse models (Stuckey DJ, 2012).). Interestingly, the tagged CINE CMR could assess the STE and morphology which illustrated changes in the myocardial infarction model by taking time to scan 15 minutes (Karthikeyan B, 2020).

9.2 Computed tomography scan (CT-scan)

The CT scan was developed in the 1970s. It comes from two words, ‘computed’ which means processing through the computer, and ‘tomography’ which means cutting an image into slices (Caldemeyer KS, 1999; Das BK, 2015). Briefly, the principle of CT-scan is the use of ionizing radiation or X-rays rotated 360° around the organs coupled with a detector. The images are scanned slice to slice and reconstructed into 3D images with computer processing (Das BK, 2015). The X-rays can pass through the organs and then are attenuated. The difference in attenuated radiation depends on the type of tissue. The high attenuation is brighter in the image (bone, metal, dense organs) and the low attenuation is darker in the images (air, fat, water) (Caldemeyer KS, 1999). CT-Scan of the brain may be performed to assess the brain for tumors, after TBI, intracranial bleeding, and structural anomalies (e.g., hydrocephalus, infections,...), particularly when another type of examination (e.g., X-rays or a physical exam) are inconclusive.

9.2.1 CT-scan in neurological study

Because some organs or pre-clinical studies need higher spatial resolution, the micro-CT or μCT was developed for serving this purpose (Boerckel JD, 2014). The μCT-scan was addressed in the brain for anatomical and structural studies with or without the contrast agents to increase the resolution of the images. The previous study showed the μCT-scan coupled with iodine contrast medium could define the middle cerebral artery occlusion *in vivo* mouse model (Hayasaka N, 2012). The study showed the development of last-longer iodine contrast with micro-CT to study brain structure and blood vessel formation (Starosolski Z, 2015).

9.2.2 CT-scan in cardiovascular study

Interestingly, the μCT-scan could apply to measure the cardiac function and synchronization with the heart rate, previously study showed the combine between μCT-scan and ECG recording (respiratory gating) could generate 4D micro-CT that achieved to evaluation LV diastolic-systolic volume, EF, CO, SV couple with heart rate in the healthy mouse model (Christian TF, 2005)(Kojonazarov B, 2018).

9.3 Positron emission tomography (PET)

PET is the nuclear medicine imaging technique, which contains possibly to quantify cellular and molecular processes (metabolism quantification) in humans. The detection of PET determines pairs of γ-rays, which are emitted indirectly by radioisotopes administered into the body. The radiopharmaceuticals are indicators for detecting receptor binding capacity, molecular metabolism, and cerebral blood flow (Mishina M, 2008). Due to the lack of quality in anatomical structure imaging of PET, PET/MRI or PET/CT was combined to improve the resolution (Tarkin JM, 2020).

9.3.1 PET in neurological study

The brain oxygen saturation is the parameter that indicates oxygen condition, which can be measured by radiopharmaceuticals. The [18 F]-FMISO tracer demonstrated extensive properties to detect the Fraction of Inspired Oxygen (FiO2) and construct mapping for discriminating between the healthy and tumoral murine brain (Valable S, 2017). The specific molecule to neuroinflammation is like 18 -kDa translocator protein (TSPO), which indicates activation of microglia. The [18 F] DPA-714, the radiotracer for targeting TSPO, enabled quantification of radioactivity uptake and constructed mapping in mTBI and moderate-severe TBI murine model (Israel I, 2016).

9.3.2 PET in cardiovascular study

In pre-clinical studies, PET could assess various strategies. The 18F-FDG radionuclide tracer showed efficient cardiac function and histology evaluation in the myocardial infarction murine model, consisting of LV metabolic volume, EDV, ESV, SV, and EF (Fischer M, 2021). The specific molecule in the heart could also be detected by radiopharmaceuticals such as 68Ga-NODAGA-RGD, which could attach the αvβ3 integrin for investigating angiogenesis in the myocardium (Lang CI, 2020). The other strategy for detecting ROS production using 18F-DHMT showed possibly measuring ROS in the doxorubicin-cardiac toxicity murine model (Boutagy NE, 2018).

9.4 Ultrasound imaging

Ultrasound (US) is a non-invasive diagnostic medical imaging technique performed to view a patient's internal soft tissues and organs (heart, bladder, etc.) and to assess blood flow through various vessels. Unlike other imaging techniques, the US do not use radiation, but instead, rely on sound waves and echoes that can recreate images. Therefore, patients are not

exposed to ionizing radiation, making the procedure safer than diagnostic techniques such as X-rays and CT scans.

The frequency of the transducer is an important parameter for the resulting image as the high-frequency (25-55 MHz) transducer gives a higher resolution (less than 100 μm) of the image but reduces the scope of the image depth (4 to 1cm). On the opposite, the low-frequency transducer (2-15 MHz) gives a more depth scope (up to 40 cm) of the image but a lower resolution image (mm-cm). For preclinical imaging, frequencies between 15-55 MHz are generally used for rats and mice.

9.4.1 US in neurological study

The emergence of new ultrasound technologies is to flip the hand from conventional ultrasound to ultra-fast ultrasound. The plane-wave compounding with multiple angles pushes the limit of ultrasound imaging resolution to more than 1,000 frames per second, which gives the possibility of brain assessment of blood flow (motion), contrast agents, and neurovascular brain activity (Tanter M, 2014).

9.4.1.1 Power Doppler for determining change of blood flow

The functional ultrasound (fUS) technique was developed to evaluate the whole-brain microvasculature dynamics, increasing sensitivity and spatial-temporal resolution by compound plane-wave emission and multiple angles (Macé E, 2011). This fUS scans the main arteries in the whole brain with a short acquisition time (200 ms) (**Figure 9**). The power Doppler was selected for determining the change of blood volume in microvascular in the brain by detecting and calculating the red cells with the axial velocity >4mm s^{-1} (Macé E, 2011). Although the fUS is highly capable, it was limited with the ultrasound emission frequency 15 MHz that could not cover the blood velocity in capillaries < 1mm s^{-1} (Macé E, 2011).

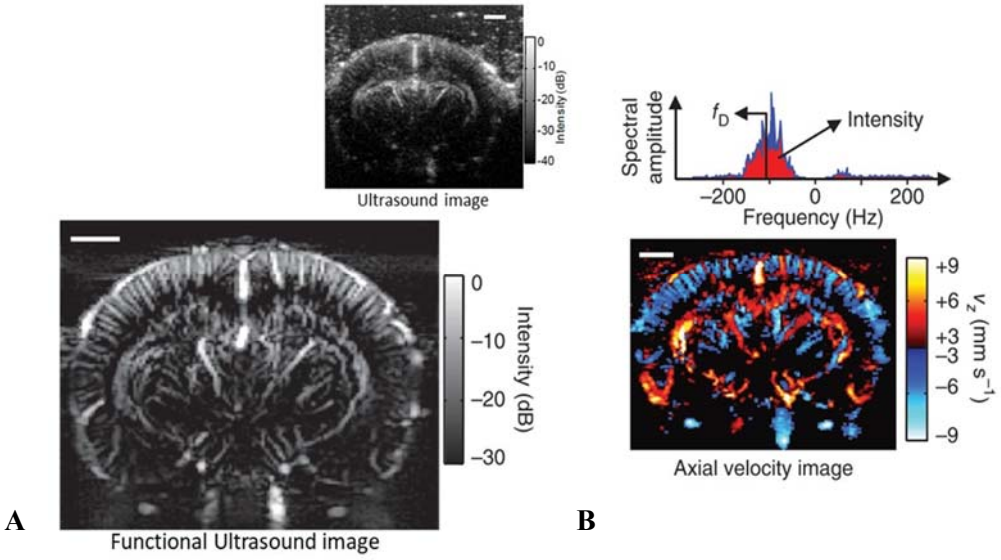

Figure 9. The comparison resolution between conventional-functional ultrasound and measurement of blood volume. (A) fUS revealed the high resolution of small vessels when compared to the conventional US. (B) Power Doppler assessment changes blood volume by axial velocity (Modified from (Macé E, 2011)

9.4.1.2 Micro bubble tracking

The CBV changes by using a non-linear contrast (NLC) ultrasound imaging mode, which employs an ultrasound pulse sequence designed to receive only backscattered ultrasound from nonlinear scatterers of microbubbles and reject signals from linear scatterers like tissue or red blood cells (Goertz DE, 2005; Needles A, 2010). For the low concentrations of bubbles, the signal intensity in this imaging mode depends linearly on bubble concentration, effectively making the signal a relative measure of local blood plasma volume (Lampaskis M, 2010). Since the hematocrit is largely unaffected by functional activation (van Raaij ME, 2011), the measured plasma volume changes provide an estimate of total blood volume change. The previous studies showed that the ultrafast ultrasound could detect the microbubbles in the mouse brain with a high spatial resolution in B-mode and then allows the construction of the vessels images by tracking the microbubbles (**Figure 10**) which acts as enhanced-contrast ultrasound (Errico C, 2015).

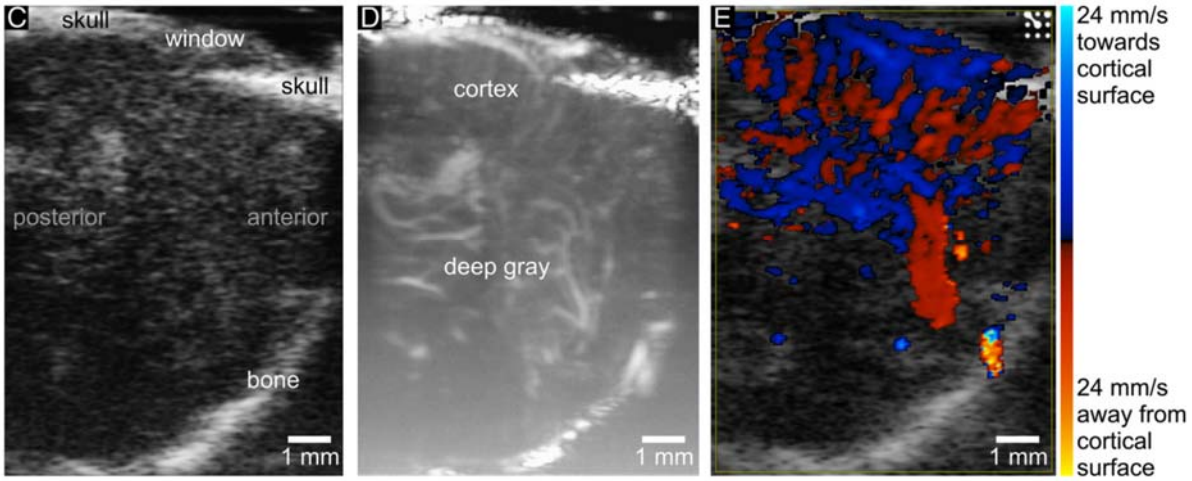

Figure 10. Tracked-micro bubbles for constructing vessels from ultrasound imaging (Errico C, 2015)

Even ultrasound imaging techniques such as functional or ultrafast-ultra could determine the functions of the brain but the limitations in terms of blood flow velocity still need to improve. The other technique that could provide the assessment of brain functions in more detail will be mentioned in the next topic.

9.4.1.3 Photoacoustic imaging for detecting oxygen saturation

Photoacoustic imaging (PAI) combines a laser light source and ultrasounds to detect endogenous molecular information (e.g., collagen, melatonin, hemoglobin, and lipid) from the tissues. The PAI still applies with the contrast to expand the resolution of detecting exogenous contrast imaging agents to detect specific molecule (Zackrisson S, 2014). Moreover, the PAI gives a high spatial resolution of molecular, functional, and anatomical imaging. PAI is a non-invasive and non-ionizing imaging technology (Zackrisson S, 2014). The principle of PAI, first described by Bell in 1880, was defined as '*sound by light*' (Bell AG, 1880). Remarkably, the pulse of the laser beam is emitted in a nano-second to the target tissues that could transfer, diffuse, and accumulate the photons in the tissues. The photons absorption in the tissues is caused by a slight increase in the

temperature inside. The phenomenon is called "*the thermoelastic expansion*", which shortly remains in the tissues and could generate a pressure wave or ultrasound. The signals could be detected by the transducer of ultrasound and construct the images.

Blood oxygen saturation is a useful biomedical index that indicates oxygen and metabolism in the whole body (Toffaletti J, 2007). The gold standard of measurement of blood oxygen saturation is arterial blood-gas analysis, which is an invasive technique that potentially causes complications during the intervention and non-specific regions (Scheer B, 2002). However, the concept of assessing oxygen saturation can be applied to the evaluation of the specific location of oxygen and activity using the PAI. The endogenous contrast or intrinsic chromophore is hemoglobin, which carries the oxygen for serving the body that could be essential to detecting oxygen saturation in regional areas or organs (**Figure 11**) (Weber J, 2016). The hemoglobin's ability to carry oxygen can divide into 2 types, i.e. oxy-hemoglobin and deoxy-hemoglobin, which distinguish wavelengths for PAI measuring oxygenation (**Figure 12**) (Needles A, 2013). The PAI demonstrated capability to determine brain oxygen saturation in various pathophysiological of ischemic preclinical models (Sun Y-Y, 2015; David H, 2020).

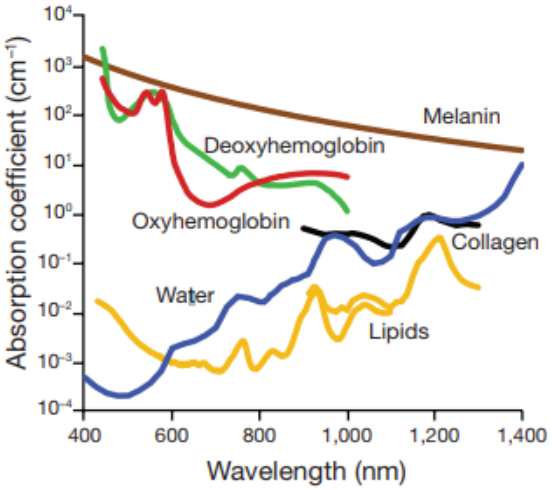

Figure 11. The intrinsic chromophores in the body in optical light wavelength (Weber J, 2016).

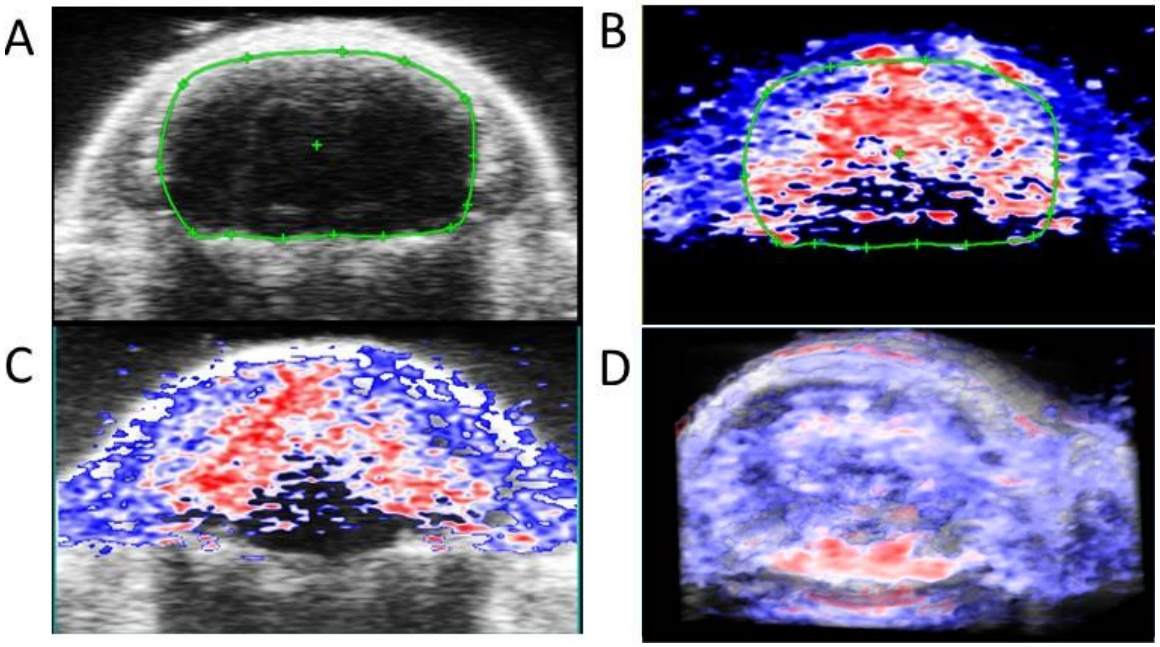

Figure 12. The brain oxygen saturation measurement with PAI. A) B-mode showed the head structure of the mouse and the brain (located in the green area). B) PA-mode showed the colorimetric map of the brain. the red represents oxy-hemoglobin and the blue represents deoxyhemoglobin. C) Merged images between B-mode and PA-mode for quantifying oxygen saturation D) The 3D computational reconstructing image of the brain

The cardiac function (right and/or left ventricle (LV)) assessment by US imaging, also called an echocardiogram, accurately defines the condition of the heart during the entire cardiac cycle. The LV systolic function and LV diastolic function provide valuable pieces of information about the heart status and the prognosis of the diseases.

9.4.2 US in cardiovascular study

9.4.2.1 LV systolic function

The assessment of systolic function indicates the performance of the heart in systole, which is the contraction period of the heart that pumps blood out from the left ventricle to the arteries to support the body with oxygenated blood (Lang RM, 2015). The systolic function could be measured by using the image of 2-dimensional (2D) echocardiogram in B-mode and M-mode (**Figure 13**) (Lang RM, 2015).

9.4.2.1.1 2D B-mode in US imaging

The Brightness mode (B-mode) is usually used to access 2D cross-sectional images. The real-time images in the display are acquired by using the transducer that emits the ultrasound waves through the skin until impact and scatters organ boundaries and tissue, and then the ultrasound waves reflect the feedback signal to the transducer (Jan MF, 2017). The received signal is constructed to the gray-scale image. The whiter scale represents the organ boundaries, and the darker scale represents the scatter area lower echoes, e.g., blood, out-of-focus areas, and the shadow of bones. The 2D B-mode is the most general and standard approach for echocardiography, enabling cardiac anatomical structures and function measurements in a real-time cross-sectional view (Jan MF, 2017) (**Figure 13A**).

9.4.2.1.2 2D M-mode ultrasound imaging

Motion-mode (M-mode) is applied to study rapidly moving structures such as valvular movement or heart-wall movement. A single section area is selected in the B-mode image across the valves or chamber walls of interest and the ultrasound image

is obtained only from the selected area shown in the M-mode (Feigenbaum H, 2010)The image with a high temporal resolution of the M-mode corresponds with the B-mode image. M-mode imaging is a mode that captures high-speed images along a single line or axis. This mode is most suitable for heart-wall anatomical and functional evaluation during the entire cardiac cycle (systole, diastole). The M-mode can provide a momentary resolution of up to 1,000 frames/sec according to the movement of the heart wall (Feigenbaum H, 2010). The resulting images reflect the contractile pattern, which can then be used to assess cardiac function (**Figure 13B**).

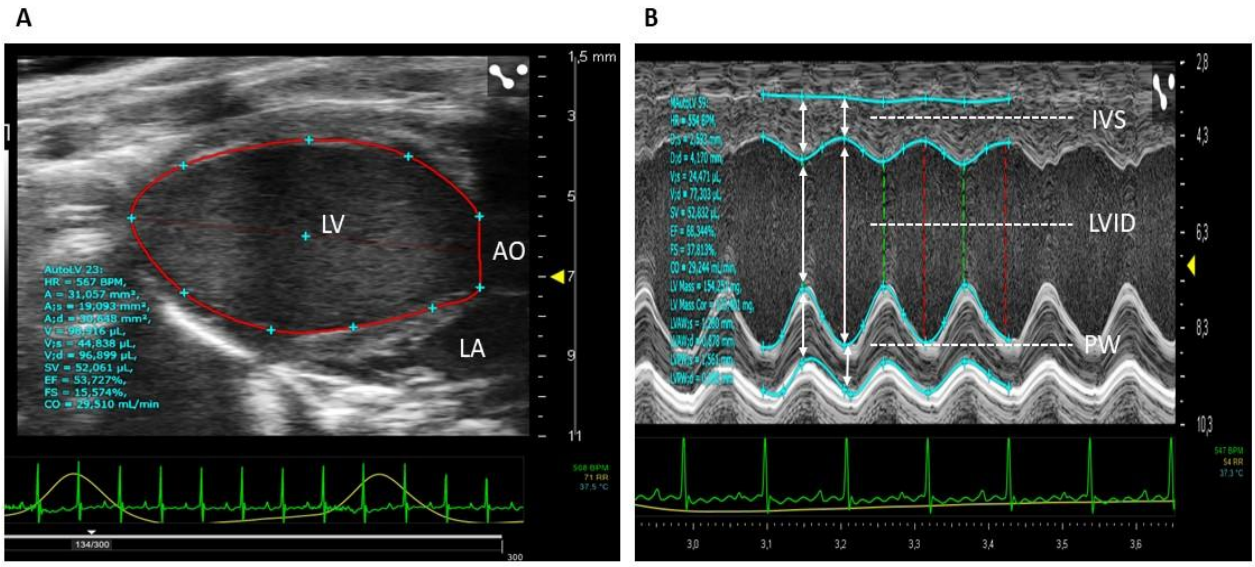

Figure 13. The images of systolic function evaluation in mice. (A) LV B-mode in parasternal long-axis view, allows for assessment of systolic function by LV. (B) LV M-mode, allow for assessment of systolic function by IVS, LVID and PW.

9.4.2.1.3 Cardiac parameters in systolic function

Based on the B-Mode and M-mode images, we can measure and calculate key cardiac anatomical and functional parameters.

a) The left ventricular ejection fraction (LVEF)

LVEF is the index indicating the percentage change of LV volume from end-diastolic volume (EDV) and end-systolic volume (ESV) (Wong ND, 1995; Tsujita Y, 2005; Bamira D, 2018). The formula for calculating EF:

$$EF = \frac{EDV - ESV}{EDV} \times 100$$

b) Stroke Volume (SV)

SV is the ejected volume of the blood in the LV during systole. SV is equal to the difference between EDV and ESV, which is an index LV function (Bruss ZS, 2022).

$$SV = EDV - ESV$$

c) Cardiac Output (CO)

CO is the volume of the blood ejected from the LV to the aorta per minute, which is the index of the LV pumping function (Bruss ZS, 2022).

$$CO = SV \times HR$$

*Note: HR - heart rate per minute

d) Left Ventricular Fractional Shortening (LVFS)

LVFS is the index that indicates percentage change of LV chamber size during systole and diastole, which represents LV myocardial contraction. This is obtained by evaluating the LV end-diastolic dimension (LVDd) and LV end-systolic dimension (LVDs) (Wong ND, 1995; Tsujita Y, 2005). The formula for calculating FS:

$$FS = \frac{LVDd - LVDs}{LVDd} \times 100$$

e) Left Ventricular Mass (LV mass)

LV mass is an anatomical index. LV mass could be obtained from the M-mode echocardiogram (Tsujita Y, 2005). The formula for calculating LV mass:

$$LV\ mass = 1.05 \times [(LVIDd + LVPWd + LVIVSd) - LVIDd^3]$$

*Note: LVIDd – LV internal dimensions at diastole

LVPWd – LV posterior wall thickness at diastole

IVSd – LV interventricular septal thickness at diastole

9.4.2.2 LV diastolic function

The diastolic function indicates the cardiac performance of the heart during the "resting" period, which results tightly from the LV relaxation phase that keeps normal cardiac blood filling. Diastole is divided into 4 phases: Isovolumic relaxation, early rapid filling, diastasis, and atrial contraction (Nishimura RA, 1997). Due to several properties that could affect the diastole in each phase, the two main determinants play a role in the diastolic function. Firstly, ventricular relaxation is the period of decreasing pressure after systole or LV contraction, which is a negative peak of LV pressure over timing (-dP/dt) (Rakowski H, 1996). Secondly, chamber compliance, which correlates with the change of volume over changing of pressure in LV (dV/dP) depends on the passive abilities of LV during blood flowing via the mitral valve from the left atrium to LV (Grossman W, 1976).

The evaluation of diastolic function in mice models is well documented. Recently, Schnelle et al developed a specific algorithm to monitor diastolic dysfunction in mice. (**Figure 14**) (Schnelle M, 2018).

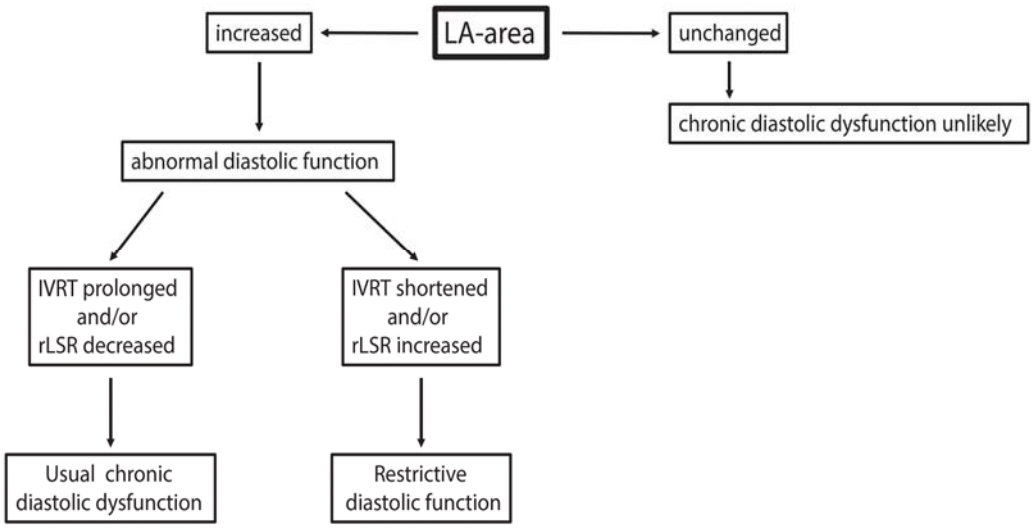

Figure 14. The algorithm for evaluation of diastolic dysfunction in mice (Schnelle M, 2018).

Using high-resolution ultrasound, the diastolic function parameters could be assessed using PW Doppler-mode, Tissue Doppler imaging, and B-mode imaging (**Figure 15**).

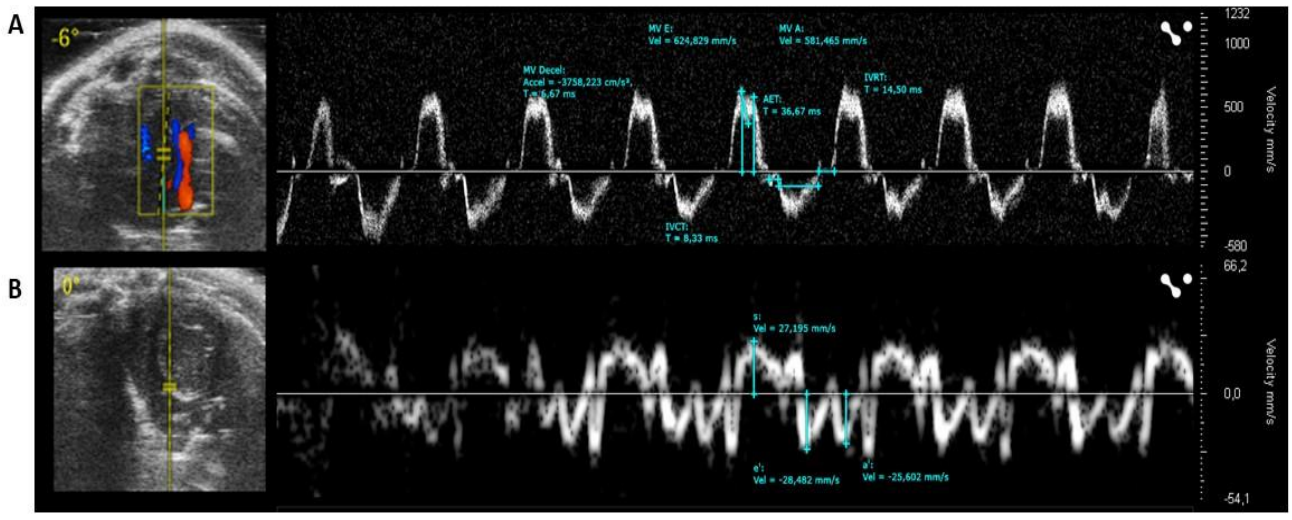

Figure 15. The images of diastolic function evaluation in mice. (A) LV PW Doppler-mode combine Color Doppler mode in apical four-chamber view, allows for assessment of mitral flow profile. (B) LV PW Doppler-mode, allow for assessment of Tissue Doppler imaging.

9.4.2.2.1 Doppler mode ultrasound imaging

The Doppler mode is used to assess blood flow direction and velocity of the myocardium. This mode could measure the systolic ventricular function and mitral annulus (Gulati VK, 1996; Pellerin D, 2003; Tassan-Mangina S, 2006). The Doppler mode imaging utilizes the Doppler shift principle reflected by moving targets such as blood cells. The changes in the Doppler shift correlate with the blood flow velocity. The Doppler shift depends on the alignment of the blood flow and ultrasound waves. The more parallel the waves, the more attenuation of the Doppler switch is. Clinically, this mode is employed to assess vascular and cardiac functions. It relates to diastolic function; pressures in the pulmonary artery, left and right atria; left ventricular stroke volume; and quantification of a regurgitant valve, if present. Assessment of the filling patterns of the left ventricle, in addition to the diastolic function of the heart, has been shown to have clinical implications as it relates to morbidity and prognostic evaluations (Jan MF, 2017). Tissue Doppler Imaging (TDI) is a mode that can detect lower-velocity and higher amplitude signals arising from heart muscle contraction (Rohde LE, 2007). The pulse-wave TDI is suitable for long-axis or apical four-chamber view monitoring of heart function because the position of the myocardium is parallel to the emitted ultrasound waves, especially when viewed through the apical view (Isaaz K, 1993). TDI is tissue motion velocity, which is obtained by assessing the mitral annulus (interventricular septum, lateral wall, and LV posterior wall). TDI usually consists of three waveforms: the peak of early diastolic velocity wave (E'), the peak of late diastolic velocity wave (A'), and the peak of systole (s) (Schmidt AG, 2002). This makes it possible to predict the filling pressure from E/E' ratio (Ommen SR, 2000).

a) Trans mitral inflow velocity pattern (Mitral flow profile)

The mitral flow profile is obtained by the mitral velocity waveforms that flow through the mitral valve from LA into LV during diastole, which is the practical index indicating diastolic function because the waveforms could reflect LV filling characteristics and compliance (Schumacher A, 2008). The mitral velocity waveforms are assessed by Pulsed-wave (PW) Doppler with a parasternal long-axis view or apical four-chamber view. They include the early filling wave (E wave) and late atrial filling wave (A wave) representing the LV filling dynamics (Schmidt AG, 2002). The E wave represents the velocity of blood flow via the mitral valve in the early filling phase, which can be affected by compliance and the rate of relaxation of the LV. The A wave represents the velocity of blood flow via the mitral valve in the atrial contraction phase, which could reflect alteration by compliance and contractility (Lester SJ, 2007). The mitral flow profile indexes include the parameters as follows:

ai) The ratio of peak velocity of early to late filing of mitral inflow (E/A)

aii) The deceleration time (DT) of early filling of mitral inflow is the time of pressure equilibration between LA and LV, which is measured from the peak of E wave to the baseline.

aiii) The isovolumetric relaxation time (IVRT) is the time from the aortic valve until the opening of the mitral valve, if high IVRT means prolonged relaxation during diastole.

b) Left Atrium (LA) Size

LA size can be used to assess the chronic elevation of LV filling pressure in diastolic dysfunction. The LA size is measured by B-mode or 3D-mode (more accurate) in parasternal long-axis view (Basu R, 2009; Jorge AJL, 2012).

c) Myocardial Performance Index (MPI)

The MPI is the index that combines both systolic and diastolic functions, involving IVRT, isovolumetric contraction time (IVCT), and ejection time (ET).

The formula for calculating MPI:

$$MPI = \frac{IVRT + IVCT}{ET}$$

The increase in MPI could indicate diastolic dysfunction when corresponding with the other parameters for diastolic function assessment (Broberg CS, 2003).

9.4.2.3 LV Strain analysis

The strain analysis assesses the myocardial LV regional functions. The strain or deformation has been defined with 3 principles: circumferential, longitudinal, and radial which are the movement or contraction directions of the heart muscle (**Figure 16**) (Gorcsan J, 2011). The term strain was defined to describe lengthening, shortening, or thickening (regional deformation) in the echocardiography assessment (D'hooge J, 2000). It can simplify the explanation of when the heart contracts and changes its structure shapes called "deformation". The strain needs to define how much it changes (extent of deformation) in the regional myocardium.

The strain could calculate by the formula (D'hooge J, 2000):

$$\text{Strain, } \varepsilon = \frac{\Delta L}{L_0}$$

*Note: where ε = strain, ΔL = change in length (end-systolic length – end-diastolic length), and L_0= original length (end-diastolic length)

The strain rate is the rate described as strain or deformation per time unit. The strain rate unit is s^{-1} and calculate by the formula (Dandel M, 2009):

$$\text{Strain rate, } \varepsilon = \frac{\Delta \varepsilon}{\Delta t} = \frac{(\Delta L/L_0)}{\Delta t} = \frac{\Delta L/(\Delta t)}{L_0} = \frac{\Delta V}{L_0}$$

*Note: where ε = strain, t = time, ΔV = the difference in velocities between two points of myocardial wall

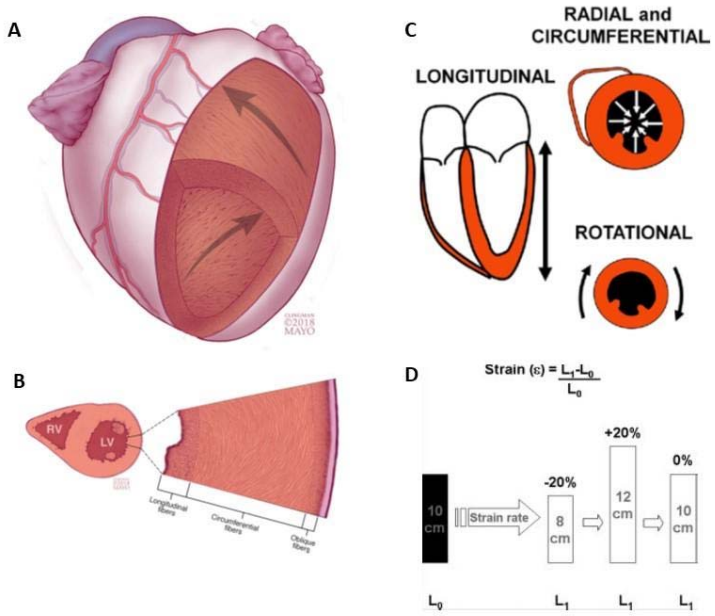

Figure 16. LV myocardium lining orientation and principal directions of strain. (A) The alignments of myocardial fibers like helical pattern. (B) A cross-sectional view of the LV myocardium demonstrates the layers of the myocardial fiber, longitudinal, circumferential, and oblique, respectively. (C) the directions or vectors of the LV strain. (D) The graphic that described strain assessment. Modified from (Abraham TP, 2007; Gorcsan J, 2011; Luis SA, 2019)

9.4.2.3.1 2D strain analysis (speckle-tracking echocardiography)

The 2D strain analysis or speckle-tracking echocardiography (STE) was introduced in the 2000s (Leitman M, 2004; Reisner SA, 2004; Ingul CB, 2005). STE is used to assess cardiac functions. STE was initiated with the recorded digital images from ultrasound in the B-mode and ECG into cine loops. The speckles occur from the scattering of the ultrasound wave with the structure, with the noise filtered out from the image maintaining the small features left which are speckles. The cine loops of the cardiac cycle could create specific speckle patterns from the myocardium movement. Specific software is used to track the speckles pattern frame to frame. The algorithm used quantifies some cardiac parameters such as strain, strain rate, displacement, and velocity directly from 2D ultrasound imaging (**Figure 17**). The STE is acquired from 2D images. The suggested resolution and quality are

approximately 40-80 frames per second (fps) for a normal heart in patients. However, the pre-clinical studies for the STE in animals such as rodents exhibiting a normal heart rate between 400-500 beats per minute need higher temporal resolution ultrasound to record cine loops 300-400 fps (Bauer M, 2011). The distinctive points of STE are global and segmental myocardial functions for giving informative data in the same analysis (**Figure 18**). The assessment of STE for cardiac function parameters (Leitman M, 2004; Mor-Avi V, 2011; Voigt J-U, 2015) as following:

Displacement

Displacement is the shortest traveled distance, which is observed in myocardium regions between epicardium and endocardium during the cardiac cycle. This displacement unit is presented in cm or mm.

Velocity

Velocity is the speed of monitored speckles moving during the cardiac cycle, presenting units in cm/s.

Strain

Strain is previously described, the change of deformation in displacement at myocardial segments. The strain is presented in percentage or fraction.

Strain rate

Strain rate as previously described; the strain dynamics change the length of myocardium per time unit. The strain rate unit is presented in s^{-1}.

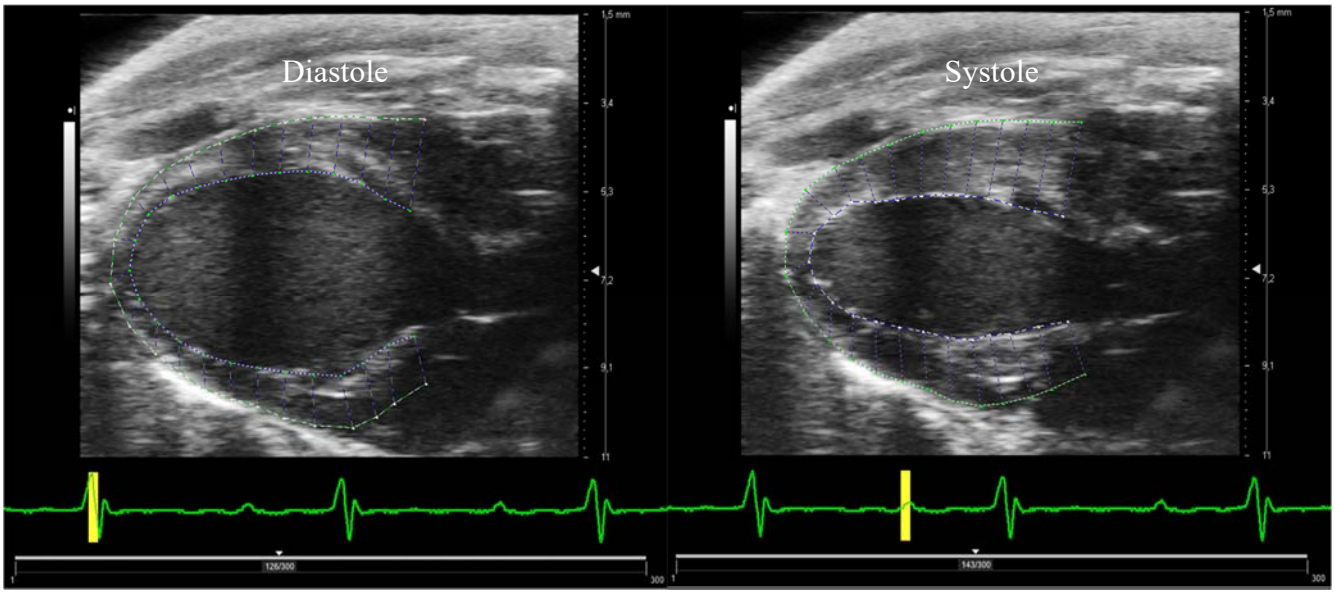

Figure 17. The figure shows the speckles-tracking selection of parasternal long-axis view – mice. (Left) The tracking of speckles between epicardium and endocardium during diastole. (Right) The tracking of speckles between epicardium and endocardium during diastole.

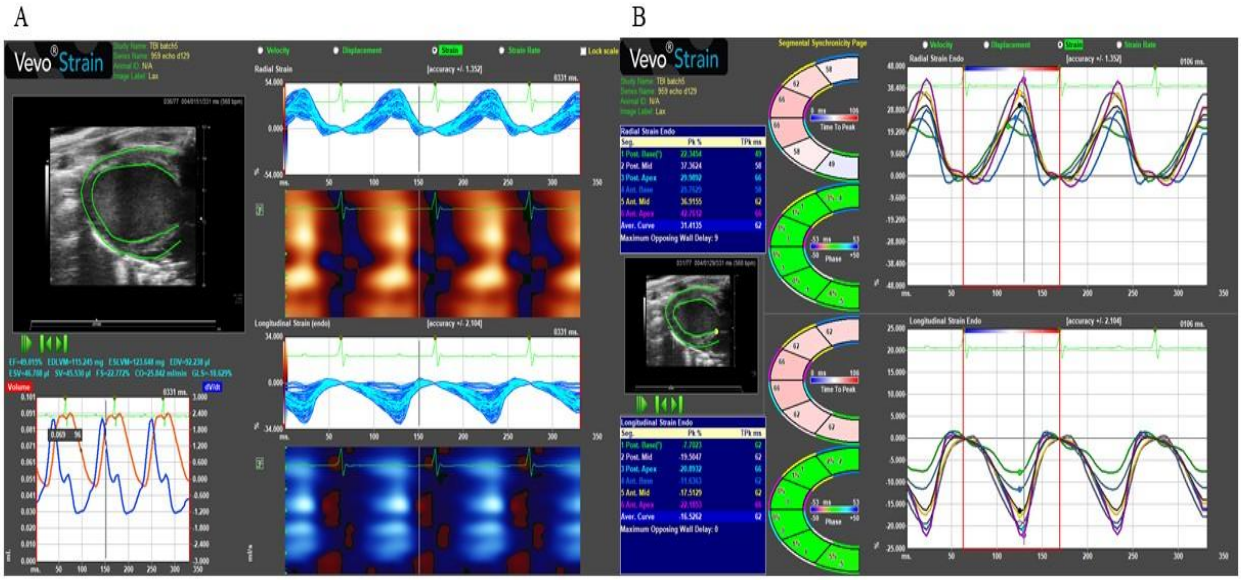

Figure 18. The Vevo strain software (VisualSonics) analysis of STE in parasternal long-axis view – mice. (Left) The global STE analysis provides the overview information for both basic cardiac functions and strain analysis during 3 cardiac cycles. (Right) The segmental STE analysis provides the data of myocardial movement in each segment, which could represent velocity, displacement, strain, and strain rate during 3 cardiac cycles.

a) The pitfalls of 2D STE

The insufficient tracking analysis at the border of the endocardium may be the problem with STE. The other major limitation is the sensitivity to shadows or artifacts that occur during the image recording, which could affect the deformation (strain) measurement (Mor-Avi V, 2011). The STE algorithm's limitation in defining the “normal” when the analysis unclearly indicated the border area between normal and dysfunctional regions will affect the segmental analysis. Moreover, the restriction of short-axis images could be an encounter with signal problems related to the dimension in systole. The LV movement is a rotation forward to the apex in systole that causes out-of-plane motion. The error in many regions in segmental strain analysis could directly introduce inaccurate global strain analysis (Mor-Avi V, 2011).

b) The pros and cons of 2D STE

The STE has the advantage to assess the motion in any plane or any direction of images. This point of STE allows measurement of radial and circumferential directions, which are disregarding the ultrasound wave direction. However, the STE is not free from all angles because the best resolution of the ultrasound image is better when in the same direction as the beam (Mor-Avi V, 2011). The 2D STE depends on the 2D ultrasound images recording which means that the quality of the images directly affects when analysis frame by frame, the out-of-plane motion could decrease the accuracy of the analysis (Mor-Avi V, 2011). The other limitation is the difference between commercial platforms and vendor software, which may be a problem with the cross-platform analysis. This issue was addressed by the American Society of Echocardiography and the European Association of Echocardiography.

9.4.3.2.2 4D strain analysis (4D STE)

Although 2D STE is widely used for evaluation of the LV function, limitations of the 2D STE are accuracy of quantification and plain of speckles tracking because of volumetric complexity motion of the heart contraction. The gated volumetric ultrasound overcomes the obstacles in geometric assumptions from the 2D STE (Hoole SP, 2008). The 4D image can generate more than 3,000 vectors/volume and the temporal resolution of real-time data sets is approximately 20-30 volumes/sec (Pérez de Isla L, 2009). The 4D imaging was developed pre-clinically for covering the restrictions introduced by the scanning-tracking motion of speckles in irrespective directions from ultrasound waves and constructing the heart in volume for measuring (Soepriatna AH, 2018; Damen FW, 2021). These important advantages might allow more potential and more accurate analysis of cardiac assessment (**Figure 19**).

a) The pitfalls of 4D STE

The main problems of analysis are related to consuming the time for acquisition of the image and stable collection of the ECG signal for gating with the corresponding image (Soepriatna AH, 2018).

b) The pros of 4D STE

The outstanding benefits of 4D STE cover the movement motion in geometric volume and a more accurate assessment of segmental analysis of Soepriatna with high spatiotemporal resolution (Soepriatna AH, 2018).

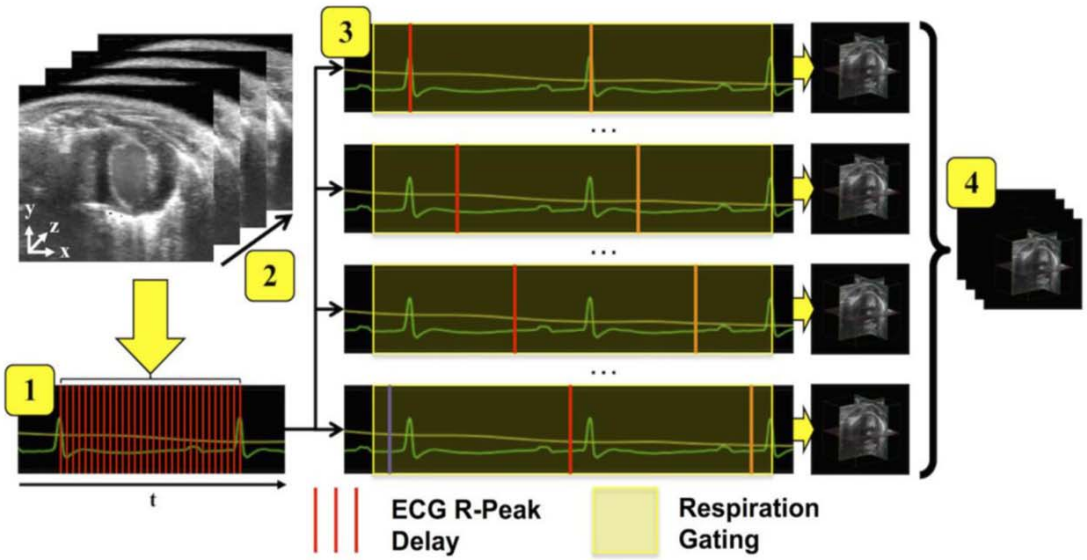

Figure 19. A schematic of the construct 4D imaging for speckles analysis in the mouse heart. The steps include 1) and 2) collecting the images by scanning from apex forward to the base and recording the ECG 3) combining the extracted frames from each cine loop, dependent on their timing within the cardiac cycles, to create 3D volumes at each respective time-point, and 4) temporally concatenating said volumes to create 4D datasets (Soepriatna AH, 2018).

The advantages and disadvantages of imaging techniques described above to assess the brain and the heart in clinical and/or preclinical studies are summarized in **Table 8.** However, US imaging has numerous advantages compared to other techniques. High resolution US is non ionizing, reproducible, fast, cost effective and reliable for cardiac measurement. Interestingly, the combination between US and PAI gives us the possibility to assess molecular imaging in the heart and the brain. These promising tools could provide more understanding of TBI and cardiac dysfunction.

Table 8. Comparison table of imaging techniques for accessing the heart and brain

Imaging technique	Model	Heart	Brain	Time	Cost	Ironizing radiation
❖ Ultrasound imaging	compatible with small animal model	1) fully accessible cardiac measurement both LV systolic and diastolic function 2) 4D cine loop	1) brain vessels structure 2) brain blood volume changes	low operations 5-15 mins/animal	1) low to medium purchase costs 2) low maintenance costs	-
❖Photoacoustic imaging	compatible with small animal model	1) heart tissue oxygen saturation 2) contrast agents or nanoparticle approaches	1) brain oxygen saturation 2) contrast agents or nanoparticle approaches	low operations 5-10 mins/animal	1) medium purchase costs 2) low maintenance costs	-
MRI	compatible with small animal model	1) morphology and LV function 2) strain analysis *limit in do both analysis in the same time	1) quality image for brain structure 2) contrast agents approach	medium operations 20 – 30 mins/animal	1) high purchase costs 2) medium maintenance costs	-
(μ)CT-SCAN	compatible with small animal model	1) morphology and LV function	1) quality image for brain structure 2) contrast agents approach	high operations 20 – 30 mins/animal	1) high purchase costs 2) medium maintenance costs	yes
PET, PET/MRI, PET/CT	compatible with small animal model	1) high biogenic sensitivity 2) measure cardiac function if combined with MRI or CT		high operations 30-60 mins/animal	1) high purchase costs 2) medium maintenance costs	yes

❖ ultrasound and photoacoustic imaging techniques could perform in the same machine platform.

Objective

Objective

My thesis project was to emphasize three research contents:

Firstly, we investigated the interaction between mTBI and cardiac dysfunction in the pediatric population via closed-head injury with long-term disorders (CHILD) in the juvenile mouse model. We have introduced the novel imaging techniques, 4D echocardiography, from our collaboration with Purdue University to evaluate the progression of mTBI and cardiac function. We intensively assess cardiac function in stress conditions by dobutamine stress which provides more information about the heart contractility. Finally, we are interested in the correlation between PAI brain imaging after mTBI affects the long-term cardiac dysfunction.

To determine correlation between jmTBI and cardiac dysfunction by ultrasound techniques in juvenile mice

We want to monitor in longitudinal study of jmTBI model which affect to cardiac dysfunction via echocardiography, PAI, and 4D-US.

We hypothesized that the TBI in the juvenile mice could be alteration the cardiac dysfunction during the growth development to adult.

The first, we performed the experiment setting to confirm the outcome of mTBI that affect cardiac dysfunction from the CHILD protocol (Rodriguez-Grande B, 2018; Ichkova A, 2020). The varies of impact parameters including velocity and depth were determined in juvenile mice and monitored the changes by photoacoustic imaging and echocardiography. Then, the jmTBI model was established for longitudinal study. The PAI was used to monitor the brain oxygen saturation post impact, meanwhile the echocardiography was used to assess the cardiac function, these measurements were simultaneously performed for evaluating the brain and heart changes. Additionally, the 4D-US was performed to assess the strain analysis, which will give the intensive results in cardiac function.

The monitoring of longitudinal study in jmTBI could be give the information about the changes of brain tissue oxygen level and reflect patterns of cardiac dysfunction, which might tell us about the linkages between brain and heart in this model.

Materials and Methodology

Materials and Methodology

1. Experimental animal

According to the European Directive (2010/63/EU), we conducted experiments and the French laws governing laboratory animal use. Local Ethics Committees approved the experiments (authorization #17133-2018101615211943 v3) and followed ARRIVE guidelines for animal reporting.

We obtained Swiss breeder mice from Janvier Labs (Le Genest-Saint-Isle, France) and bred pups in-house. All animals were maintained under an environmental control condition (21 ± 1 °C with 55± 1% humidity, and 12 h light/12 h dark cycle) and provided food-water at all times at animal house of Physiologie et médecine expérimentale du cœur et des muscle (PhyMedExp, Inserm1046, Montpellier, France). Only pup mice greater than 6 grams were used in this protocol.

All experiments were performed under anesthesia as described in the respective method parts, and all efforts were to reduce the animal's pain, suffering, and distress. The animals consisted of enrichment materials and standard bedding.

2. Juvenile mTBI model

The closed-head juvenile mild traumatic brain injury (jmTBI), we modified from the closed-head injury with long-term disorders (CHILD) model as previously described (Rodriguez-Grande B, 2018). Briefly, the perinatal (P) 17 pup mice were anesthetized using 2.5-3% isoflurane and 1.5 L/min air for 5 min and then placed on the aluminum foil sheet under the cortical controlled impactor (CCI) without head restraint. The lack of head restraint allowed for head rotation and limited the accumulation of focal damage. The aluminum foil supported the weight of the animal, and its free-form stereotactic frame also allowed a greater degree of rotation. We applied depilatory cream on the cranial area. We did not make a skin incision or perform a craniotomy to avoid surgical artifacts and limit severity of the TBI. The impact was

directly to the intact head of the mice. We performed the mTBI with a CCI (Leica Impact One Stereotaxic impactor, Leica Biosystems, Richmond, IL) with a 3 mm diameter round impactor tip. The various impact velocity was 2,3, and 6 m/s with a depth of 1,3, and 3 mm into the head, respectively. The tip impacted the left somatosensory parietal cortex 1.7 mm from bregma and 1.5 mm from midline. We anesthetized sham mice and performed an identical procedure without an impact. After that, we placed the mice in an empty cage for recovery, then returned them to housing cages. We record the time from anesthetization, preparation, time to stand, and time to explore for comparing the effect of mTBI (**Figure 20**).

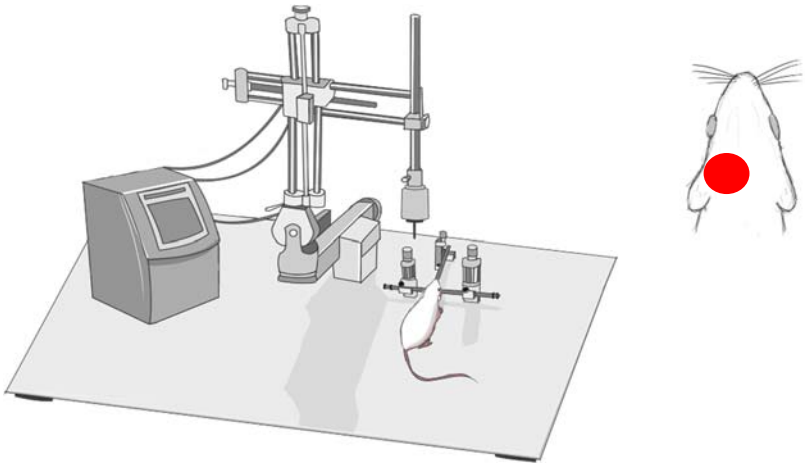

Figure 20. The schematic establishment TBI on the mouse under CCI impactor (red circle: area of impact)

These schematic timelines show the experimental designs of thesis:

Figure 21. jmTBI 1- establishment jmTBI with varies grade of impact

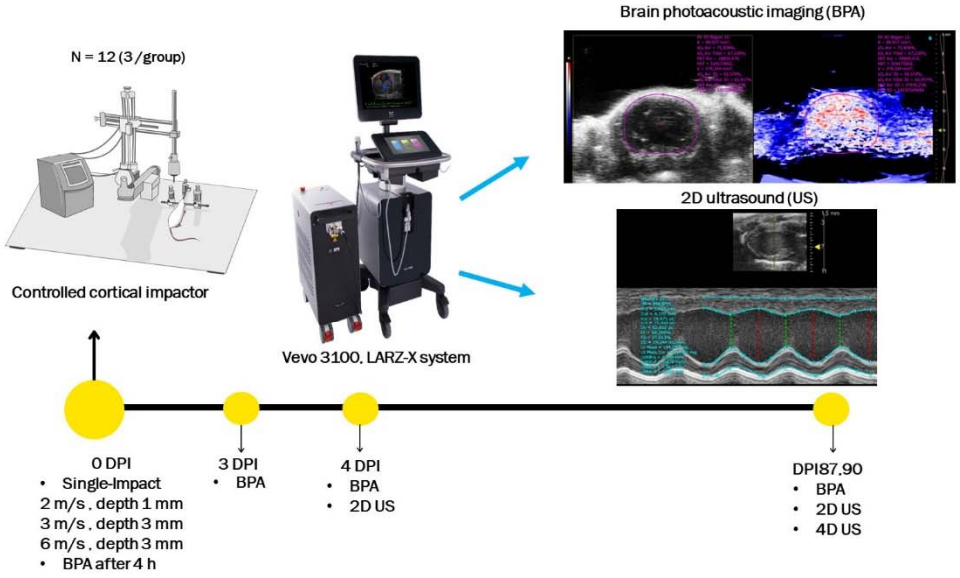

Figure 22. jmTBI 2- the longitudinal study

(selected grade of impact at 6 m/s, depth 3 mm)

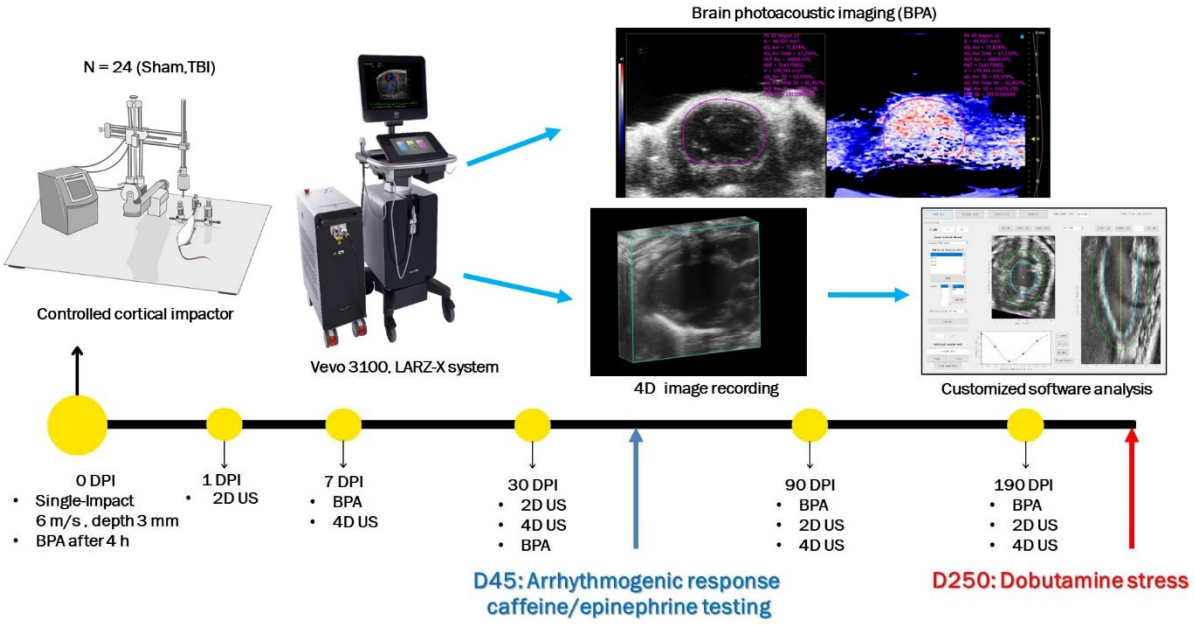

3. Photoacoustic imaging

3.1 Photoacoustic imaging for brain oxygen saturation

The level of cerebrovascular oxygenation for monitoring the animals after mTBI was measured by PAI. PAI is a combination of ultrasound and optical imaging for constructing functional and anatomical imaging. PAI has the possibility to detect optical absorption from endogenous contrasts consist of oxygenated and deo-oxygenated hemoglobin. Brain oxygen saturation imaging was monitored on the mice following above protocols. The PAI was performed by using a Vevo3100 LAZR-X imaging system and laser optical source Nd:YAG 680-2000 nm (FUJIFILM VisualSonics INC., Toronto, ON, Canada) and using a 15-30 MHz MX250D probe to assess brain tissue oxygenation. The mice were depilated hair on cranium surface before performed PAI. The animals were anesthetized with 2.5-3% isoflurane and placed on the heated platform in the prone position and maintained body temperature at 37°C. We centrifuged ultrasound gel to eliminate bubble artifacts and applied it to the cranium. The transducer probe combined two lines of 4 channels laser optic fiber were put on the gel and we performed scanning by slice steps in the horizontal axis from the occipital region to the frontal region of the brain (**Figure 23**). The PAI was used to measure parametric maps of oxygen saturation (sO2) by dual-wavelength at 750/850 nm. We adjusted the parameters toa PA gain of 40 dB, a 2D gain of 18 dB, an image depth of 22 mm, and an image width of 21 mm. The PAI recoding was setting acquisition motor and adjusted range of scanning 10 mm, step size 0.15 mm and adjusted depth of image 19 mm, width of image 16 mm, then recorded 4-5 min/session for creating 3D PAI approximately 70 frames. The 3D PAI image was composed of b-mode and optical images. The area of impact or region of interest (ROI) was manually defined based on the anatomic ultrasound images. We achieved offline quantitative image analysis in Vevo LAB (v5.5.1, FUJIFILM VisualSonics) to get measurements of mean and total oxygen saturation (sO2) and hemoglobin (HbT). The Mean sO2 indicates average blood

oxygenation within tissue factoring out measures of 0% sO2, while total sO2represents tissue oxygenation, including 0% sO2 measurements.

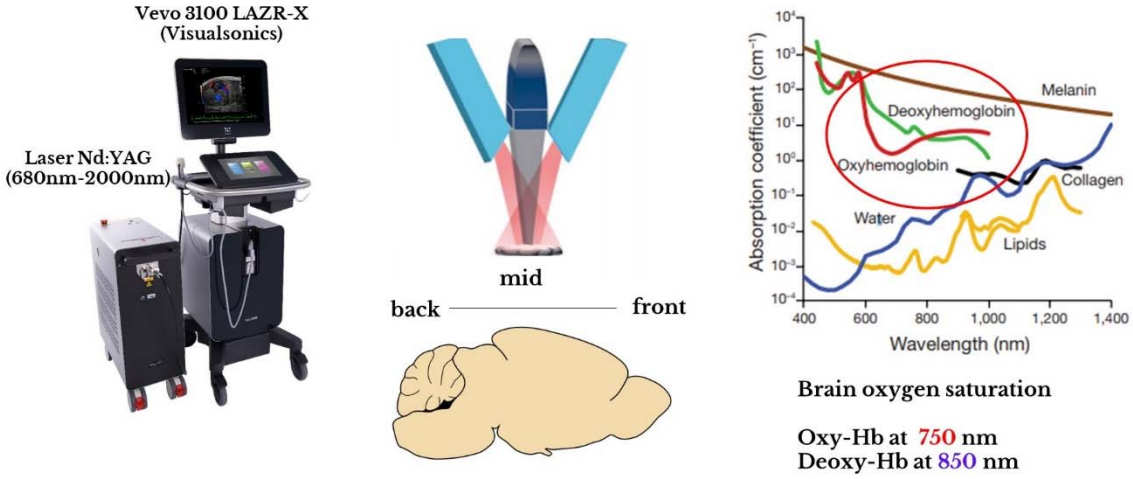

Figure 23. The schematic diagram PAI for monitoring brain oxygen saturation (Modified from FUJIFILM VisualSonics and (Weber J, 2016)

4. The cardiac measurement

We obtained high-resolution 2D and 4DUS data with the Vevo 3100 high-frequency ultrasound system (FUJIFILM VisualSonics) using a 40 MHz center frequency MX550D probe to assess left ventricular function. We anesthetized mice with 2.5 -3% isoflurane at 2.0 mL/min, and the body temperature was controlled with a heating pad. We secured the mice to a stage for imaging, and the ventral thorax hair was depilated. The ECG and respiratory rate were monitored throughout the imaging process.

4.1 2D Ultrasound imaging

We assessed cardiac functions measurement for monitoring the animals after mTBI model. We performed following the American Physiological Society guidelines for cardiac measuring in mice (Lindsey ML, 2018). We obtained multiple views of parasternal short (PSAX) and long axis (PSLAX) were used to assess Left Ventricle (LV) wall thickness at the intraventricular septum and posterior wall, LV volume calculated from Simpson's method of disks and the LV ejection fraction calculated by (LV end diastolic – end systolic volume) /LV end diastolic volume

both b-mode and m-mode. We performed longitudinal strain under long axis view and circumferential strain under short axis. We obtained a four-chamber in b-mode view was used to assess at mitral valve (MV) leaflet for MV flow and MV tissular doppler which measured Isovolumic Relaxation Time (IVRT), peak early filling (E wave), late diastolic filling (A wave), E/A ratio and peak early filling to early diastolic mitral annular velocity (E') as E/E' ratio (Schnelle M, 2018). The offline image analysis was conducted in Vevo Lab Software 5.5.1. (FUJIFILM VisualSonics).

4.2 4D Ultrasound imaging

We assessed 4US by using attached probe with a linear step motor scanning in the parasternal short axis (PSAX) view from below the apex to above the aortic arch. We adjusted acquisition parameters as following gain 48 dB, 3D ranges 12 mm, 3D steps size 0.08 mm, and approximately 300 frames/sec, which used total recording time 10-15 min to create a 4D image that corresponded with the cardiac cycle from base to apex. The 4DUS dataset was submitted to the customized and developed interactive toolbox in MATLAB 2021a (MathWorks Inc., Natick, MA, USA) (**Figure 24**).

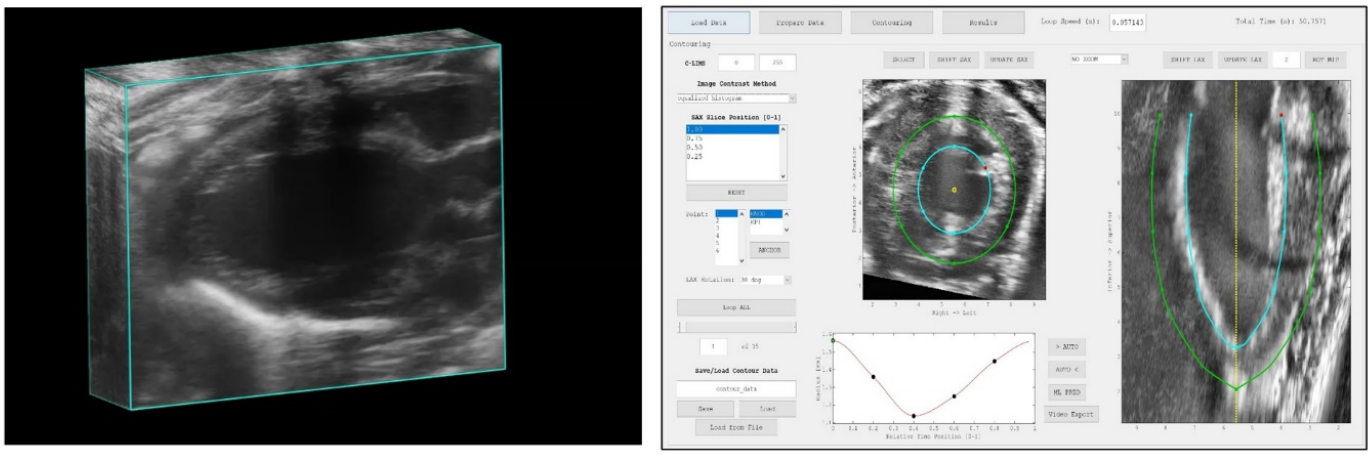

Figure 24. The 4D imaging assessment: 4DUS image dataset and Interface of customized and developed MATLAB software

5. 4D ultrasound and photoacoustic imaging for cardiac oxygen saturation in dobutamine stress test

We performed the assessment of heart functions and structures under the mimic effect of exercise on the heart by dobutamine stress. At day 250 post-impact, we anesthetized the animals as previously described and performed 4DUS to record baseline cardiac function. Then, we performed an intraperitoneal injection (IP) of dobutamine (4.5 μg/g body weight) on each animal. We conducted 4DUS 15 min after IP once the animal reached the plateau phase of induced stress (Salami CO, 2020).

For the level of cardiac tissue oxygenation was measured as previous described in PAI in the brain tissue. We used PAI to record cardiac perfusion of the heart at baseline and 15 min after administration of dobutamine. PAI acquisition was combined with ECG-gated kilohertz visualization (EKV). We adjusted imaging parameters to PA gain of 40 dB, 2D gain of 18 dB, image depth of 22 mm, image width of 21 mm, high PAI sensitivity, and standard acquisition with EKV 250 Hz. We recorded 4-5 min/session for creating PAI image approximately 150 frames. The anterior myocardial wall was manually defined based on the anatomic ultrasound images. The offline image analysis was conducted in Vevo Lab Software 5.5.1.

6. 4D Ultrasound data strain analysis

We conducted the strain analysis using a 4D Strain Toolbox (**Figure 24**). This custom software enables the visualization and quantification of 4DUS data to produce a 3D strain map over an entire cardiac cycle (Damen FW, 2021; Dann MM, 2022). We first oriented the 4D images and centered them to PLAX, SAX, and coronal views of the left ventricle. Endocardial boundaries were set at peak systole and diastole for the apex and base. Then, we added automated endo-and epicardial contours to the images based on initial estimates. We manually adjusted the contours over the cardiac cycle using four SAX planes and three PLAX planes. Next, the software created a 4D mesh of the contours from which measurements of global

cardiac function (e.g., ejection fraction, stroke volume) and regional function (strain, volume) can be extracted. The cardiac regions included the anterior free wall, anterior septum, posterior septum, posterior, and posterior free wall. The peak strain, systolic strain rate, early diastolic strain rate, and late diastolic strain rate were calculated for each region and then averaged into global strain metrics.

7. Statistical analysis

All values were expressed as Mean ± SD. All comparisons involving more than one group were assessed for significance using one-way analysis of variance (ANOVA), followed when appropriate by the Bonferroni test. The statistical tests were performed using commercially available software Prism version 9.3(GraphPad Software, San Diego, CA, USA. A *p*-value less than 0.05 was considered statistically significant and levels of significance were depicted as $*p < 0.05$, $**p < 0.01$, and $***p < 0.001$.

Results

Results

The longitudinal study for monitoring and evaluating brain tissue oxygen saturation and cardiac function after mTBI in a juvenile mouse model

Context

TBI causes brain tissue injury and hypoxia following secondary injury, which could affect peripheral organs such as the heart. Significantly, the mTBI in the pediatric population was taken less care of when the clinical appearance was not found, which could be an unnoticed problem in the future. The CT scan, clinical questionnaires, and observations might be inadequate (Lumba-Brown A, 2018). The PAI and US are potent tools and promise to assess both brain and heart complications in jmTBI. However, these tools are not routinely used in clinical approaches. However, convenient and efficient tools are to be desired.

This study aimed to test the combination techniques in ultrasound platforms to monitor jmTBI over time, which are PAI for assessing brain oxygen saturation in the brain and the 2D and the 4D US for evaluating cardiac function in the heart for the long term. We hypothesized that mTBI induces localized brain hypoxia that influences the trajectories of cardiac function.

To summarize, we show quantitative correlations between the initial decline in cerebrovascular oxygenation and cardiac diastolic dysfunction observed long-term in the same animal and, over time, extending to negative adaptations during an extra-physiological cardiac challenge. We report specific long-term behavioral adaptations that are mouse-specific and cross-correlate with PAI read-outs. Collectively, this data establishes a direct link between early cerebrovascular hypoxia occurring after mTBI in juvenile mice and cardiac maladaptation that persist into adulthood.

Discussions

Discussion

mTBI in pediatrics followed by cardiac dysfunction in adulthood

In this work, we have demonstrated that cerebrovascular hypoxia after juvenile mild traumatic brain injury correlates with chronic cardiac and cognitive dysfunctions. Our research highlights that mTBI induces diastolic dysfunction characterized by preserved ejection fraction in juvenile mice. The response of a TBI heart to stress conditions revealed global and regional LV dysfunction. More importantly, our data suggest that the short-term hypoxic brain tissue after mTBI correlates with long-term cardiac dysfunction. Our data also show the efficacy of a combination between PAI and 4D-US high-resolution ultrasound in evaluating both brain and heart during post-TBI disease progression.

Previous studies showed the involvement of TBI and cardiac dysfunction both in the short and long term, focusing on moderate to severe TBI both in pre-clinical and clinical models as we summarized (**Tables 6 & 7**). Although the clinical studies included approximately 30-40% of mTBI, a lack of evidence suggests that mTBI individually affects cardiac dysfunction. Recently, Izzy *et al.* reported that mTBI, from moderate to severe forms, is associated with a risk to promote cardiovascular disease, in addition to endocrine, neurological and psychotic disorders (Izzy S, 2022). A study of the European pediatric population reported a year of loss of about 184.4 per 100000 due to TBI, demonstrating the burden problems of TBI (Majdan M, 2022). Clinical studies have shown that severe TBI in pediatric patients also affects cardiac dysfunction such as decreased LVEF, RWMA (Krishnamoorthy V, 2015) and increased cTnI (Lele AV, 2020). Here, we showed the consequences of mTBI with acute brain tissue hypoxia in a juvenile mouse model after several months. The major cardiac consequence is diastolic dysfunction with preserved EF by altering LV mass, LA volume, IRVT, and early diastolic strain rate.

Takotsubo cardiomyopathy is known as the '*stress heart disease'* that occurs from catecholamine surge following acute emotional or physical stress, thereby causing reversible LV wall motion abnormality with specific heart morphology changes. Gruhl *et al.* reported that post-moderate to severe TBI patients exhibited RWMA with reduced EF of less than 55%, systolic dysfunction, and morphology abnormality (Gruhl SL, 2022). However, in contrast, our results showed no change in cardiac morphometry when comparing PSV, EDV, and LV mass in the jmTBI group. Moreover, the cardiac systolic function is preserved in this model.

Interestingly, relying on the algorithm used for evaluation of the diastolic dysfunction in the murine model (**Figure 14**; also, (Schnelle M, 2018), we interpret our results as reflecting usual chronic diastolic dysfunction with increased LA area and abnormal chronic diastolic function (prolonged IVRT and decreased rLSR). Our results match those of Cuisinier *et al.* who showed no changes in systolic function but genuine diastolic function alteration in clinical adult patients by IVRT elongation and RWMA (Cuisinier A, 2016). Additionally, Chaikittisilpa *et al.* and Krishnamoorthy *et al.* reported both systolic and diastolic dysfunction with RWMA occurring within hours and reverting to baseline in a week after moderate to severe TBI in the adult population (Chaikittisilpa N, 2018; Krishnamoorthy V, 2020). In our preclinical work, our results suggest the development of chronic diastolic dysfunction after mTBI in juvenile mice. Further, clinical investigation in the pediatric population is needed to validate or not our preclinical data.

The shreds of evidence of non-neurologic organ failure were found in the patients with severe TBI, which includes cardiovascular dysfunction and failure (Ramtinfar S, 2016). Interestingly, myocardial O2 consumption (MVO2) is increased in heart failure with preserved ejection fraction (HFpEF) (AbouEzzeddine OF, 2019). We investigated this possibility by using dobutamine stress tests to increase heart rate and O2 consumption from the heart. In our conditions, compared to sham animals, the mTBI mice failed to respond correctly to the

dobutamine challenge. Consistently, Nomad *et al.* work showed an impaired contractile function of the myocardium when stimulated with dobutamine in HFpEF patients (Norman HS, 2011). Additionally, Van Empel *et al.* and Houstis *et al.* demonstrated that HFpEF encounters oxygen transport and utilization pathway defects in the myocardium during stress conditions with exercise (van Empel VPM, 2014; Houstis NE, 2018). Our data support the idea that mTBI in pediatrics contributes to contractility impairment and increase oxygen consumption when responding to stress conditions in adulthood.

The interaction between brain and heart in TBI is currently under investigation, especially focusing on the mechanisms that could affect the non-injury peripheral organs. One of the theories is that neuroinflammation after TBI could induce low-grade chronic and systemic inflammation. This low-grade systemic inflammation may affect both the brain and heart from the organ level to the cellular level (Chang JJJ, 2009; McDonald SJ, 2020). Zhao *et al.*'s work supported the view that splenectomy after moderate-severe TBI for one month improves cardiac function, reduces fibrosis, and decreases the number of invasive immune cells in the heart (Zhao Q, 2019). In this direction, MAPKs could play a major role in neuro-cardiovascular communication. MAPKs are known to regulate various cellular functions including inflammation, immunity response, cell death/survival, proliferation, and differentiation (Otani N, 2011; Bourgeois-Tardif S, 2021). The p38α MAPK activation has an important noxious role in cardiac function (Jacquet S, 2008; Sicard P, 2010; Kumphune S, 2010; DeNicola GF, 2013; Lucas A, 2015) and for microglia (brain macrophage) by releasing pro-inflammatory cytokines after TBI (Bachstetter AD, 2013; Morganti JM, 2019). Chu *et al.*'s work showed evidence of systemic inflammation after splenectomy in the severe TBI model, down-regulated MAPK (p-p38 MPAK and p-ERK), and NF-κB-mediated decrease if pro-inflammatory cytokines levels (Chu W, 2013). Future extensive work is warranted to evaluate the communication role of MAPK between the brain and the heart after injury.

Apart from the physical injury and consequences that affect peripheral organs, mTBI is the major cause of post-concussive symptoms after injury for several months followed by long-term behavior problems such as social and learning problems (Keightley ML, 2014). Recently, Ledoux *et al.* 's work supported the notion that the pediatric mTBI population is associated with a higher risk of mental health issues, psychiatric hospitalization, and self-harm (Ledoux AA, 2022). In the pre-clinical setting, Griffiths *et al.* 's work showed that mTBI correlates with the impairment of cognitive function and cerebrovascular function after 6 months in the FPI rat model (Griffiths DR, 2022). Previously, Rodriguez-Grande *et al.* 's work reported that long-term behavioral deficits consisting of cognitive features, motor and exploration/anxiety are observed with a protocol similar to ours (Rodriguez-Grande B, 2018).

Biomarkers imaging for assessment of TBI and cardiac dysfunction

Neuroimaging is the first diagnostic tool to assess TBI after injury consisting of CT scanning and MRI. However, most mTBI patients have not found significant anatomical modification in neuroimaging (Bigler ED, Abildskov TJ, 2016). For this reason, mTBI may receive inappropriate medical care, especially in the pediatric population (Lumba-Brown A, 2018). In this study, we showed that PAI and US could evaluate the brain tissue hypoxia in mTBI by using the sO2 and hemoglobin intensity, which could be assessed and monitored hours after injury for several months. These results corresponded to those of Ichokova *et al*. showing decreased cerebrovascular oxygen saturation in mTBI six hours after impact by using PAI imaging (Ichkova A, 2020). The potential of PAI imaging to detect the sO2 in the brain is widely used in pre-clinical studies (Guevara E, 2013; Lv J, 2020; Qiu T, 2021). Moreover, hemodynamic and vascularization can be performed in real-time (Yao J, 2022). Beyond the pre-clinical setting, photoacoustic computed tomography (PACT) and ultrafast ultrasound imaging demonstrate high efficiency, which allows for constructing the vascularization,

hemodynamics patterns, and measuring sO2 in the human brain (Demené C, 2021; Na S, 2022). The other non-invasive technique, near-infrared spectroscopy (NIRS) can also measure regional brain oxygen saturation, but limit the area of detection (Barud M, 2021). The PAI imaging shows great promise to be a novel technique for brain sO2 measurement, hemodynamics, and vessel structure, which is greater than other techniques **(Table 8)**, especially the gold standard as the cerebral metabolic rate of oxygen (CMRO2) in PET (Ssali T, 2018), because non-radiation ionizing, less time-consuming, and more accessible. However, the challenge for PAI imaging is the ability to penetrate the human skull, due to the thickness (>7mm) and the complexity of skull structure could block both light and sound signals from transcranial brain imaging (Manwar R, 2020). Additionally, Zhao et al used the PAI systems with nanosecond laser power sources, the penetration of light also struggles at a few centimeters of depth through the human skin in the clinical setting (Zhao T, 2019). The development of the US probe and higher energy of the laser still need more investigation to reach the capacity for TBI clinical usage. Interestingly, the combination of PAI and US was approved to perform in the clinical application in breast cancer, which offers a promising alternative to other strategies in the future (Kratkiewicz K, 2022).

To enhance the performance of US/PAI, researchers have developed several exogenous contrast agents such as carbon-based nanomaterial. Recently, Jiang et al. ‘s work showed that the use of nanoparticle-based photoacoustic nano-transducers (PANs) with NIR-II dyes could stimulate neuronal modulation at both the cellular level and the murine model (Jiang Y, 2021). For cell targeting purposes, Liu et al. reported that the construction of Croconaine-based NPs coupled with CR780 dyes (CR780RGD-NPs) could specifically detect brain tumors in a murine model (Liu N, 2021). Additionally, the NPS has been used to increase sensitivity and precision for sO2 in the stroke murine model by generating biodegradable MnCO3@BSA-ICG NPs as an exogenous contrast (Song G, 2022). The multi-usage of NPs to improve the capability of

PAI could be the alternative approach to adapting to TBI. In our collaboration with the University of Toulouse, we attempt to develop various NPs for increasing the power of the detection of PAI (**Figure 27**). On our hand, NPs showed the capacity for improving the signal of both PAI and US. The next interesting experiment could be investigated and developed to detect NPs in the phantom and pre-clinical models, revealing intensive information rather than in-vitro study.

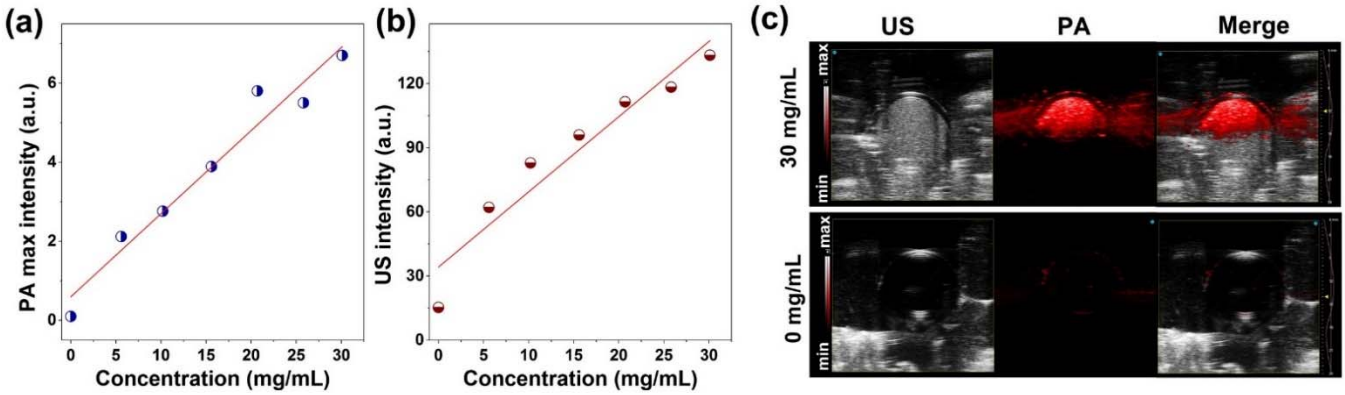

Figure 25. PAI and US luminescence imaging one of NPs ($Gd_{0.8}Nd_{1.2}O_2S$ NPs). Plot of PA (A) and US (B) intensities as detection of NPs concentration from 0-30 mg/mL. (C) Comparison images obtained under PA, US, and merge channels for NPs of concentrations 0 and 30 mg/mL. (In-preparation for publication)

The other challenge is the possibility to use brain oxygenation for discriminating TBI alignment as a GCS score. Here, we showed a decrease of 8% of brain sO2, in line with Ichokova *et al*'s work showing a 15% decrease after mTBI (Ichkova A, 2020) at 3m/sec. Combine together, these results support the idea that the high-resolution ultrasound coupled with PAI could be used to evaluate cerebrovascular oxygen saturation and molecular changes in mTBI in pre-clinical settings.

PAI and the US could also be used to study the heart. David *et al*.' showed decreased sO2 in multi-organs (brain, heart, kidney, liver) by using PAI after myocardial infarction,

which correlated with cardiac dysfunction with reduced LVEF and GLS (David H, 2020). This evidence enlightens that PAI assessment for sO2 in the brain-heart and US imaging for cardiac function might be a powerful tool to evaluate during brain-heart interaction. Generally, US imaging is used to assess cardiac function by measuring LV performance with various parameters during systole and diastole (Thomas JD, 2006). For the last decades, strain analysis or STE from 2D US imaging has emerged as a valuable method to quantify regional myocardial function and improve understanding of systolic and diastolic function (Gorcsan J, 2011). However, the conventional 2D STE requires geometric assumptions for accurate LV function calculation since the disease's asymmetric heart morphology could affect the measurement (Dawson D, 2004; Yuan L-J, 2011). Here, we established a collaboration with Dr. Craig GOERGEN's team at Purdue University (USA) to use the 4D STE for assessing cardiac dysfunction after long-term mTBI. The 4D (3-Dimensional + Time) could be performed to measure cardiac function with improved accuracy and precision in high-spatiotemporal resolution, especially acquisition time for constructing images when compared to the gold standard method of MRI (Damen FW, 2017). Recently, Dann *et al* 's work showed that the advantages of 4D STE are greater than 2D with histological analysis and corrected strain analysis in MI murine model (Dann MM, 2022).

The perspective of PAI and US imaging could determine the brain and heart function in one platform by non-invasive, non-ionizing, and less time-consuming approaches, which might give promise to biomarker imaging of TBI, especially in pediatric mTBI. However, the properties of biomarker imaging still need more investigation further both in pre-clinical and clinical settings.

Even so, the PAI and US imaging show the capabilities to detect endogenous contrast agents like deoxyhemoglobin and oxy-hemoglobin for assessing the sO2, which demonstrate

in this study. These agents are poorly detected if they are at a depth of more than 10 mm (Jiang Y, 2017). The NPs could be a novel approach, increasing the capabilities of PAI.

Limitations

Even though our results show that diastolic dysfunction is the consequence of mTBI in the juvenile mouse model, our results cannot be directly extrapolated to the pediatric population. Additionally, humans and murine have differences in terms of size, metabolic rate, life history, and microenvironment which might affect the responses to the injury (Perlman RL, 2016). The other factor is sex matter. In our study, we performed experiments on both male and female mice. The heart-brain interaction depends on complex multisystem interactions consisting of the vascular system, neurohormonal system, immune system, and inflammation, which are differently affected by sex (Rossi A, 2022). This could be one reason impacting various results of cardiac dysfunction after mTBI. We use the closed-head TBI model with restraint to introduce a greater degree of variability that could reflect the real clinical setting of TBI in humans (Rodriguez-Grande B, 2018). However, it might be the cause of variation in decreased sO2 even if performed in a similar protocol. Over these conflicts, the usage murine TBI model contains advantages such as convenience and reproducibility (Wiegand TLT, 2021). As mentioned, we support long-term diastolic dysfunction after mTBI which is brain-heart interaction in disease conditions. The underlying mechanisms are still inadequately investigated, which are two main streams autonomic dysregulation and systemic inflammation (McDonald SJ, 2020).

Conclusion

In conclusion, this study reveals that mTBI contributes to brain hypoxia in the short term and promotes diastolic dysfunction with preserved ejection fraction in the long term, which was detected by high-resolution 2D-4D US and PAI in the juvenile mouse model.

Additionally, the dobutamine stress unraveled systolic cardiac dysfunction and impaired LV myocardium oxygen consumption after several months. Lastly, initial hypoxia correlated with cardiac alteration, and multivariate analyses elucidate comprehension in this interaction, which might be helpful in the clinical decision. In perspectivity, we encourage the future development of US and PAI imaging into biomarkers imaging for the cerebrovascular and cardiovascular in clinical approaches.

References

References

AbouEzzeddine OF, Kemp BJ, Borlaug BA, Mullan BP, Behfar A, Pislaru SV, Fudim M, Redfield MM [Margaret M.], Chareonthaitawee P (2019). Myocardial Energetics in Heart Failure With Preserved Ejection Fraction. *Circulation. Heart Failure*, *12*(10), e006240. https://doi.org/10.1161/CIRCHEARTFAILURE.119.006240

Abraham TP, Dimaano VL, Liang H-Y (2007). Role of tissue Doppler and strain echocardiography in current clinical practice. *Circulation*, *116*(22), 2597–2609. https://doi.org/10.1161/CIRCULATIONAHA.106.647172

Aggarwal M, Zhang J [Jiangyang], Mori S (2012). Magnetic Resonance Imaging of the Mouse Brain, 473–488. https://doi.org/10.1016/B978-0-12-369497-3.10015-9

Ahmad A, Crupi R, Impellizzeri D, Campolo M, Marino A, Esposito E, Cuzzocrea S (2012). Administration of palmitoylethanolamide (PEA) protects the neurovascular unit and reduces secondary injury after traumatic brain injury in mice. *Brain, Behavior, and Immunity*, *26*(8), 1310–1321. https://doi.org/10.1016/j.bbi.2012.07.021

Akashi YJ, Goldstein DS, Barbaro G, Ueyama T (2008). Takotsubo cardiomyopathy: A new form of acute, reversible heart failure. *Circulation*, *118*(25), 2754–2762. https://doi.org/10.1161/CIRCULATIONAHA.108.767012

Amyot F, Arciniegas DB, Brazaitis MP, Curley KC, Diaz-Arrastia R, Gandjbakhche A, Herscovitch P, Hinds SR, Manley GT, Pacifico A, Razumovsky A, Riley J, Salzer W, Shih R, Smirniotopoulos JG, Stocker D (2015). A Review of the Effectiveness of Neuroimaging Modalities for the Detection of Traumatic Brain Injury. *Journal of Neurotrauma*, *32*(22), 1693–1721. https://doi.org/10.1089/neu.2013.3306

An C, Jiang X, Pu H, Hong D, Zhang W [Wenting], Hu X, Gao Y (2016). Severity-Dependent Long-Term Spatial Learning-Memory Impairment in a Mouse Model of Traumatic Brain Injury. *Translational Stroke Research*, *7*(6), 512–520. https://doi.org/10.1007/s12975-016-0483-5

Anderson, V., Catroppa, C., Morse, S., Haritou, F., & Rosenfeld, J. (2005). Attentional and processing skills following traumatic brain injury in early childhood. Brain injury, 19(9), 699–710. https://doi.org/10.1080/02699050400025281 [Add to Citavi project by DOI]

Andkhoie M, Meyer D, Szafron M (2018). Factors underlying treatment decision-making for localized prostate cancer in the U.S. And Canada: A scoping review using principal component analysis. *Canadian Urological Association Journal = Journal De L'association Des Urologues Du Canada*, E220-E225. https://doi.org/10.5489/cuaj.5538

Armstead WM, Vavilala MS (2019). Cerebral Perfusion Pressure Directed-Therapy Modulates Cardiac Dysfunction After Traumatic Brain Injury to Influence Cerebral Autoregulation in Pigs. *Neurocritical Care*, *31*(3), 476–485. https://doi.org/10.1007/s12028-019-00735-2

Atkins CM, Cepero ML, Kang Y, Liebl DJ, Dietrich WD (2013). Effects of early rolipram treatment on histopathological outcome after controlled cortical impact injury in mice. *Neuroscience Letters*, *532*, 1–6. https://doi.org/10.1016/j.neulet.2012.10.019

Ay H, Koroshetz WJ, Benner T, Vangel MG, Melinosky C, Arsava EM, Ayata C, Zhu M, Schwamm LH, Sorensen AG (2006). Neuroanatomic correlates of stroke-related myocardial injury. *Neurology*, *66*(9), 1325–1329. https://doi.org/10.1212/01.wnl.0000206077.13705.6d

Bachstetter AD, Rowe RK, Kaneko M, Goulding D, Lifshitz J, van Eldik LJ (2013). The p38α MAPK regulates microglial responsiveness to diffuse traumatic brain injury. *The Journal of Neuroscience : The Official Journal of the Society for Neuroscience*, *33*(14), 6143–6153. https://doi.org/10.1523/JNEUROSCI.5399-12.2013

Bailes JE, Dashnaw ML, Petraglia AL, Turner RC (2014). Cumulative effects of repetitive mild traumatic brain injury. *Progress in Neurological Surgery*, *28*, 50–62. https://doi.org/10.1159/000358765

Bajwa NM, Halavi S, Hamer M, Semple BD, Noble-Haeusslein LJ, Baghchechi M, Hiroto A, Hartman RE, Obenaus A [André] (2016). Mild Concussion, but Not Moderate Traumatic Brain Injury, Is Associated with Long-Term Depression-Like Phenotype in Mice. *PloS One*, *11*(1), e0146886. https://doi.org/10.1371/journal.pone.0146886

Bamira D, Picard MH [M. H.]. (2018). Imaging: Echocardiology—Assessment of Cardiac Structure and Function. In *Encyclopedia of Cardiovascular Research and Medicine* (pp. 35–54). Elsevier. https://doi.org/10.1016/B978-0-12-809657-4.10953-6

Barlow KM, Crawford S, Brooks BL, Turley B, Mikrogianakis A (2015). The Incidence of Postconcussion Syndrome Remains Stable Following Mild Traumatic Brain Injury in Children. *Pediatric Neurology*, *53*(6), 491–497. https://doi.org/10.1016/j.pediatrneurol.2015.04.011

Barud M, Dabrowski W, Siwicka-Gieroba D, Robba C, Bielacz M, Badenes R (2021). Usefulness of Cerebral Oximetry in TBI by NIRS. *Journal of Clinical Medicine*, *10*(13). https://doi.org/10.3390/jcm10132938

Basu R, Oudit GY, Wang X [Xiuhua], Zhang L [Liyan], Ussher JR, Lopaschuk GD, Kassiri Z (2009). Type 1 diabetic cardiomyopathy in the Akita (Ins2WT/C96Y) mouse model is characterized by lipotoxicity and diastolic dysfunction with preserved systolic function. *American Journal of Physiology. Heart and Circulatory Physiology*, *297*(6), H2096-108. https://doi.org/10.1152/ajpheart.00452.2009

Bauer M, Cheng S, Jain M, Ngoy S, Theodoropoulos C, Trujillo A, Lin F-C, Liao R (2011). Echocardiographic speckle-tracking based strain imaging for rapid cardiovascular phenotyping in mice. *Circulation Research*, *108*(8), 908–916. https://doi.org/10.1161/CIRCRESAHA.110.239574

Bell AG (1880). On the production and reproduction of sound by light. *American Journal of Science*, *s3-20*(118), 305–324. https://doi.org/10.2475/ajs.s3-20.118.305

Beschorner R, Simon P, Schauer N, Mittelbronn M, Schluesener HJ, Trautmann K, Dietz K, Meyermann R (2007). Reactive astrocytes and activated microglial cells express EAAT1, but not EAAT2, reflecting a neuroprotective potential following ischaemia. *Histopathology*, *50*(7), 897–910. https://doi.org/10.1111/j.1365-2559.2007.02703.x

Bigler ED (2016). Systems Biology, Neuroimaging, Neuropsychology, Neuroconnectivity and Traumatic Brain Injury. *Frontiers in Systems Neuroscience*, *10*, 55. https://doi.org/10.3389/fnsys.2016.00055

Bigler ED, Abildskov TJ, Goodrich-Hunsaker NJ, Black G, Christensen ZP, Huff T, Wood D-MG, Hesselink JR, Wilde EA, Max JE (2016). Structural Neuroimaging Findings in Mild Traumatic Brain Injury. *Sports Medicine and Arthroscopy Review*, *24*(3), e42-52. https://doi.org/10.1097/JSA.0000000000000119

Blackwell, L S., Ono, K E., & Howarth, R. (2016, May 30). Acute and Long-Term Outcomes Following Pediatric Traumatic Brain Injury. Thieme Medical Publishers (Germany), 05(01), 026-031. https://doi.org/10.1055/s-0036-1584285

Boerckel JD, Mason DE, McDermott AM, Alsberg E (2014). Microcomputed tomography: Approaches and applications in bioengineering. *Stem Cell Research & Therapy*, *5*(6), 144. https://doi.org/10.1186/scrt534

Borg J, Holm L, Cassidy JD, Peloso PM, Carroll LJ, Holst H von, Ericson K (2004). Diagnostic procedures in mild traumatic brain injury: Results of the WHO Collaborating Centre Task Force on Mild Traumatic Brain Injury. *Journal of Rehabilitation Medicine*(43 Suppl), 61–75. https://doi.org/10.1080/16501960410023822

Bourgeois-Tardif S, Louis De Beaumont, José Carlos Rivera, Sylvain Chemtob, Alexander G Weil (2021). Review Article. *Economica*, *70*(280), 691–697. https://doi.org/10.1046/j.0013-0427.2003.00027.x

Boutagy NE, Wu J, Cai Z, Zhang W [Wenjie], Booth CJ, Kyriakides TC, Pfau D, Mulnix T, Liu Z, Miller EJ, Young LH, Carson RE, Huang Y [Yiyun], Liu C [Chi], Sinusas AJ (2018). In Vivo Reactive Oxygen Species Detection With a Novel Positron Emission Tomography Tracer, 18F-DHMT, Allows for Early Detection of Anthracycline-Induced Cardiotoxicity in Rodents. *JACC. Basic to Translational Science*, *3*(3), 378–390. https://doi.org/10.1016/j.jacbts.2018.02.003

Bretzin AC, Covassin T, Fox ME, Petit KM, Savage JL, Walker LF, Gould D (2018). Sex Differences in the Clinical Incidence of Concussions, Missed School Days, and Time Loss in High School Student-Athletes: Part 1. *The American Journal of Sports Medicine*, *46*(9), 2263–2269. https://doi.org/10.1177/0363546518778251

Brickler T, Morton P, Hazy A, Theus MH (2017). Age-Dependent Responses Following Traumatic Brain Injury. Advance online publication. https://doi.org/10.5772/intechopen.71344

Broberg CS, Pantely GA, Barber BJ, Mack GK, Lee K, Thigpen T, Davis LE, Sahn D, Hohimer AR (2003). Validation of the myocardial performance index by echocardiography in mice: A noninvasive measure of left ventricular function. *Journal of the American Society of Echocardiography*, *16*(8), 814–823. https://doi.org/10.1067/S0894-7317(03)00399-7

Brookes PS, Yoon Y, Robotham JL, Anders MW, Sheu S-S (2004). Calcium, ATP, and ROS: A mitochondrial love-hate triangle. *American Journal of Physiology. Cell Physiology*, *287*(4), C817-33. https://doi.org/10.1152/ajpcell.00139.2004

Bruce ED, Konda S, Dean DD, Wang EW, Huang JH, Little DM (2015). Neuroimaging and traumatic brain injury: State of the field and voids in translational knowledge. *Molecular and Cellular Neurosciences*, *66*(Pt B), 103–113. https://doi.org/10.1016/j.mcn.2015.03.017

Bruss ZS, Raja A. (2022). *StatPearls: Physiology, Stroke Volume.*

Bye N, Habgood MD, Callaway JK, Malakooti N, Potter A, Kossmann T [Thomas], Morganti-Kossmann MC [M. Cristina] (2007). Transient neuroprotection by minocycline following traumatic brain injury is associated with attenuated microglial activation but no changes in cell apoptosis or neutrophil infiltration. *Experimental Neurology*, *204*(1), 220–233. https://doi.org/10.1016/j.expneurol.2006.10.013

Caldemeyer KS, Buckwalter KA (1999). The basic principles of computed tomography and magnetic resonance imaging. *Journal of the American Academy of Dermatology*, *41*(5), 768–771. https://doi.org/10.1016/s0190-9622(99)70015-0

Cao F, Jiang Y [Yong], Wu Y, Zhong J, Liu J, Qin X, Chen L [Ligang], Vitek MP, Li F [Fengqiao], Xu L [Lu], Sun X (2016). Apolipoprotein E-Mimetic COG1410 Reduces Acute Vasogenic Edema following Traumatic Brain Injury. *Journal of Neurotrauma*, *33*(2), 175–182. https://doi.org/10.1089/neu.2015.3887

CDC (2003). National Center for Injury Prevention and Control. Report to Congress on Mild Traumatic Brain Injury in the United States: Steps to Prevent a Serious Public Health Problem. Atlanta, GA: Centers for Disease Control and Prevention; 2003. http://www.cdc.gov/traumaticbraininjury/pdf/mtbireport-a.pdf.

Chaikittisilpa N, Krishnamoorthy V, Lele AV, Qiu Q, Vavilala MS (2018). Characterizing the relationship between systemic inflammatory response syndrome and early cardiac dysfunction in traumatic brain injury. *Journal of Neuroscience Research*, *96*(4), 661–670. https://doi.org/10.1002/jnr.24100

Chamoun R, Suki D, Gopinath SP, Goodman JC, Robertson C (2010). Role of extracellular glutamate measured by cerebral microdialysis in severe traumatic brain injury. *Journal of Neurosurgery*, *113*(3), 564–570. https://doi.org/10.3171/2009.12.JNS09689

Chang JJJ, Youn TS, Benson D, Mattick H, Andrade N, Harper CR, Moore CB, Madden CJ, Diaz-Arrastia RR (2009). Physiologic and functional outcome correlates of brain tissue hypoxia in traumatic brain injury. *Critical Care Medicine*, *37*(1), 283–290. https://doi.org/10.1097/CCM.0b013e318192fbd7

Chen, X., Gao, C., Yan, Y., Cheng, Z., Chen, G., Rui, T., Luo, C., Gao, Y., Wang, T., Chen, X., & Tao, L. (2021). Ruxolitinib exerts neuroprotection via repressing ferroptosis in a mouse model of traumatic brain injury. Experimental neurology, 342, 113762. https://doi.org/10.1016/j.expneurol.2021.113762 [Add to Citavi project by DOI]

Chou A, Morganti JM, Rosi S (2016). Frontal Lobe Contusion in Mice Chronically Impairs Prefrontal-Dependent Behavior. *PloS One*, *11*(3), e0151418. https://doi.org/10.1371/journal.pone.0151418

Christian TF (2005). Anatomy of an emerging diagnostic test: Computed tomographic coronary angiography. *Circulation*, *112*(15), 2222–2225. https://doi.org/10.1161/CIRCULATIONAHA.105.572826

Chu W, Li M, Li F [Fei], Hu R, Chen Z [Zhi], Lin J, Feng H (2013). Immediate splenectomy down-regulates the MAPK-NF-κB signaling pathway in rat brain after severe traumatic brain injury. *The Journal of Trauma and Acute Care Surgery*, *74*(6), 1446–1453. https://doi.org/10.1097/TA.0b013e31829246ad

Coote JH (2007). Landmarks in understanding the central nervous control of the cardiovascular system. *Experimental Physiology*, *92*(1), 3–18. https://doi.org/10.1113/expphysiol.2006.035378

Corps KN, Roth TL, McGavern DB (2015). Inflammation and neuroprotection in traumatic brain injury. *JAMA Neurology*, *72*(3), 355–362. https://doi.org/10.1001/jamaneurol.2014.3558

Courville, E., Kazim, S F., Vellek, J., Tarawneh, O H., Stack, J., Roster, K., Roy, J M., Schmidt, M H., & Bowers, C A. (2023, July 28). Machine learning algorithms for predicting outcomes of traumatic brain injury: A systematic review and meta-analysis. Medknow, 14, 262-262. https://doi.org/10.25259/sni_312_2023

Cuisinier A, Maufrais C, Payen J-F, Nottin S, Walther G, Bouzat P (2016). Myocardial function at the early phase of traumatic brain injury: A prospective controlled study. *Scandinavian Journal of Trauma, Resuscitation and Emergency Medicine*, *24*(1), 129. https://doi.org/10.1186/s13049-016-0323-3

Damen FW, Berman AG, Soepriatna AH, Ellis JM, Buttars SD, Aasa KL, Goergen CJ (2017). High-Frequency 4-Dimensional Ultrasound (4DUS): A Reliable Method for Assessing Murine Cardiac Function. *Tomography (Ann Arbor, Mich.)*, *3*(4), 180–187. https://doi.org/10.18383/j.tom.2017.00016

Damen FW, Salvas JP, Pereyra AS, Ellis JM, Goergen CJ (2021). Improving characterization of hypertrophy-induced murine cardiac dysfunction using four-dimensional ultrasound-derived strain mapping. *American Journal of Physiology. Heart and Circulatory Physiology*, *321*(1), H197-H207. https://doi.org/10.1152/ajpheart.00133.2021

Dandel M, Lehmkuhl H, Knosalla C, Suramelashvili N, Hetzer R (2009). Strain and strain rate imaging by echocardiography - basic concepts and clinical applicability. *Current Cardiology Reviews*, *5*(2), 133–148. https://doi.org/10.2174/157340309788166642

Dann MM, Clark SQ, Trzaskalski NA, Earl CC, Schepers LE, Pulente SM, Lennord EN, Annamalai K, Gruber JM, Cox AD, Lorenzen-Schmidt I, Seymour R, Kim K-H, Goergen CJ, Mulvihill EE (2022). Quantification of murine myocardial infarct size using 2-D and 4-D high-frequency ultrasound. *American Journal of Physiology. Heart and Circulatory Physiology*, *322*(3), H359-H372. https://doi.org/10.1152/ajpheart.00476.2021

Danna-Dos-Santos A, Mohapatra S, Santos M, Degani AM (2018). Long-term effects of mild traumatic brain injuries to oculomotor tracking performances and reaction times to simple

environmental stimuli. *Scientific Reports*, *8*(1), 4583. https://doi.org/10.1038/s41598-018-22825-5

Das BK (2015). Basic Principles of CT Imaging, 181–184. https://doi.org/10.1007/978-81-322-2098-5_20

David H, Ughetto A, Gaudard P, Plawecki M, Paiyabhroma N, Zub E, Colson P, Richard S, Marchi N, Sicard P (2020). Experimental Myocardial Infarction Elicits Time-Dependent Patterns of Vascular Hypoxia in Peripheral Organs and in the Brain. *Frontiers in Cardiovascular Medicine*, *7*, 615507. https://doi.org/10.3389/fcvm.2020.615507

Dawson D, Lygate CA, Saunders J, Schneider JE, Ye X, Hulbert K, Noble JA, Neubauer S (2004). Quantitative 3-dimensional echocardiography for accurate and rapid cardiac phenotype characterization in mice. *Circulation*, *110*(12), 1632–1637. https://doi.org/10.1161/01.CIR.0000142049.14227.AD

Dean PJA, Sterr A (2013). Long-term effects of mild traumatic brain injury on cognitive performance. *Frontiers in Human Neuroscience*, *7*, 30. https://doi.org/10.3389/fnhum.2013.00030

Delage C, Taib T, Mamma C, Lerouet D, Besson VC (2021). Traumatic Brain Injury: An Age-Dependent View of Post-Traumatic Neuroinflammation and Its Treatment. *Pharmaceutics*, *13*(10). https://doi.org/10.3390/pharmaceutics13101624

Demené C, Robin J, Dizeux A, Heiles B, Pernot M, Tanter M, Perren F (2021). Transcranial ultrafast ultrasound localization microscopy of brain vasculature in patients. *Nature Biomedical Engineering*, *5*(3), 219–228. https://doi.org/10.1038/s41551-021-00697-x

DeNicola GF, Martin ED, Chaikuad A, Bassi R, Clark J, Martino L, Verma S, Sicard P, Tata R, Atkinson RA, Knapp S, Conte MR, Marber MS (2013). Mechanism and consequence of the autoactivation of p38α mitogen-activated protein kinase promoted by TAB1. *Nature Structural & Molecular Biology*, *20*(10), 1182–1190. https://doi.org/10.1038/nsmb.2668

Dewan MC, Rattani A, Gupta S, Baticulon RE, Hung Y-C, Punchak M, Agrawal A, Adeleye AO, Shrime MG, Rubiano AM, Rosenfeld JV, Park KB (2018). Estimating the global incidence of traumatic brain injury. *Journal of Neurosurgery*, 1–18. https://doi.org/10.3171/2017.10.JNS17352

Dewey M, Laule M, Taupitz M, Kaufels N, Hamm B, Kivelitz D (2006). Myocardial viability: Assessment with three-dimensional MR imaging in pigs and patients. *Radiology*, *239*(3), 703–709. https://doi.org/10.1148/radiol.2393050586

DeWitt DS, Hawkins BE, Dixon CE, Kochanek PM, Armstead W, Bass CR, Bramlett HM, Buki A, Dietrich WD, Ferguson AR, Hall ED, Hayes RL, Hinds SR, LaPlaca MC, Long JB, Meaney DF, Mondello S, Noble-Haeusslein LJ, Poloyac SM, . . . Zhang L [Liying] (2018). Pre-Clinical Testing of Therapies for Traumatic Brain Injury. *Journal of Neurotrauma*, *35*(23), 2737–2754. https://doi.org/10.1089/neu.2018.5778

D'hooge J, Heimdal A, Jamal F, Kukulski T, Bijnens B, Rademakers F, Hatle L, Suetens P, Sutherland GR (2000). Regional strain and strain rate measurements by cardiac ultrasound:

Principles, implementation and limitations. *European Journal of Echocardiography : The Journal of the Working Group on Echocardiography of the European Society of Cardiology*, *1*(3), 154–170. https://doi.org/10.1053/euje.2000.0031

Dixon CE, Clifton GL, Lighthall JW, Yaghmai AA, Hayes RL (1991). A controlled cortical impact model of traumatic brain injury in the rat. *Journal of Neuroscience Methods*, *39*(3), 253–262. https://doi.org/10.1016/0165-0270(91)90104-8

Dombrowski K, Laskowitz D (2014). Cardiovascular manifestations of neurologic disease. *Handbook of Clinical Neurology*, *119*, 3–17. https://doi.org/10.1016/B978-0-7020-4086-3.00001-1

Ellis MJ, Ritchie LJ, Koltek M, Hosain S, Cordingley D, Chu S, Selci E, Leiter J, Russell K (2015). Psychiatric outcomes after pediatric sports-related concussion. *Journal of Neurosurgery. Pediatrics*, *16*(6), 709–718. https://doi.org/10.3171/2015.5.PEDS15220

El-Menyar A, Sathian B, Wahlen BM, Al-Thani H (2019). Serum cardiac troponins as prognostic markers in patients with traumatic and non-traumatic brain injuries: A meta-analysis. *The American Journal of Emergency Medicine*, *37*(1), 133–142. https://doi.org/10.1016/j.ajem.2018.10.002

Emery CA, Barlow KM, Brooks BL, Max JE, Villavicencio-Requis A, Gnanakumar V, Robertson HL, Schneider K, Yeates KO (2016). A Systematic Review of Psychiatric, Psychological, and Behavioural Outcomes following Mild Traumatic Brain Injury in Children and Adolescents. *Canadian Journal of Psychiatry. Revue Canadienne De Psychiatrie*, *61*(5), 259–269. https://doi.org/10.1177/0706743716643741

Errico C, Pierre J, Pezet S, Desailly Y, Lenkei Z, Couture O, Tanter M (2015). Ultrafast ultrasound localization microscopy for deep super-resolution vascular imaging. *Nature*, *527*(7579), 499–502. https://doi.org/10.1038/nature16066

Evans AM (1986). Age at puberty and first litter size in early and late paired rats. *Biology of Reproduction*, *34*(2), 322–326. https://doi.org/10.1095/biolreprod34.2.322

Fan X, DU F-H, Tian J-P (2012). The electrocardiographic changes in acute brain injury patients. *Chinese Medical Journal*, *125*(19), 3430–3433.

Feigenbaum H (2010). Role of M-mode technique in today's echocardiography. *Journal of the American Society of Echocardiography : Official Publication of the American Society of Echocardiography*, *23*(3), 240-57; 335-7. https://doi.org/10.1016/j.echo.2010.01.015

Ferdinand P, Roffe C [Christine] (2016). Hypoxia after stroke: A review of experimental and clinical evidence. *Experimental & Translational Stroke Medicine*, *8*, 9. https://doi.org/10.1186/s13231-016-0023-0

Fernandez-Ortega JF, Baguley IJ, Gates TA, Garcia-Caballero M, Quesada-Garcia JG, Prieto-Palomino MA (2017). Catecholamines and Paroxysmal Sympathetic Hyperactivity after Traumatic Brain Injury. *Journal of Neurotrauma*, *34*(1), 109–114. https://doi.org/10.1089/neu.2015.4364

Fischer M, Zacherl MJ, Weckbach L, Paintmayer L, Weinberger T, Stark K, Massberg S, Bartenstein P, Lehner S, Schulz C, Todica A (2021). Cardiac 18F-FDG Positron Emission Tomography: An Accurate Tool to Monitor In vivo Metabolic and Functional Alterations in Murine Myocardial Infarction. *Frontiers in Cardiovascular Medicine*, *8*, 656742. https://doi.org/10.3389/fcvm.2021.656742

Franzoso M, Zaglia T, Mongillo M (2016). Putting together the clues of the everlasting neuro-cardiac liaison. *Biochimica Et Biophysica Acta*, *1863*(7 Pt B), 1904–1915. https://doi.org/10.1016/j.bbamcr.2016.01.009

Fraunberger E, Esser MJ (2019). Neuro-Inflammation in Pediatric Traumatic Brain Injury-from Mechanisms to Inflammatory Networks. *Brain Sciences*, *9*(11). https://doi.org/10.3390/brainsci9110319

Gao W-M, Chadha MS, Kline AE, Clark RSB, Kochanek PM, Dixon CE, Jenkins LW (2006). Immunohistochemical analysis of histone H3 acetylation and methylation--evidence for altered epigenetic signaling following traumatic brain injury in immature rats. *Brain Research*, *1070*(1), 31–34. https://doi.org/10.1016/j.brainres.2005.11.038

Gao N, Zhang-Brotzge X, Wali B, et al. Plasma osteopontin may predict neuroinflammation and the severity of pediatric traumatic brain injury. Journal of Cerebral Blood Flow & Metabolism. 2020;40(1):35-43. doi:10.1177/0271678X19836412

Gardner AJ, Zafonte R [R.] (2016). Neuroepidemiology of traumatic brain injury. *Handbook of Clinical Neurology*, *138*, 207–223. https://doi.org/10.1016/B978-0-12-802973-2.00012-4

Girgis, F., Pace, J., Sweet, J., & Miller, J. P. (2016). Hippocampal Neurophysiologic Changes after Mild Traumatic Brain Injury and Potential Neuromodulation Treatment Approaches. Frontiers in systems neuroscience, 10, 8. https://doi.org/10.3389/fnsys.2016.00008

Giza, C. C., & Difiori, J. P. (2011). Pathophysiology of sports-related concussion: an update on basic science and translational research. Sports health, 3(1), 46–51. https://doi.org/10.1177/1941738110391732

Goertz DE, Needles A [Andrew], Burns PN, Foster FS [F. Stuart] (2005). High-frequency, nonlinear flow imaging of microbubble contrast agents. *IEEE Transactions on Ultrasonics, Ferroelectrics, and Frequency Control*, *52*(3), 495–502. https://doi.org/10.1109/tuffc.2005.1417273

Gorcsan J, Tanaka H (2011). Echocardiographic assessment of myocardial strain. *Journal of the American College of Cardiology*, *58*(14), 1401–1413. https://doi.org/10.1016/j.jacc.2011.06.038

Gorina R, Font-Nieves M, Márquez-Kisinousky L, Santalucia T, Planas AM (2011). Astrocyte TLR4 activation induces a proinflammatory environment through the interplay between MyD88-dependent NFκB signaling, MAPK, and Jak1/Stat1 pathways. *Glia*, *59*(2), 242–255. https://doi.org/10.1002/glia.21094

Greenhalgh AD, Zarruk JG, Healy LM, Baskar Jesudasan SJ, Jhelum P, Salmon CK, Formanek A, Russo MV, Antel JP, McGavern DB, McColl BW, David S (2018). Peripherally derived

macrophages modulate microglial function to reduce inflammation after CNS injury. *PLoS Biology*, *16*(10), e2005264. https://doi.org/10.1371/journal.pbio.2005264

Gregory T, Smith M (2012). Cardiovascular complications of brain injury. *Continuing Education in Anaesthesia Critical Care & Pain*, *12*(2), 67–71. https://doi.org/10.1093/bjaceaccp/mkr058

Greve MW, Zink BJ (2009). Pathophysiology of traumatic brain injury. *The Mount Sinai Journal of Medicine, New York*, *76*(2), 97–104. https://doi.org/10.1002/msj.20104

Griffiths DR, Law LM, Young C, Fuentes A, Truran S, Karamanova N, Bell LC, Turner G, Emerson H, Mastroeni D, Gonzales R, Reaven PD, Quarles CC, Migrino RQ, Lifshitz J (2022). Chronic Cognitive and Cerebrovascular Function Following Mild Traumatic Brain Injury in Rats. Advance online publication. https://doi.org/10.1101/2022.01.05.474992

Grin'kina NM, Li Y [Yang], Haber M, Sangobowale M, Nikulina E, Le'Pre C, El Sehamy AM, Dugue R, Ho JS, Bergold PJ (2016). Righting Reflex Predicts Long-Term Histological and Behavioral Outcomes in a Closed Head Model of Traumatic Brain Injury. *PloS One*, *11*(9), e0161053. https://doi.org/10.1371/journal.pone.0161053

Grossman W, McLaurin LP (1976). Diastolic properties of the left ventricle. *Annals of Internal Medicine*, *84*(3), 316–326. https://doi.org/10.7326/0003-4819-84-3-316

Gruhl SL, Su J, Chua WC, Tay KV (2022). Takotsubo cardiomyopathy in post-traumatic brain injury: A systematic review of diagnosis and management. *Clinical Neurology and Neurosurgery*, *213*, 107119. https://doi.org/10.1016/j.clineuro.2021.107119

Guevara E, Berti R, Londono I, Xie N, Bellec P, Lesage F, Lodygensky GA (2013). Imaging of an inflammatory injury in the newborn rat brain with photoacoustic tomography. *PloS One*, *8*(12), e83045. https://doi.org/10.1371/journal.pone.0083045

Gulati VK, Katz WE, Follansbee WP, Gorcsan J (1996). Mitral annular descent velocity by tissue Doppler echocardiography as an index of global left ventricular function. *The American Journal of Cardiology*, *77*(11), 979–984. https://doi.org/10.1016/s0002-9149(96)00033-1

Gunnoo T, Hasan N, Khan MS, Slark J, Bentley P, Sharma P (2016). Quantifying the risk of heart disease following acute ischaemic stroke: A meta-analysis of over 50,000 participants. *BMJ Open*, *6*(1), e009535. https://doi.org/10.1136/bmjopen-2015-009535

Guo M-F, Yu J-Z, Ma C-G (2011). Mechanisms related to neuron injury and death in cerebral hypoxic ischaemia. *Folia Neuropathologica*, *49*(2), 78–87. https://doi.org/Review

Harvey LA, Close JCT (2012). Traumatic brain injury in older adults: Characteristics, causes and consequences. *Injury*, *43*(11), 1821–1826. https://doi.org/10.1016/j.injury.2012.07.188

Hasanin A, Kamal A, Amin S, Zakaria D, El Sayed R, Mahmoud K, Mukhtar A (2016). Incidence and outcome of cardiac injury in patients with severe head trauma. *Scandinavian Journal of Trauma, Resuscitation and Emergency Medicine*, *24*, 58. https://doi.org/10.1186/s13049-016-0246-z

Hawryluk GWJ, Manley GT (2015). Classification of traumatic brain injury: Past, present, and future. *Handbook of Clinical Neurology*, *127*, 15–21. https://doi.org/10.1016/b978-0-444-52892-6.00002-7

Hayasaka N, Nagai N, Kawao N, Niwa A, Yoshioka Y, Mori Y, Shigeta H, Kashiwagi N, Miyazawa M, Satou T, Higashino H, Matsuo O, Murakami T [Takamichi] (2012). In vivo diagnostic imaging using micro-CT: Sequential and comparative evaluation of rodent models for hepatic/brain ischemia and stroke. *PloS One*, *7*(2), e32342. https://doi.org/10.1371/journal.pone.0032342

Hoiland RL, Bain AR, Rieger MG, Bailey DM, Ainslie PN (2016). Hypoxemia, oxygen content, and the regulation of cerebral blood flow. *American Journal of Physiology. Regulatory, Integrative and Comparative Physiology*, *310*(5), R398-413. https://doi.org/10.1152/ajpregu.00270.2015

Hoole SP, Boyd J, Ninios V, Parameshwar J, Rusk RA (2008). Measurement of cardiac output by real-time 3D echocardiography in patients undergoing assessment for cardiac transplantation. *European Journal of Echocardiography : The Journal of the Working Group on Echocardiography of the European Society of Cardiology*, *9*(3), 334–337. https://doi.org/10.1016/j.euje.2007.03.033

Houstis NE, Eisman AS, Pappagianopoulos PP, Wooster L, Bailey CS, Wagner PD, Lewis GD (2018). Exercise Intolerance in Heart Failure With Preserved Ejection Fraction: Diagnosing and Ranking Its Causes Using Personalized O2 Pathway Analysis. *Circulation*, *137*(2), 148–161. https://doi.org/10.1161/CIRCULATIONAHA.117.029058

Hrishi PA, Ruby Lionel K, Prathapadas U (2019). Head Rules Over the Heart: Cardiac Manifestations of Cerebral Disorders. *Indian Journal of Critical Care Medicine : Peer-Reviewed, Official Publication of Indian Society of Critical Care Medicine*, *23*(7), 329–335. https://doi.org/10.5005/jp-journals-10071-23208

Huang L, Obenaus A [Andre], Hamer M, Zhang JH (2016). Neuroprotective effect of hyperbaric oxygen therapy in a juvenile rat model of repetitive mild traumatic brain injury. *Medical Gas Research*, *6*(4), 187–193. https://doi.org/10.4103/2045-9912.196900

Ichkova A, Rodriguez-Grande B, Zub E, Saudi A, Fournier M-L, Aussudre J, Sicard P, Obenaus A [André], Marchi N, Badaut J (2020). Early cerebrovascular and long-term neurological modifications ensue following juvenile mild traumatic brain injury in male mice. *Neurobiology of Disease*, *141*, 104952. https://doi.org/10.1016/j.nbd.2020.104952

Ingul CB, Torp H, Aase SA, Berg S, Stoylen A, Slordahl SA (2005). Automated analysis of strain rate and strain: Feasibility and clinical implications. *Journal of the American Society of Echocardiography*, *18*(5), 411–418. https://doi.org/10.1016/j.echo.2005.01.032

Isaaz K, Del Romeral LM, Lee E, Schiller NB (1993). Quantitation of the Motion of the Cardiac Base in Normal Subjects by Doppler Echocardiography. *Journal of the American Society of Echocardiography*, *6*(2), 166–176. https://doi.org/10.1016/s0894-7317(14)80487-2

Israel I, Ohsiek A, Al-Momani E, Albert-Weissenberger C, Stetter C, Mencl S, Buck AK, Kleinschnitz C, Samnick S, Sirén A-L (2016). Combined (18)FDPA-714 micro-positron emission tomography and autoradiography imaging of microglia activation after closed head injury in mice. *Journal of Neuroinflammation*, *13*(1), 140. https://doi.org/10.1186/s12974-016-0604-9

Izzy S, Chen PM, Tahir Z, Grashow R, Radmanesh F, Cote DJ, Yahya T, Dhand A, Taylor H, Shih SL, Albastaki O, Rovito C, Snider SB, Whalen M, Nathan DM, Miller KK, Speizer FE, Baggish A, Weisskopf MG, Zafonte R [Ross] (2022). Association of Traumatic Brain Injury With the Risk of Developing Chronic Cardiovascular, Endocrine, Neurological, and Psychiatric Disorders. *JAMA Network Open*, *5*(4), e229478. https://doi.org/10.1001/jamanetworkopen.2022.9478

Jacquet S, Nishino Y, Kumphune S, Sicard P, Clark JE, Kobayashi KS, Flavell RA, Eickhoff J, Cotten M, Marber MS (2008). The role of RIP2 in p38 MAPK activation in the stressed heart. *The Journal of Biological Chemistry*, *283*(18), 11964–11971. https://doi.org/10.1074/jbc.M707750200

Jafari AA, Shah M, Mirmoeeni S, Hassani MS, Nazari S, Fielder T, Godoy DA, Seifi A (2022). Paroxysmal sympathetic hyperactivity during traumatic brain injury. *Clinical Neurology and Neurosurgery*, *212*, 107081. https://doi.org/10.1016/j.clineuro.2021.107081

Jan MF, Tajik AJ [A. Jamil] (2017). Modern Imaging Techniques in Cardiomyopathies. *Circulation Research*, *121*(7), 874–891. https://doi.org/10.1161/CIRCRESAHA.117.309600

Jarrahi A, Braun M, Ahluwalia M, Gupta RV, Wilson M, Munie S, Ahluwalia P, Vender JR, Vale FL, Dhandapani KM, Vaibhav K (2020). Revisiting Traumatic Brain Injury: From Molecular Mechanisms to Therapeutic Interventions. *Biomedicines*, *8*(10). https://doi.org/10.3390/biomedicines8100389

Jassam YN, Izzy S, Whalen M, McGavern DB, El Khoury J (2017). Neuroimmunology of Traumatic Brain Injury: Time for a Paradigm Shift. *Neuron*, *95*(6), 1246–1265. https://doi.org/10.1016/j.neuron.2017.07.010

Jiang Y [Yuting], Peng C, Zhu Y, Ma X, Xu G, Yuan J, Wang X [Xueding], Carson P (2021). Biomedical Photoacoustic Imaging With Unknown Spatially Distributed Ultrasound Sensor Array. *IEEE Transactions on Bio-Medical Engineering*, *68*(10), 2948–2956. https://doi.org/10.1109/TBME.2021.3056715

Jiang Y, Pu K (2017). Advanced Photoacoustic Imaging Applications of Near-Infrared Absorbing Organic Nanoparticles. *Small (Weinheim an Der Bergstrasse, Germany)*, *13*(30). https://doi.org/10.1002/smll.201700710

Johnson, L. W., & Hall, K. D. (2022). A Scoping Review of Cognitive Assessment in Adults With Acute Traumatic Brain Injury. American journal of speech-language pathology, 31(2), 739–756. https://doi.org/10.1044/2021_AJSLP-21-00132 [Add to Citavi project by DOI]

Johnson VE, Meaney DF, Cullen DK, Smith DH (2015). Animal models of traumatic brain injury. *Handbook of Clinical Neurology*, *127*, 115–128. https://doi.org/10.1016/B978-0-444-52892-6.00008-8

Jolliffe IT, Cadima J (2016). Principal component analysis: A review and recent developments. *Philosophical Transactions. Series A, Mathematical, Physical, and Engineering Sciences*, *374*(2065), 20150202. https://doi.org/10.1098/rsta.2015.0202

Freeman-Jones E, Miller WH, Work LM, Fullerton JL. Polypathologies and Animal Models of Traumatic Brain Injury. Brain Sci. 2023 Dec 12;13(12):1709. doi: 10.3390/brainsci13121709 [Add to Citavi project by DOI] . PMID: 38137157 [Add to Citavi project by Pubmed ID] ; PMCID: PMC10741988. [Add to Citavi project by PMC ID]

Jorge AJL, Ribeiro ML, Rosa MLG, Licio FV, Fernandes LCM, Lanzieri PG, Jorge BAL, Brito FOX, Mesquita ET (2012). Left atrium measurement in patients suspected of having heart failure with preserved ejection fraction. *Arquivos Brasileiros De Cardiologia*, *98*(2), 175–181. https://doi.org/10.1590/s0066-782x2012005000009

Kane MJ, Angoa-Pérez M, Briggs DI, Viano DC, Kreipke CW, Kuhn DM (2012). A mouse model of human repetitive mild traumatic brain injury. *Journal of Neuroscience Methods*, *203*(1), 41–49. https://doi.org/10.1016/j.jneumeth.2011.09.003

Karr, J. E., Areshenkoff, C. N., & Garcia-Barrera, M. A. (2014). The neuropsychological outcomes of concussion: a systematic review of meta-analyses on the cognitive sequelae of mild traumatic brain injury. Neuropsychology, 28(3), 321–336. https://doi.org/10.1037/neu0000037

Karthikeyan B, Sonkawade SD, Pokharel S, Preda M, Schweser F, Zivadinov R, Kim M, Sharma UC (2020). Tagged cine magnetic resonance imaging to quantify regional mechanical changes after acute myocardial infarction. *Magnetic Resonance Imaging*, *66*, 208–218. https://doi.org/10.1016/j.mri.2019.09.010

Kazl C, Torres A (2019). Definition, Classification, and Epidemiology of Concussion. *Seminars in Pediatric Neurology*, *30*, 9–13. https://doi.org/10.1016/j.spen.2019.03.003

Keightley ML, Côté P, Rumney P, Hung R, Carroll LJ, Cancelliere C, Cassidy JD (2014). Psychosocial consequences of mild traumatic brain injury in children: Results of a systematic review by the International Collaboration on Mild Traumatic Brain Injury Prognosis. *Archives of Physical Medicine and Rehabilitation*, *95*(3 Suppl), S192-200. https://doi.org/10.1016/j.apmr.2013.12.018

Kim W, Kim EJ (2018). Heart Failure as a Risk Factor for Stroke. *Journal of Stroke*, *20*(1), 33–45. https://doi.org/10.5853/jos.2017.02810

Kinder HA, Baker EW, Howerth EW, Duberstein KJ, West FD (2019). Controlled Cortical Impact Leads to Cognitive and Motor Function Deficits that Correspond to Cellular Pathology in a Piglet Traumatic Brain Injury Model. *Journal of Neurotrauma*, *36*(19), 2810–2826. https://doi.org/10.1089/neu.2019.6405

King MD, Laird MD, Ramesh SS, Youssef P, Shakir B, Vender JR, Alleyne CH, Dhandapani KM (2010). Elucidating novel mechanisms of brain injury following subarachnoid hemorrhage: An emerging role for neuroproteomics. *Neurosurgical Focus*, *28*(1), E10. https://doi.org/10.3171/2009.10.FOCUS09223

Kochanek PM, Wallisch JS, Bayır H, Clark RSB (2017). Pre-clinical models in pediatric traumatic brain injury-challenges and lessons learned. *Child's Nervous System : ChNS : Official Journal of the International Society for Pediatric Neurosurgery*, *33*(10), 1693–1701. https://doi.org/10.1007/s00381-017-3474-2

Koerte IK, Hufschmidt J, Muehlmann M, Lin AP, Shenton ME. (2016). *Translational Research in Traumatic Brain Injury: Advanced Neuroimaging of Mild Traumatic Brain Injury* (D. Laskowitz, & G. Grant, Eds.).

Kojonazarov B, Belenkov A, Shinomiya S, Wilchelm J, Kampschulte M, Mizuno S, Ghofrani HA, Grimminger F, Weissmann N, Seeger W, Schermuly RT (2018). Evaluating Systolic and Diastolic Cardiac Function in Rodents Using Microscopic Computed Tomography. *Circulation. Cardiovascular Imaging*, *11*(12), e007653. https://doi.org/10.1161/CIRCIMAGING.118.007653

Kratkiewicz K, Pattyn A, Alijabbari N, Mehrmohammadi M (2022). Ultrasound and Photoacoustic Imaging of Breast Cancer: Clinical Systems, Challenges, and Future Outlook. *Journal of Clinical Medicine*, *11*(5). https://doi.org/10.3390/jcm11051165

Kraus JF, Nourjah P (1988). The epidemiology of mild, uncomplicated brain injury. *The Journal of Trauma*, *28*(12), 1637–1643. https://doi.org/10.1097/00005373-198812000-00004

Krishnamoorthy V, Chaikittisilpa N, Lee J [James], Mackensen GB, Gibbons EF, Laskowitz D, Hernandez A, Velazquez E, Lele AV, Vavilala MS (2020). Speckle Tracking Analysis of Left Ventricular Systolic Function Following Traumatic Brain Injury: A Pilot Prospective Observational Cohort Study. *Journal of Neurosurgical Anesthesiology*, *32*(2), 156–161. https://doi.org/10.1097/ANA.0000000000000578

Krishnamoorthy V, Mackensen GB, Gibbons EF, Vavilala MS (2016). Cardiac Dysfunction After Neurologic Injury: What Do We Know and Where Are We Going? *Chest*, *149*(5), 1325–1331. https://doi.org/10.1016/j.chest.2015.12.014

Krishnamoorthy V, Prathep S, Sharma D, Fujita Y, Armstead W, Vavilala MS (2015). Cardiac dysfunction following brain death after severe pediatric traumatic brain injury: A preliminary study of 32 children. *International Journal of Critical Illness and Injury Science*, *5*(2), 103–107. https://doi.org/10.4103/2229-5151.158409

Krishnamoorthy V, Prathep S, Sharma D, Gibbons E, Vavilala MS (2014). Association between electrocardiographic findings and cardiac dysfunction in adult isolated traumatic brain injury. *Indian Journal of Critical Care Medicine : Peer-Reviewed, Official Publication of Indian Society of Critical Care Medicine*, *18*(9), 570–574. https://doi.org/10.4103/0972-5229.140144

Krishnamoorthy V, Rowhani-Rahbar A, Gibbons EF, Rivara FP, Temkin NR, Pontius C, Luk K, Graves M, Lozier D, Chaikittisilpa N, Kiatchai T, Vavilala MS (2017). Early Systolic Dysfunction Following Traumatic Brain Injury: A Cohort Study. *Critical Care Medicine*, *45*(6), 1028–1036. https://doi.org/10.1097/CCM.0000000000002404

Kumphune S, Bassi R, Jacquet S, Sicard P, Clark JE, Verma S, Avkiran M, O'Keefe SJ, Marber MS (2010). A chemical genetic approach reveals that p38alpha MAPK activation by

diphosphorylation aggravates myocardial infarction and is prevented by the direct binding of SB203580. *The Journal of Biological Chemistry*, *285*(5), 2968–2975. https://doi.org/10.1074/jbc.M109.079228

Kurland D, Hong C, Aarabi B, Gerzanich V, Simard JM (2012). Hemorrhagic progression of a contusion after traumatic brain injury: A review. *Journal of Neurotrauma*, *29*(1), 19–31. https://doi.org/10.1089/neu.2011.2122

Lackner I, Weber B, Haffner-Luntzer M, Hristova S, Gebhard F, Lam C, Morioka K, Marcucio RS, Miclau T, Kalbitz M (2021). Systemic and local cardiac inflammation after experimental long bone fracture, traumatic brain injury and combined trauma in mice. *Journal of Orthopaedic Translation*, *28*, 39–46. https://doi.org/10.1016/j.jot.2020.12.003

Lambert E, Du X-J, Percy E, Lambert G (2002). Cardiac response to norepinephrine and sympathetic nerve stimulation following experimental subarachnoid hemorrhage. *Journal of the Neurological Sciences*, *198*(1-2), 43–50. https://doi.org/10.1016/S0022-510X(02)00073-4

Lampaskis M, Averkiou M (2010). Investigation of the relationship of nonlinear backscattered ultrasound intensity with microbubble concentration at low MI. *Ultrasound in Medicine & Biology*, *36*(2), 306–312. https://doi.org/10.1016/j.ultrasmedbio.2009.09.011

Lang CI, Döring P, Gäbel R, Vasudevan P, Lemcke H, Müller P, Stenzel J, Lindner T, Joksch M, Kurth J, Bergner C, Wester H-J, Ince H, Steinhoff G, Vollmar B, David R, Krause BJ (2020). 68ga-NODAGA-RGD Positron Emission Tomography (PET) for Assessment of Post Myocardial Infarction Angiogenesis as a Predictor for Left Ventricular Remodeling in Mice after Cardiac Stem Cell Therapy. *Cells*, *9*(6). https://doi.org/10.3390/cells9061358.

Lang RM, Badano LP [Luigi P.], Mor-Avi V, Afilalo J, Armstrong A, Ernande L, Flachskampf FA, Foster E, Goldstein SA, Kuznetsova T, Lancellotti P, Muraru D, Picard MH [Michael H.], Rietzschel ER, Rudski L, Spencer KT, Tsang W, Voigt J-U (2015). Recommendations for cardiac chamber quantification by echocardiography in adults: An update from the American Society of Echocardiography and the European Association of Cardiovascular Imaging. *Journal of the American Society of Echocardiography : Official Publication of the American Society of Echocardiography*, *28*(1), 1-39.e14. https://doi.org/10.1016/j.echo.2014.10.003

Langlois JA, Rutland-Brown W, Wald MM (2006). The epidemiology and impact of traumatic brain injury: A brief overview. *The Journal of Head Trauma Rehabilitation*, *21*(5), 375–378. https://doi.org/10.1097/00001199-200609000-00001

Larson BE, Stockwell DW, Boas S, Andrews T, Wellman GC, Lockette W, Freeman K (2012). Cardiac reactive oxygen species after traumatic brain injury. *The Journal of Surgical Research*, *173*(2), e73-81. https://doi.org/10.1016/j.jss.2011.09.056

Ledoux AA, Webster RJ, Clarke AE, Fell DB, Knight BD, Gardner W, Cloutier P, Gray C, Tuna M, Zemek R (2022). Risk of Mental Health Problems in Children and Youths Following Concussion. *JAMA Network Open*, *5*(3), e221235. https://doi.org/10.1001/jamanetworkopen.2022.1235

Lee LK, Monroe D, Bachman MC, Glass TF, Mahajan PV, Cooper A, Stanley RM, Miskin M, Dayan PS, Holmes JF, Kuppermann N (2014). Isolated loss of consciousness in children with

minor blunt head trauma. *JAMA Pediatrics*, *168*(9), 837–843. https://doi.org/10.1001/jamapediatrics.2014.361

Lee YL, Lim S-W, Zheng H-X, Chang W-T, Nyam T-TE, Chio C-C, Kuo J-R, Wang C-C (2020). The Short-Term Effects of Isolated Traumatic Brain Injury on the Heart in Experimental Healthy Rats. *Neurocritical Care*, *33*(2), 438–448. https://doi.org/10.1007/s12028-019-00902-5

Leftin A, Rosenberg JT, Solomon E, Calixto Bejarano F, Grant SC, Frydman L (2015). Ultrafast in vivo diffusion imaging of stroke at 21.1 T by spatiotemporal encoding. *Magnetic Resonance in Medicine*, *73*(4), 1483–1489. https://doi.org/10.1002/mrm.25271

Leitman M, Lysyansky P, Sidenko S, Shir V, Peleg E, Binenbaum M, Kaluski E, Krakover R, Vered Z (2004). Two-dimensional strain-a novel software for real-time quantitative echocardiographic assessment of myocardial function. *Journal of the American Society of Echocardiography*, *17*(10), 1021–1029. https://doi.org/10.1016/j.echo.2004.06.019

Lele AV, Alunpipatthanachai B, Clark-Bell C, Watanitanon A, Min Xu M, Anne Moore RVT, Zimmerman JJ, Portman MA, Chesnut RM, Vavilala MS (2020). Cardiac-cerebral-renal associations in pediatric traumatic brain injury: Preliminary findings. *Journal of Clinical Neuroscience : Official Journal of the Neurosurgical Society of Australasia*, *76*, 126–133. https://doi.org/10.1016/j.jocn.2020.04.021

Lester SJ, Wilansky S (2007). Endocarditis and associated complications. *Critical Care Medicine*, *35*(8 Suppl), S384-91. https://doi.org/10.1097/01.CCM.0000270275.89478.5F

Lindsey ML, Kassiri Z, Virag JAI, Castro Brás LE de, Scherrer-Crosbie M (2018). Guidelines for measuring cardiac physiology in mice. *American Journal of Physiology. Heart and Circulatory Physiology*, *314*(4), H733-H752. https://doi.org/10.1152/ajpheart.00339.2017

Liu N [Nian], Gujrati V, Malekzadeh-Najafabadi J, Werner JPF, Klemm U, Tang L, Chen Z [Zhenyue], Prakash J, Huang Y [Yuanhui], Stiel A, Mettenleiter G, Aichler M, Blutke A, Walch A, Kleigrewe K, Razansky D, Sattler M, Ntziachristos V (2021). Croconaine-based nanoparticles enable efficient optoacoustic imaging of murine brain tumors. *Photoacoustics*, *22*, 100263. https://doi.org/10.1016/j.pacs.2021.100263

Ljubicic ML, Madsen A, Juul A, Almstrup K, Johannsen TH (2021). The Application of Principal Component Analysis on Clinical and Biochemical Parameters Exemplified in Children With Congenital Adrenal Hyperplasia. *Frontiers in Endocrinology*, *12*, 652888. https://doi.org/10.3389/fendo.2021.652888

Loane DJ, Faden AI (2010). Neuroprotection for traumatic brain injury: Translational challenges and emerging therapeutic strategies. *Trends in Pharmacological Sciences*, *31*(12), 596–604. https://doi.org/10.1016/j.tips.2010.09.005

Lowry R, Haarbauer-Krupa J, Breiding MJ, Simon TR (2021). Sports- and Physical Activity-Related Concussion and Risk for Youth Violence. *American Journal of Preventive Medicine*, *60*(3), 352–359. https://doi.org/10.1016/j.amepre.2020.10.018

Lucas A, Mialet-Perez J, Daviaud D, Parini A, Marber MS, Sicard P (2015). Gadd45γ regulates cardiomyocyte death and post-myocardial infarction left ventricular remodelling. *Cardiovascular Research*, *108*(2), 254–267. https://doi.org/10.1093/cvr/cvv219

Luis SA, Chan J, Pellikka PA (2019). Echocardiographic Assessment of Left Ventricular Systolic Function: An Overview of Contemporary Techniques, Including Speckle-Tracking Echocardiography. *Mayo Clinic Proceedings*, *94*(1), 125–138. https://doi.org/10.1016/j.mayocp.2018.07.017

Lumba-Brown A, Yeates KO, Sarmiento K, Breiding MJ, Haegerich TM, Gioia GA, Turner M, Benzel EC, Suskauer SJ, Giza CC, Joseph M, Broomand C, Weissman B, Gordon W, Wright DW, Moser RS, McAvoy K, Ewing-Cobbs L, Duhaime A-C, . . . Timmons SD (2018). Centers for Disease Control and Prevention Guideline on the Diagnosis and Management of Mild Traumatic Brain Injury Among Children. *JAMA Pediatrics*, *172*(11), e182853. https://doi.org/10.1001/jamapediatrics.2018.2853.

Lv J, Li S, Zhang J [Jinde], Duan F, Wu Z, Chen R, Chen M, Huang S, Ma H, Nie L (2020). In vivo photoacoustic imaging dynamically monitors the structural and functional changes of ischemic stroke at a very early stage. *Theranostics*, *10*(2), 816–828. https://doi.org/10.7150/thno.38554

Macé E, Montaldo G, Cohen I, Baulac M, Fink M, Tanter M (2011). Functional ultrasound imaging of the brain. *Nature Methods*, *8*(8), 662–664. https://doi.org/10.1038/nmeth.1641

Majdan M, Melichova J, Plancikova D, Sivco P, Maas AIR, Feigin VL, Polinder S, Haagsma JA (2022). Burden of Traumatic Brain Injuries in Children and Adolescents in Europe: Hospital Discharges, Deaths and Years of Life Lost. *Children (Basel, Switzerland)*, *9*(1). https://doi.org/10.3390/children9010105

Manwar R, Kratkiewicz K, Avanaki K (2020). Overview of Ultrasound Detection Technologies for Photoacoustic Imaging. *Micromachines*, *11*(7). https://doi.org/10.3390/mi11070692

Maria, N S S., Sargolzaei, S., Prins, M L., Dennis, E L., Asarnow, R F., Hovda, D A., Harris, N G., & Giza, C C. (2019, May 2). Bridging the gap: Mechanisms of plasticity and repair after pediatric TBI. Elsevier BV, 318, 78-91. https://doi.org/10.1016/j.expneurol.2019.04.016

Marmarou A, Foda MA, van den Brink W, Campbell J, Kita H, Demetriadou K (1994). A new model of diffuse brain injury in rats. Part I: Pathophysiology and biomechanics. *Journal of Neurosurgery*, *80*(2), 291–300. https://doi.org/10.3171/jns.1994.80.2.0291

Masuda T [Takashi], Sato K, Yamamoto S, Matsuyama N, Shimohama T, Matsunaga A, Obuchi S, Shiba Y, Shimizu S, Izumi T (2002). Sympathetic nervous activity and myocardial damage immediately after subarachnoid hemorrhage in a unique animal model. *Stroke*, *33*(6), 1671–1676. https://doi.org/10.1161/01.STR.0000016327.74392.02

Matta A, Delmas C, Campelo-Parada F, Lhermusier T, Bouisset F, Elbaz M, Nader V, Blanco S, Roncalli J, Carrié D (2022). Takotsubo cardiomyopathy. *Reviews in Cardiovascular Medicine*, *23*(1), 38. https://doi.org/10.31083/j.rcm2301038

McDonald SJ, Sharkey JM, Sun M, Kaukas LM, Shultz SR, Turner RJ, Leonard AV, Brady RD, Corrigan F (2020). Beyond the Brain: Peripheral Interactions after Traumatic Brain Injury. *Journal of Neurotrauma*, *37*(5), 770–781. https://doi.org/10.1089/neu.2019.6885

McIntosh TK, Vink R, Noble L, Yamakami I, Fernyak S, Soares H, Faden AL (1989). Traumatic brain injury in the rat: Characterization of a lateral fluid-percussion model. *Neuroscience*, *28*(1), 233–244. https://doi.org/10.1016/0306-4522(89)90247-9

Mckee AC, Daneshvar DH (2015). The neuropathology of traumatic brain injury. *Handbook of Clinical Neurology*, *127*, 45–66. https://doi.org/10.1016/B978-0-444-52892-6.00004-0

McKinlay A, Grace RC, Horwood LJ, Fergusson DM, Ridder EM, MacFarlane MR (2008). Prevalence of traumatic brain injury among children, adolescents and young adults: Prospective evidence from a birth cohort. *Brain Injury*, *22*(2), 175–181. https://doi.org/10.1080/02699050801888824

Meldrum BS (2000). Glutamate as a neurotransmitter in the brain: Review of physiology and pathology. *The Journal of Nutrition*, *130*(4S Suppl), 1007S-15S. https://doi.org/10.1093/jn/130.4.1007S

Mele C, Pingue V, Caputo M, Zavattaro M, Pagano L, Prodam F, Nardone A, Aimaretti G, Marzullo P (2021). Neuroinflammation and Hypothalamo-Pituitary Dysfunction: Focus of Traumatic Brain Injury. *International Journal of Molecular Sciences*, *22*(5). https://doi.org/10.3390/ijms22052686

Menon DK, Schwab K, Wright DW, Maas AI (2010). Position statement: Definition of traumatic brain injury. *Archives of Physical Medicine and Rehabilitation*, *91*(11), 1637–1640. https://doi.org/10.1016/j.apmr.2010.05.017

Meyfroidt G, Baguley IJ, Menon DK (2017). Paroxysmal sympathetic hyperactivity: the storm after acute brain injury. *The Lancet Neurology*, *16*(9), 721–729. https://doi.org/10.1016/S1474-4422(17)30259-4

Mishina M (2008). Positron emission tomography for brain research. *Journal of Nippon Medical School = Nippon Ika Daigaku Zasshi*, *75*(2), 68–76. https://doi.org/10.1272/jnms.75.68

Morales DM, Marklund N, Lebold D, Thompson HJ, Pitkanen A, Maxwell WL, Longhi L, Laurer H, Maegele M, Neugebauer E, Graham DI, Stocchetti N, McIntosh TK (2005). Experimental models of traumatic brain injury: Do we really need to build a better mousetrap? *Neuroscience*, *136*(4), 971–989. https://doi.org/10.1016/j.neuroscience.2005.08.030

Mor-Avi V, Lang RM, Badano LP [Luigi P.], Belohlavek M, Cardim NM, Derumeaux G, Galderisi M, Marwick T, Nagueh SF, Sengupta PP, Sicari R, Smiseth OA, Smulevitz B, Takeuchi M, Thomas JD, Vannan M, Voigt J-U, Zamorano JL (2011). Current and evolving echocardiographic techniques for the quantitative evaluation of cardiac mechanics: Ase/eae consensus statement on methodology and indications endorsed by the Japanese Society of Echocardiography. *Journal of the American Society of Echocardiography : Official Publication*

of the American Society of Echocardiography, *24*(3), 277–313. https://doi.org/10.1016/j.echo.2011.01.015

Morgan CD, Zuckerman SL, Lee YM, King L, Beaird S, Sills AK, Solomon GS (2015). Predictors of postconcussion syndrome after sports-related concussion in young athletes: A matched case-control study. *Journal of Neurosurgery. Pediatrics*, *15*(6), 589–598. https://doi.org/10.3171/2014.10.PEDS14356

Morganti JM, Goulding DS, van Eldik LJ (2019). Deletion of p38α MAPK in microglia blunts trauma-induced inflammatory responses in mice. *Journal of Neuroinflammation*, *16*(1), 98. https://doi.org/10.1186/s12974-019-1493-5

Morganti-Kossmann MC [M. C.], Rancan M, Otto VI, Stahel PF, Kossmann T [T.] (2001). Role of cerebral inflammation after traumatic brain injury: A revisited concept. *Shock (Augusta, Ga.)*, *16*(3), 165–177. https://doi.org/10.1097/00024382-200116030-00001

Morrison G, Fraser DD, Cepinskas G (2013). Mechanisms and consequences of acquired brain injury during development. *Pathophysiology : The Official Journal of the International Society for Pathophysiology*, *20*(1), 49–57. https://doi.org/10.1016/j.pathophys.2012.02.006

Mouzon, B. C., Bachmeier, C., Ojo, J. O., Acker, C. M., Ferguson, S., Paris, D., Ait-Ghezala, G., Crynen, G., Davies, P., Mullan, M., Stewart, W., & Crawford, F. (2017). Lifelong behavioral and neuropathological consequences of repetitive mild traumatic brain injury. Annals of clinical and translational neurology, 5(1), 64–80. https://doi.org/10.1002/acn3.510

Miller, H. A., Magsam, A. W., Tarudji, A. W., Romanova, S., Weber, L., Gee, C. C., Madsen, G. L., Bronich, T. K., & Kievit, F. M. (2019). Evaluating differential nanoparticle accumulation and retention kinetics in a mouse model of traumatic brain injury via Ktrans mapping with MRI. Scientific reports, 9(1), 16099. https://doi.org/10.1038/s41598-019-52622-7 [Add to Citavi project by DOI]

Murakami T [Taro], Hama S, Yamashita H, Onoda K, Hibino S, Sato H, Ogawa S, Yamawaki S, Kurisu K (2014). Neuroanatomic pathway associated with attentional deficits after stroke. *Brain Research*, *1544*, 25–32. https://doi.org/10.1016/j.brainres.2013.11.029

Na S, Russin JJ, Lin L, Yuan X, Hu P, Jann KB, Yan L, Maslov K, Shi J, Wang DJ, Liu CY, Wang LV (2022). Massively parallel functional photoacoustic computed tomography of the human brain. *Nature Biomedical Engineering*, *6*(5), 584–592. https://doi.org/10.1038/s41551-021-00735-8

Najafipour H, Siahposht Khachaki A, Khaksari M, Shahouzehi B, Joukar S, Poursalehi HR (2014). Traumatic brain injury has not prominent effects on cardiopulmonary indices of rat after 24 hours: Hemodynamic, histopathology, and biochemical evidence. *Iranian Biomedical Journal*, *18*(4), 225–231. https://doi.org/10.6091/ibj.13222.2014

Najem D, Rennie K, Ribecco-Lutkiewicz M, Ly D, Haukenfrers J, Liu Q, Nzau M, Fraser DD, Bani-Yaghoub M (2018). Traumatic brain injury: Classification, models, and markers. *Biochemistry and Cell Biology = Biochimie Et Biologie Cellulaire*, *96*(4), 391–406. https://doi.org/10.1139/bcb-2016-0160

Nakano T, Onoue K, Nakada Y, Nakagawa H, Kumazawa T, Ueda T, Nishida T, Soeda T, Okayama S, Watanabe M, Kawata H, Kawakami R, Horii M, Okura H, Uemura S, Hatakeyama K, Sakaguchi Y, Saito Y (2018). Alteration of β-Adrenoceptor Signaling in Left Ventricle of Acute Phase Takotsubo Syndrome: A Human Study. *Scientific Reports*, *8*(1), 12731. https://doi.org/10.1038/s41598-018-31034-z

Namjoshi DR, Cheng WH, McInnes KA, Martens KM, Carr M, Wilkinson A, Fan J, Robert J, Hayat A, Cripton PA, Wellington CL (2014). Merging pathology with biomechanics using CHIMERA (Closed-Head Impact Model of Engineered Rotational Acceleration): A novel, surgery-free model of traumatic brain injury. *Molecular Neurodegeneration*, *9*, 55. https://doi.org/10.1186/1750-1326-9-55

Nathaniel TI, Williams-Hernandez A, Hunter AL, Liddy C, Peffley DM, Umesiri FE, Imeh-Nathaniel A (2015). Tissue hypoxia during ischemic stroke: Adaptive clues from hypoxia-tolerant animal models. *Brain Research Bulletin*, *114*, 1–12. https://doi.org/10.1016/j.brainresbull.2015.02.006

Needles A [A.], Arditi M, Rognin NG, Mehi J, Coulthard T, Bilan-Tracey C, Gaud E, Frinking P, Hirson D [D.], Foster FS [F. S.] (2010). Nonlinear contrast imaging with an array-based micro-ultrasound system. *Ultrasound in Medicine & Biology*, *36*(12), 2097–2106. https://doi.org/10.1016/j.ultrasmedbio.2010.08.012

Needles A, Heinmiller A, Sun J, Theodoropoulos C, Bates D, Hirson D [Desmond], Yin M, Foster FS [F. Stuart] (2013). Development and initial application of a fully integrated photoacoustic micro-ultrasound system. *IEEE Transactions on Ultrasonics, Ferroelectrics, and Frequency Control*, *60*(5), 888–897. https://doi.org/10.1109/TUFFC.2013.2646

Nencka AS, Meier TB, Wang Y, Muftuler LT, Wu YC, Saykin AJ, Harezlak J, Brooks MA, Giza CC, Difiori J, Guskiewicz KM, Mihalik JP, LaConte SM, Duma SM, Broglio S, McAllister T, McCrea MA, Koch KM. Stability of MRI metrics in the advanced research core of the NCAA-DoD concussion assessment, research and education (CARE) consortium. Brain Imaging Behav. 2018 Aug;12(4):1121-1140. doi: 10.1007/s11682-017-9775-y. PMID: 29064019; PMCID: PMC6445663.

Ng SY, Lee AYW (2019). Traumatic Brain Injuries: Pathophysiology and Potential Therapeutic Targets. *Frontiers in Cellular Neuroscience*, *13*, 528. https://doi.org/10.3389/fncel.2019.00528

Nguembu S, Meloni M, Endalle G, Dokponou H, Dada OE, Senyuy WP, Kanmounye US (2021). Paroxysmal Sympathetic Hyperactivity in Moderate-to-Severe Traumatic Brain Injury and the Role of Beta-Blockers: A Scoping Review. *Emergency Medicine International*, *2021*, 5589239. https://doi.org/10.1155/2021/5589239

Nguyen H, Zaroff JG (2009). Neurogenic stunned myocardium. *Current Neurology and Neuroscience Reports*, *9*(6), 486–491. https://doi.org/10.1007/s11910-009-0071-0

Nikolakopoulou AM, Koeppen J, Garcia M, Leish J, Obenaus A [Andre], Ethell IM (2016). Astrocytic Ephrin-B1 Regulates Synapse Remodeling Following Traumatic Brain Injury. *ASN Neuro*, *8*(1), 1–18. https://doi.org/10.1177/1759091416630220

Nishimura RA, Tajik AJ [A. J.] (1997). Evaluation of diastolic filling of left ventricle in health and disease: Doppler echocardiography is the clinician's Rosetta Stone. *Journal of the American College of Cardiology*, *30*(1), 8–18. https://doi.org/10.1016/s0735-1097(97)00144-7

Norman HS, Oujiri J, Larue SJ, Chapman CB, Margulies KB, Sweitzer NK (2011). Decreased cardiac functional reserve in heart failure with preserved systolic function. *Journal of Cardiac Failure*, *17*(4), 301–308. https://doi.org/10.1016/j.cardfail.2010.11.004

Ommen SR, Nishimura RA, Appleton CP, Miller FA, Oh JK, Redfield MM [M. M.], Tajik AJ [A. J.] (2000). Clinical utility of Doppler echocardiography and tissue Doppler imaging in the estimation of left ventricular filling pressures: A comparative simultaneous Doppler-catheterization study. *Circulation*, *102*(15), 1788–1794. https://doi.org/10.1161/01.cir.102.15.1788

Onrat ST, Dural İE, Yalım Z, Onrat E (2021). Investigating changes in β-adrenergic gene expression (ADRB1 and ADRB2) in Takotsubo (stress) cardiomyopathy syndrome; a pilot study. *Molecular Biology Reports*, *48*(12), 7893–7900. https://doi.org/10.1007/s11033-021-06816-w

Oppenheimer SM (1994). Neurogenic cardiac effects of cerebrovascular disease. *Current Opinion in Neurology*, *7*(1), 20–24. https://doi.org/10.1097/00019052-199402000-00005

Oppenheimer SM, Cechetto DF (1990). Cardiac chronotropic organization of the rat insular cortex. *Brain Research*, *533*(1), 66–72. https://doi.org/10.1016/0006-8993(90)91796-J

Osier ND, Dixon CE (2016). The Controlled Cortical Impact Model: Applications, Considerations for Researchers, and Future Directions. *Frontiers in Neurology*, *7*, 134. https://doi.org/10.3389/fneur.2016.00134

Otani N, Nawashiro H, Nagatani K, Takeuchi S, Kobayashi H, Shima K (2011). Mitogen-Activated Protein Kinase Pathways Following Traumatic Brain Injury. *Neuroscience and Medicine*, *02*(03), 208–216. https://doi.org/10.4236/nm.2011.23028

Ouellet M-C, Beaulieu-Bonneau S, Morin CM (2015). Sleep-wake disturbances after traumatic brain injury. *The Lancet Neurology*, *14*(7), 746–757. https://doi.org/10.1016/S1474-4422(15)00068-X

Owens TS, Calverley TA, Stacey BS, Rose G, Fall L, Tsukamoto H, Jones G, Corkill R, Tuaillon E, Hirtz C, Lehmann S, Marchi N, Marley CJ, Bailey DM (2021). Concussion history in rugby union players is associated with depressed cerebrovascular reactivity and cognition. *Scandinavian Journal of Medicine & Science in Sports*, *31*(12), 2291–2299. https://doi.org/10.1111/sms.14046

Ozisik K, Yildirim E, Kaplan S, Solaroglu I, Sargon MF, Kilinc K (2004). Ultrastructural changes of rat cardiac myocytes in a time-dependent manner after traumatic brain injury. *American Journal of Transplantation : Official Journal of the American Society of Transplantation and the American Society of Transplant Surgeons*, *4*(6), 900–904. https://doi.org/10.1111/j.1600-6143.2004.00448.x

Park, M. K., Choi, B. Y., Kho, A. R., Lee, S. H., Hong, D. K., Jeong, J. H., Kang, D. H., Kang, B. S., & Suh, S. W. (2020). Effects of Transient Receptor Potential Cation 5 (TRPC5) Inhibitor,

NU6027, on Hippocampal Neuronal Death after Traumatic Brain Injury. International journal of molecular sciences, 21(21), 8256. https://doi.org/10.3390/ijms21218256

Palma J-A, Benarroch EE (2014). Neural control of the heart: Recent concepts and clinical correlations. *Neurology*, *83*(3), 261–271. https://doi.org/10.1212/WNL.0000000000000605

Paxinos G, Franklin KBJ. (2019). *Paxinos and Franklin's the mouse brain in stereotaxic coordinates* (Fifth edition). *Expert consult*. Academic Press, an imprint of Elsevier. https://doi.org/George

Pellerin D, Sharma R, Elliott P, Veyrat C (2003). Tissue Doppler, strain, and strain rate echocardiography for the assessment of left and right systolic ventricular function. *Heart (British Cardiac Society)*, *89 Suppl 3*, iii9-17. https://doi.org/10.1136/heart.89.suppl_3.iii9

Petersen, A., Soderstrom, M., Saha, B., & Sharma, P. (2021). Animal models of traumatic brain injury: a review of pathophysiology to biomarkers and treatments. Experimental brain research, 239(10), 2939–2950. https://doi.org/10.1007/s00221-021-06178-6

Pérez de Isla L, Balcones DV, Fernández-Golfín C, Marcos-Alberca P, Almería C, Rodrigo JL, Macaya C, Zamorano J (2009). Three-dimensional-wall motion tracking: A new and faster tool for myocardial strain assessment: Comparison with two-dimensional-wall motion tracking. *Journal of the American Society of Echocardiography : Official Publication of the American Society of Echocardiography*, *22*(4), 325–330. https://doi.org/10.1016/j.echo.2009.01.001

Perez Garcia, G., Perez, G. M., De Gasperi, R., Gama Sosa, M. A., Otero-Pagan, A., Pryor, D., Abutarboush, R., Kawoos, U., Hof, P. R., Cook, D. G., Gandy, S., Ahlers, S. T., & Elder, G. A. (2021). Progressive Cognitive and Post-Traumatic Stress Disorder-Related Behavioral Traits in Rats Exposed to Repetitive Low-Level Blast. Journal of neurotrauma, 38(14), 2030–2045. https://doi.org/10.1089/neu.2020.7398

Perlman RL (2016). Mouse models of human disease: An evolutionary perspective. *Evolution, Medicine, and Public Health*, *2016*(1), 170–176. https://doi.org/10.1093/emph/eow014

Pleasant JM, Carlson SW, Mao H [Haojie], Scheff SW, Yang KH, Saatman KE (2011). Rate of neurodegeneration in the mouse controlled cortical impact model is influenced by impactor tip shape: Implications for mechanistic and therapeutic studies. *Journal of Neurotrauma*, *28*(11), 2245–2262. https://doi.org/10.1089/neu.2010.1499

Prasad A, Lerman A, Rihal CS (2008). Apical ballooning syndrome (Tako-Tsubo or stress cardiomyopathy): A mimic of acute myocardial infarction. *American Heart Journal*, *155*(3), 408–417. https://doi.org/10.1016/j.ahj.2007.11.008

Prathep S, Sharma D, Hallman M, Joffe A, Krishnamoorthy V, Mackensen GB, Vavilala MS (2014). Preliminary report on cardiac dysfunction after isolated traumatic brain injury. *Critical Care Medicine*, *42*(1), 142–147. https://doi.org/10.1097/CCM.0b013e318298a890

Qian Y, Gao C, Zhao X, Song Y, Luo H, An S, Huang J, Zhang J [Jianning], Jiang R (2020). Fingolimod Attenuates Lung Injury and Cardiac Dysfunction after Traumatic Brain Injury. *Journal of Neurotrauma*, *37*(19), 2131–2140. https://doi.org/10.1089/neu.2019.6951

Qian R, Yang W, Wang X [Xiumei], Xu Z, Liu X, Sun B (2015). Evaluation of cerebral-cardiac syndrome using echocardiography in a canine model of acute traumatic brain injury. *American Journal of Cardiovascular Disease*, *5*(1), 72–76.

Qiu T, Lan Y, Gao W, Zhou M, Liu S, Huang W, Zeng S, Pathak JL, Yang B, Zhang J [Jian] (2021). Photoacoustic imaging as a highly efficient and precise imaging strategy for the evaluation of brain diseases. *Quantitative Imaging in Medicine and Surgery*, *11*(5), 2169–2186. https://doi.org/10.21037/qims-20-845

Raible DJ, Frey LC, Del Angel YC, Carlsen J, Hund D, Russek SJ, Smith B, Brooks-Kayal AR (2015). Jak/stat pathway regulation of GABAA receptor expression after differing severities of experimental TBI. *Experimental Neurology*, *271*, 445–456. https://doi.org/10.1016/j.expneurol.2015.07.001

Rakowski H, Appleton C, Chan K-L, Dumesni JG, Honos G, Jue J, Koilpillai C, Lepage S, Martin RP, Mercier L-A, O'Kelly B, Prieur T, Sanfilippo A, Sasson Z, Alvarez N, Pruitt R, Thompson C, Tomlinson C (1996). Canadian consensus recommendations for the measurement and reporting of diastolic dysfunction by echocardiography. *Journal of the American Society of Echocardiography*, *9*(5), 736–760. https://doi.org/10.1016/s0894-7317(96)90076-0

Ramtinfar S, Chabok SY, Chari AJ, Reihanian Z, Leili EK, Alizadeh A (2016). Early detection of nonneurologic organ failure in patients with severe traumatic brain injury: Multiple organ dysfunction score or sequential organ failure assessment? *Indian Journal of Critical Care Medicine : Peer-Reviewed, Official Publication of Indian Society of Critical Care Medicine*, *20*(10), 575–580. https://doi.org/10.4103/0972-5229.192042

Reis C, Wang Y, Akyol O, Ho WM, Ii RA, Stier G, Martin R, Zhang JH (2015). What's New in Traumatic Brain Injury: Update on Tracking, Monitoring and Treatment. *International Journal of Molecular Sciences*, *16*(6), 11903–11965. https://doi.org/10.3390/ijms160611903

Reisner SA, Lysyansky P, Agmon Y, Mutlak D, Lessick J, Friedman Z (2004). Global longitudinal strain: A novel index of left ventricular systolic function. *Journal of the American Society of Echocardiography*, *17*(6), 630–633. https://doi.org/10.1016/j.echo.2004.02.011

Rodriguez-Grande B, Obenaus A [Andre], Ichkova A, Aussudre J, Bessy T, Barse E, Hiba B, Catheline G, Barrière G, Badaut J (2018). Gliovascular changes precede white matter damage and long-term disorders in juvenile mild closed head injury. *Glia*, *66*(8), 1663–1677. https://doi.org/10.1002/glia.23336

Roffe C [C.], Corfield D (2008). Hypoxaemia and stroke. *Reviews in Clinical Gerontology*, *18*(4), 299–311. https://doi.org/10.1017/S095925980900286X

Rohde LE, Baldi A, Weber C, Geib G, Mazzotti NG, Fiorentini M, Roggia M, Pereira R, Clausell N (2007). Tei index in adult patients submitted to adriamycin chemotherapy: Failure to predict early systolic dysfunction. Diagnosis of adriamycin cardiotoxicity. *The International Journal of Cardiovascular Imaging*, *23*(2), 185–191. https://doi.org/10.1007/s10554-006-9145-0

Romine J, Gao X, Chen J [Jinhui] (2014). Controlled cortical impact model for traumatic brain injury. *Journal of Visualized Experiments : JoVE*(90), e51781. https://doi.org/10.3791/51781

Rossi A, Mikail N, Bengs S, Haider A, Treyer V, Buechel RR, Wegener S, Rauen K, Tawakol A, Bairey Merz CN, Regitz-Zagrosek V, Gebhard C (2022). Heart-brain interactions in cardiac and brain diseases: Why sex matters. *European Heart Journal.* Advance online publication. https://doi.org/10.1093/eurheartj/ehac061

Roth TL, Nayak D, Atanasijevic T, Koretsky AP, Latour LL, McGavern DB (2014). Transcranial amelioration of inflammation and cell death after brain injury. *Nature*, *505*(7482), 223–228. https://doi.org/10.1038/nature12808

Rusnak M (2013). Traumatic brain injury: Giving voice to a silent epidemic. *Nature Reviews. Neurology*, *9*(4), 186–187. https://doi.org/10.1038/nrneurol.2013.38

Sabet N, Soltani Z, Khaksari M (2021). Multipotential and systemic effects of traumatic brain injury. *Journal of Neuroimmunology*, *357*, 577619. https://doi.org/10.1016/j.jneuroim.2021.577619

Saeed M, Van TA, Krug R, Hetts SW, Wilson MW (2015). Cardiac MR imaging: Current status and future direction. *Cardiovascular Diagnosis and Therapy*, *5*(4), 290–310. https://doi.org/10.3978/j.issn.2223-3652.2015.06.07

Salami CO, Jackson K, Jose C, Alyass L, Cisse G-I, De BP, Stiles KM, Chiuchiolo MJ, Sondhi D, Crystal RG, Kaminsky SM (2020). Stress-Induced Mouse Model of the Cardiac Manifestations of Friedreich's Ataxia Corrected by AAV-mediated Gene Therapy. *Human Gene Therapy*, *31*(15-16), 819–827. https://doi.org/10.1089/hum.2019.363

Samuels MA (2007). The brain-heart connection. *Circulation*, *116*(1), 77–84. https://doi.org/10.1161/CIRCULATIONAHA.106.678995

Sanders VM, Kohm AP. (2002). Sympathetic nervous system interaction with the immune system. In *International Review of Neurobiology. Neurobiology of the Immune System* (Vol. 52, pp. 17–41). Elsevier. https://doi.org/10.1016/S0074-7742(02)52004-3

Sarah Thompson, Kaitlin Hays, Alan Weintraub, Jessica M Ketchum, Robert G Kowalski, Rhythmic Auditory Stimulation and Gait Training in Traumatic Brain Injury: A Pilot Study, Journal of Music Therapy, Volume 58, Issue 1, Spring 2021, Pages 70–94, https://doi.org/10.1093/jmt/thaa016

Scanzano A, Cosentino M (2015). Adrenergic regulation of innate immunity: A review. *Frontiers in Pharmacology*, *6*, 171. https://doi.org/10.3389/fphar.2015.00171

Scheer B, Perel A, Pfeiffer UJ (2002). Clinical review: Complications and risk factors of peripheral arterial catheters used for haemodynamic monitoring in anaesthesia and intensive care medicine. *Critical Care (London, England)*, *6*(3), 199–204. https://doi.org/10.1186/cc1489

Schmidt O, Infanger M, Heyde C, Ertel W, Stahel P (2004). The Role of Neuroinflammation in Traumatic Brain Injury. *European Journal of Trauma*, *30*(3). https://doi.org/10.1007/s00068-004-1394-9

Schmidt AG, Gerst M, Zhai J, Carr AN, Pater L, Kranias EG, Hoit BD (2002). Evaluation of left ventricular diastolic function from spectral and color M-mode Doppler in genetically altered mice. *Journal of the American Society of Echocardiography*, *15*(10 Pt 1), 1065–1073. https://doi.org/10.1067/mje.2002.121863

Schneider B, Athanasiadis A, Schwab J, Pistner W, Gottwald U, Schoeller R, Toepel W, Winter K-D, Stellbrink C, Müller-Honold T, Wegner C, Sechtem U (2014). Complications in the clinical course of tako-tsubo cardiomyopathy. *International Journal of Cardiology*, *176*(1), 199–205. https://doi.org/10.1016/j.ijcard.2014.07.002

Schnelle M, Catibog N, Zhang M, Nabeebaccus AA, Anderson G, Richards DA, Sawyer G, Zhang X, Toischer K, Hasenfuss G, Monaghan MJ, Shah AM (2018). Echocardiographic evaluation of diastolic function in mouse models of heart disease. *Journal of Molecular and Cellular Cardiology*, *114*, 20–28. https://doi.org/10.1016/j.yjmcc.2017.10.006

Schumacher A, Khojeini E, Larson D (2008). Echo parameters of diastolic dysfunction. *Perfusion*, *23*(5), 291–296. https://doi.org/10.1177/0267659109102485

Semple BD, Trivedi A, Gimlin K, Noble-Haeusslein LJ (2015). Neutrophil elastase mediates acute pathogenesis and is a determinant of long-term behavioral recovery after traumatic injury to the immature brain. *Neurobiology of Disease*, *74*, 263–280. https://doi.org/10.1016/j.nbd.2014.12.003

Sengupta P (2013). The Laboratory Rat: Relating Its Age With Human's. *International Journal of Preventive Medicine*, *4*(6), 624–630.

Serri K, El Rayes M, Giraldeau G, Williamson D, Bernard F (2016). Traumatic brain injury is not associated with significant myocardial dysfunction: An observational pilot study. *Scandinavian Journal of Trauma, Resuscitation and Emergency Medicine*, *24*, 31. https://doi.org/10.1186/s13049-016-0217-4

Sharp DJ, Jenkins PO (2015). Concussion is confusing us all. *Practical Neurology*, *15*(3), 172–186. https://doi.org/10.1136/practneurol-2015-001087

Sicard P, Clark JE, Jacquet S, Mohammadi S, Arthur JSC, O'Keefe SJ, Marber MS (2010). The activation of p38 alpha, and not p38 beta, mitogen-activated protein kinase is required for ischemic preconditioning. *Journal of Molecular and Cellular Cardiology*, *48*(6), 1324–1328. https://doi.org/10.1016/j.yjmcc.2010.02.013

Siebold L, Obenaus A [Andre], Goyal R (2018). Criteria to define mild, moderate, and severe traumatic brain injury in the mouse controlled cortical impact model. *Experimental Neurology*, *310*, 48–57. https://doi.org/10.1016/j.expneurol.2018.07.004

Siedler DG, Chuah MI, Kirkcaldie MTK, Vickers JC, King AE (2014). Diffuse axonal injury in brain trauma: Insights from alterations in neurofilaments. *Frontiers in Cellular Neuroscience*, *8*, 429. https://doi.org/10.3389/fncel.2014.00429

Simon DW, McGeachy MJ, Bayır H, Clark RSB, Loane DJ, Kochanek PM (2017). The far-reaching scope of neuroinflammation after traumatic brain injury. *Nature Reviews. Neurology*, *13*(3), 171–191. https://doi.org/10.1038/nrneurol.2017.13

Singh IN, Sullivan PG, Deng Y, Mbye LH, Hall ED (2006). Time course of post-traumatic mitochondrial oxidative damage and dysfunction in a mouse model of focal traumatic brain injury: Implications for neuroprotective therapy. *Journal of Cerebral Blood Flow and Metabolism : Official Journal of the International Society of Cerebral Blood Flow and Metabolism*, *26*(11), 1407–1418. https://doi.org/10.1038/sj.jcbfm.9600297

Skandsen T, Kvistad KA, Solheim O, Strand IH, Folvik M, Vik A (2010). Prevalence and impact of diffuse axonal injury in patients with moderate and severe head injury: A cohort study of early magnetic resonance imaging findings and 1-year outcome. *Journal of Neurosurgery*, *113*(3), 556–563. https://doi.org/10.3171/2009.9.JNS09626

Smith DH, Kochanek PM, Rosi S, Meyer R, Ferland-Beckham C, Prager EM, Ahlers ST, Crawford F (2021). Roadmap for Advancing Pre-Clinical Science in Traumatic Brain Injury. *Journal of Neurotrauma*, *38*(23), 3204–3221. https://doi.org/10.1089/neu.2021.0094

Smith DH, Meaney DF (2000). Axonal Damage in Traumatic Brain Injury. *The Neuroscientist*, *6*(6), 483–495. https://doi.org/10.1177/107385840000600611

Soepriatna AH, Damen FW, Vlachos PP, Goergen CJ (2018). Cardiac and respiratory-gated volumetric murine ultrasound. *The International Journal of Cardiovascular Imaging*, *34*(5), 713–724. https://doi.org/10.1007/s10554-017-1283-z

Song G, Zhang B, Song L, Li W [Wenzhe], Liu C [Chuxuan], Chen L [Leshan], Liu A (2022). Mnco3@bsa-ICG nanoparticles as a magnetic resonance/photoacoustic dual-modal contrast agent for functional imaging of acute ischemic stroke. *Biochemical and Biophysical Research Communications*, *614*, 125–131. https://doi.org/10.1016/j.bbrc.2022.04.143

Sposato LA, Hilz MJ, Aspberg S, Murthy SB, Bahit MC, Hsieh C-Y, Sheppard MN, Scheitz JF (2020). Post-Stroke Cardiovascular Complications and Neurogenic Cardiac Injury: Jacc State-of-the-Art Review. *Journal of the American College of Cardiology*, *76*(23), 2768–2785. https://doi.org/10.1016/j.jacc.2020.10.009

Ssali T, Anazodo UC, Thiessen JD, Prato FS, St Lawrence K (2018). A Noninvasive Method for Quantifying Cerebral Blood Flow by Hybrid PET/MRI. *Journal of Nuclear Medicine : Official Publication, Society of Nuclear Medicine*, *59*(8), 1329–1334. https://doi.org/10.2967/jnumed.117.203414

Stanley RM, Hoyle JD, Dayan PS, Atabaki S, Lee L, Lillis K, Gorelick MH, Holubkov R, Miskin M, Holmes JF, Dean JM, Kuppermann N (2014). Emergency department practice variation in computed tomography use for children with minor blunt head trauma. *The Journal of Pediatrics*, *165*(6), 1201-1206.e2. https://doi.org/10.1016/j.jpeds.2014.08.008

Starosolski Z, Villamizar CA, Rendon D, Paldino MJ, Milewicz DM, Ghaghada KB, Annapragada AV (2015). Ultra High-Resolution In vivo Computed Tomography Imaging of

Mouse Cerebrovasculature Using a Long Circulating Blood Pool Contrast Agent. *Scientific Reports*, *5*, 10178. https://doi.org/10.1038/srep10178

Stoffey RD, Mizrachi JS (2012). MRI in Practice, 4th ed. *American Journal of Roentgenology*, *198*(5), W501-W501. https://doi.org/10.2214/AJR.11.8252

Stuckey DJ, Carr CA, Camelliti P, Tyler DJ, Davies KE, Clarke K (2012). In vivo MRI characterization of progressive cardiac dysfunction in the mdx mouse model of muscular dystrophy. *PloS One*, *7*(1), e28569. https://doi.org/10.1371/journal.pone.0028569

Sturgill MG, Kelly M, Notterman DA. (2011). Pharmacology of the Cardiovascular System. In *Pediatric Critical Care* (pp. 277–305). Elsevier. https://doi.org/10.1016/B978-0-323-07307-3.10025-4

Steyerberg, E. W., Wiegers, E., Sewalt, C., Buki, A., Citerio, G., De Keyser, V., Ercole, A., Kunzmann, K., Lanyon, L., Lecky, F., Lingsma, H., Manley, G., Nelson, D., Peul, W., Stocchetti, N., von Steinbüchel, N., Vande Vyvere, T., Verheyden, J., Wilson, L., Maas, A. I. R., … CENTER-TBI Participants and Investigators (2019). Case-mix, care pathways, and outcomes in patients with traumatic brain injury in CENTER-TBI: a European prospective, multicentre, longitudinal, cohort study. The Lancet. Neurology, 18(10), 923–934. https://doi.org/10.1016/S1474-4422(19)30232-7

Sun Y-Y, Li Y [Yikun], Wali B, Li Y [Yuancheng], Lee J [Jolly], Heinmiller A, Abe K, Stein DG, Mao H [Hui], Sayeed I, Kuan C-Y (2015). Prophylactic Edaravone Prevents Transient Hypoxic-Ischemic Brain Injury: Implications for Perioperative Neuroprotection. *Stroke*, *46*(7), 1947–1955. https://doi.org/10.1161/STROKEAHA.115.009162

Sword J, Masuda T [Tadashi], Croom D, Kirov SA (2013). Evolution of neuronal and astroglial disruption in the peri-contusional cortex of mice revealed by in vivo two-photon imaging. *Brain : A Journal of Neurology*, *136*(Pt 5), 1446–1461. https://doi.org/10.1093/brain/awt026

Tanter M, Fink M (2014). Ultrafast imaging in biomedical ultrasound. *IEEE Transactions on Ultrasonics, Ferroelectrics, and Frequency Control*, *61*(1), 102–119. https://doi.org/10.1109/TUFFC.2014.2882

Tarkin JM, Ćorović A, Wall C, Gopalan D, Rudd JH (2020). Positron emission tomography imaging in cardiovascular disease. *Heart (British Cardiac Society)*, *106*(22), 1712–1718. https://doi.org/10.1136/heartjnl-2019-315183

Tassan-Mangina S, Codorean D, Metivier M, Costa B, Himberlin C, Jouannaud C, Blaise AM, Elaerts J, Nazeyrollas P (2006). Tissue Doppler imaging and conventional echocardiography after anthracycline treatment in adults: Early and late alterations of left ventricular function during a prospective study. *European Journal of Echocardiography : The Journal of the Working Group on Echocardiography of the European Society of Cardiology*, *7*(2), 141–146. https://doi.org/10.1016/j.euje.2005.04.009

Tatara Y, Shimada R, Kibayashi K (2021). Effects of Preexisting Diabetes Mellitus on the Severity of Traumatic Brain Injury. *Journal of Neurotrauma*, *38*(7), 886–902. https://doi.org/10.1089/neu.2020.7118

Taylor CA, Bell JM, Breiding MJ, Xu L [Likang] (2017). Traumatic Brain Injury-Related Emergency Department Visits, Hospitalizations, and Deaths - United States, 2007 and 2013. *Morbidity and Mortality Weekly Report. Surveillance Summaries (Washington, D.C. : 2002)*, *66*(9), 1–16. https://doi.org/10.15585/mmwr.ss6609a1

Thomas JD, Popović ZB (2006). Assessment of left ventricular function by cardiac ultrasound. *Journal of the American College of Cardiology*, *48*(10), 2012–2025. https://doi.org/10.1016/j.jacc.2006.06.071

Thomsen GM, Ko A, Harada MY, Ma A, Wyss L, Haro P, Vit J-P, Avalos P, Dhillon NK, Cho N, Shelest O, Ley EJ (2017). Clinical correlates to assist with chronic traumatic encephalopathy diagnosis: Insights from a novel rodent repeat concussion model. *The Journal of Trauma and Acute Care Surgery*, *82*(6), 1039–1048. https://doi.org/10.1097/TA.0000000000001443

Thompson, W. H., Thelin, E. P., Lilja, A., Bellander, B. M., & Fransson, P. (2016). Functional resting-state fMRI connectivity correlates with serum levels of the S100B protein in the acute phase of traumatic brain injury. NeuroImage. Clinical, 12, 1004–1012. https://doi.org/10.1016/j.nicl.2016.05.005

Tobin RP, Mukherjee S, Kain JM, Rogers SK, Henderson SK, Motal HL, Newell Rogers MK, Shapiro LA (2014). Traumatic brain injury causes selective, CD74-dependent peripheral lymphocyte activation that exacerbates neurodegeneration. *Acta Neuropathologica Communications*, *2*, 143. https://doi.org/10.1186/s40478-014-0143-5

Toffaletti J, Zijlstra WG (2007). Misconceptions in reporting oxygen saturation. *Anesthesia and Analgesia*, *105*(6 Suppl), S5-S9. https://doi.org/10.1213/01.ane.0000278741.29274.e1

Tseng W-C, Shih H-M, Su Y-C, Chen H-W, Hsiao K-Y, Chen I-C (2011). The association between skull bone fractures and outcomes in patients with severe traumatic brain injury. *The Journal of Trauma*, *71*(6), 1611-4; discussion 1614. https://doi.org/10.1097/TA.0b013e31823a8a60

Tsujita Y, Kato T, Sussman MA (2005). Evaluation of left ventricular function in cardiomyopathic mice by tissue Doppler and color M-mode Doppler echocardiography. *Echocardiography (Mount Kisco, N.Y.)*, *22*(3), 245–253. https://doi.org/10.1111/j.0742-2822.2005.04014.x

Valable S, Corroyer-Dulmont A, Chakhoyan A, Durand L, Toutain J, Divoux D, Barré L, MacKenzie ET, Petit E, Bernaudin M, Touzani O, Barbier EL (2017). Imaging of brain oxygenation with magnetic resonance imaging: A validation with positron emission tomography in the healthy and tumoural brain. *Journal of Cerebral Blood Flow and Metabolism : Official Journal of the International Society of Cerebral Blood Flow and Metabolism*, *37*(7), 2584–2597. https://doi.org/10.1177/0271678X16671965

van Empel VPM, Mariani J, Borlaug BA, Kaye DM (2014). Impaired myocardial oxygen availability contributes to abnormal exercise hemodynamics in heart failure with preserved ejection fraction. *Journal of the American Heart Association*, *3*(6), e001293. https://doi.org/10.1161/JAHA.114.001293

van Landeghem FKH, Weiss T, Oehmichen M, Deimling A von (2006). Decreased expression of glutamate transporters in astrocytes after human traumatic brain injury. *Journal of Neurotrauma*, *23*(10), 1518–1528. https://doi.org/10.1089/neu.2006.23.1518

van Raaij ME, Lindvere L, Dorr A, He J, Sahota B, Foster FS [F. Stuart], Stefanovic B (2011). Functional micro-ultrasound imaging of rodent cerebral hemodynamics. *NeuroImage*, *58*(1), 100–108. https://doi.org/10.1016/j.neuroimage.2011.05.088

van Tassell BW, Toldo S, Mezzaroma E, Abbate A (2013). Targeting interleukin-1 in heart disease. *Circulation*, *128*(17), 1910–1923. https://doi.org/10.1161/CIRCULATIONAHA.113.003199

van Vliet EA, Marchi N (2022). Neurovascular unit dysfunction as a mechanism of seizures and epilepsy during aging. *Epilepsia*, *63*(6), 1297–1313. https://doi.org/10.1111/epi.17210

Venkata C, Kasal J (2018). Cardiac Dysfunction in Adult Patients with Traumatic Brain Injury: A Prospective Cohort Study. *Clinical Medicine & Research*, *16*(3-4), 57–65. https://doi.org/10.3121/cmr.2018.1437

Voigt J-U, Pedrizzetti G, Lysyansky P, Marwick TH, Houle H, Baumann R, Pedri S, Ito Y, Abe Y, Metz S, Song JH, Hamilton J, Sengupta PP, Kolias TJ, d'Hooge J, Aurigemma GP, Thomas JD, Badano LP [Luigi Paolo] (2015). Definitions for a common standard for 2D speckle tracking echocardiography: Consensus document of the EACVI/ASE/Industry Task Force to standardize deformation imaging. *Journal of the American Society of Echocardiography : Official Publication of the American Society of Echocardiography*, *28*(2), 183–193. https://doi.org/10.1016/j.echo.2014.11.003

Walko TD, Bola RA, Hong JD, Au AK, Bell MJ, Kochanek PM, Clark RSB, Aneja RK (2014). Cerebrospinal fluid mitochondrial DNA: A novel DAMP in pediatric traumatic brain injury. *Shock (Augusta, Ga.)*, *41*(6), 499–503. https://doi.org/10.1097/SHK.0000000000000160

Wang LV, Hu S (2012). Photoacoustic tomography: In vivo imaging from organelles to organs. *Science (New York, N.Y.)*, *335*(6075), 1458–1462. https://doi.org/10.1126/science.1216210

Wang, K. K., Yang, Z., Zhu, T., Shi, Y., Rubenstein, R., Tyndall, J. A., & Manley, G. T. (2018). An update on diagnostic and prognostic biomarkers for traumatic brain injury. Expert Review of Molecular Diagnostics, 18(2), 165–180. https://doi.org/10.1080/14737159.2018.1428089

Weber JT (2012). Altered calcium signaling following traumatic brain injury. *Frontiers in Pharmacology*, *3*, 60. https://doi.org/10.3389/fphar.2012.00060

Weber J, Beard PC, Bohndiek SE (2016). Contrast agents for molecular photoacoustic imaging. *Nature Methods*, *13*(8), 639–650. https://doi.org/10.1038/nmeth.3929

Werner C, Engelhard K (2007). Pathophysiology of traumatic brain injury. *British Journal of Anaesthesia*, *99*(1), 4–9. https://doi.org/10.1093/bja/aem131

White M, Wiechmann RJ, Roden RL, Hagan MB, Wollmering MM, Port JD, Hammond E, Abraham WT, Wolfel EE, Lindenfeld J (1995). Cardiac beta-adrenergic neuroeffector systems

in acute myocardial dysfunction related to brain injury. Evidence for catecholamine-mediated myocardial damage. *Circulation*, *92*(8), 2183–2189. https://doi.org/10.1161/01.cir.92.8.2183

Wiegand TLT, Sollmann N, Bonke EM, Umeasalugo KE, Sobolewski KR, Plesnila N, Shenton ME, Lin AP, Koerte IK (2021). Translational neuroimaging in mild traumatic brain injury. *Journal of Neuroscience Research.* Advance online publication. https://doi.org/10.1002/jnr.24840

Williams AJ (1998). Abc of oxygen: Assessing and interpreting arterial blood gases and acid-base balance. *BMJ (Clinical Research Ed.)*, *317*(7167), 1213–1216. https://doi.org/10.1136/bmj.317.7167.1213

Williams, H. C., Carlson, S. W., & Saatman, K. E. (2022). A role for insulin-like growth factor-1 in hippocampal plasticity following traumatic brain injury. Vitamins and hormones, 118, 423–455. https://doi.org/10.1016/bs.vh.2021.11.009

Wilde, E. A., McCauley, S. R., Barnes, A., Wu, T. C., Chu, Z., Hunter, J. V., & Bigler, E. D. (2012). Serial measurement of memory and diffusion tensor imaging changes within the first week following uncomplicated mild traumatic brain injury. Brain imaging and behavior, 6(2), 319–328. https://doi.org/10.1007/s11682-012-9174-3

Won SJ, Kim J-E, Cittolin-Santos GF, Swanson RA (2015). Assessment at the single-cell level identifies neuronal glutathione depletion as both a cause and effect of ischemia-reperfusion oxidative stress. *The Journal of Neuroscience : The Official Journal of the Society for Neuroscience*, *35*(18), 7143–7152. https://doi.org/10.1523/JNEUROSCI.4826-14.2015

Wong ND, Gardin JM, Kurosaki T, Anton-Culver H, Sidney S, Roseman J, Gidding S (1995). Echocardiographic left ventricular systolic function and volumes in young adults: Distribution and factors influencing variability. *American Heart Journal*, *129*(3), 571–577. https://doi.org/10.1016/0002-8703(95)90287-2

Xiong Y, Mahmood A, Chopp M (2013). Animal models of traumatic brain injury. *Nature Reviews. Neuroscience*, *14*(2), 128–142. https://doi.org/10.1038/nrn3407

Yang Z, Lin F, Weissman AS, Jaalouk E, Xue Q-S, Wang KKW (2016). A Repetitive Concussive Head Injury Model in Mice. *Journal of Visualized Experiments : JoVE.* Advance online publication. https://doi.org/10.3791/54530

Yao J, Zhu X, Huang Q, DiSpirito A, Vu T, Rong Q, Peng X, Sheng H, Shen X, Zhou Q, Jiang L, Hoffmann U (2022). Real-time whole-brain imaging of hemodynamics and oxygenation at micro-vessel resolution with ultrafast wide-field photoacoustic microscopy. Advance online publication. https://doi.org/10.21203/rs.3.rs-1230249/v1

Yuan L-J, Wang T, Kahn ML, Ferrari VA (2011). High-resolution echocardiographic assessment of infarct size and cardiac function in mice with myocardial infarction. *Journal of the American Society of Echocardiography : Official Publication of the American Society of Echocardiography*, *24*(2), 219–226. https://doi.org/10.1016/j.echo.2010.11.001

Zackrisson S, van de Ven SMWY, Gambhir SS (2014). Light in and sound out: Emerging translational strategies for photoacoustic imaging. *Cancer Research*, *74*(4), 979–1004. https://doi.org/10.1158/0008-5472.CAN-13-2387

Zamani A, O'Brien TJ, Kershaw J, Johnston LA, Semple BD, Wright DK (2021). White matter changes following experimental pediatric traumatic brain injury: An advanced diffusion-weighted imaging investigation. *Brain Imaging and Behavior.* Advance online publication. https://doi.org/10.1007/s11682-020-00433-0

Zhang Y, Zhang H, Li J, Zhao J, Chen H, Xu J, Shang X, Yu R (2021). Outcomes and Relevant Factors Associated with Cardiac Dysfunction in Patients with Traumatic Brain Injury. *OALib*, *08*(01), 1–13. https://doi.org/10.4236/oalib.1107071

Zhang YP, Cai J, Shields LBE, Liu N [Naikui], Xu X-M, Shields CB (2014). Traumatic brain injury using mouse models. *Translational Stroke Research*, *5*(4), 454–471. https://doi.org/10.1007/s12975-014-0327-0

Zhao S, Gao X, Dong W, Chen J [Jinhui] (2016). The Role of 7,8-Dihydroxyflavone in Preventing Dendrite Degeneration in Cortex After Moderate Traumatic Brain Injury. *Molecular Neurobiology*, *53*(3), 1884–1895. https://doi.org/10.1007/s12035-015-9128-z

Zhao Q, Yan T, Li L, Chopp M, Venkat P, Qian Y, Li R, Wu R, Li W [Wei], Lu M, Zhang T, Chen J [Jieli] (2019). Immune Response Mediates Cardiac Dysfunction after Traumatic Brain Injury. *Journal of Neurotrauma*, *36*(4), 619–629. https://doi.org/10.1089/neu.2018.5766

Zhao T, Desjardins AE, Ourselin S, Vercauteren T, Xia W (2019). Minimally invasive photoacoustic imaging: Current status and future perspectives. *Photoacoustics*, *16*, 100146. https://doi.org/10.1016/j.pacs.2019.100146

Zuo Z, Subgang A, Abaei A, Rottbauer W, Stiller D, Ma G, Rasche V (2017). Assessment of Longitudinal Reproducibility of Mice LV Function Parameters at 11.7 T Derived from Self-Gated CINE MRI. *BioMed Research International*, *2017*, 8392952. https://doi.org/10.1155/2017/8392952

Annexes

Annexes

A. Annexe I

This result, I contributed in all parts to establish the research work including initiated, planned, and led the study; performed the mTBI model in mice and US/PA imaging in the heart and brain; analyzed 2D and PA images in publication:

Leyba, K., Paiyabhroma, N., Salvas, J. P., Damen, F. W., Janvier, A., Zub, E., Bernis, C., Rouland, R., Dubois, C. J., Badaut, J., Richard, S., Marchi, N., Goergen, C. J., & Sicard, P. (2023). Neurovascular hypoxia after mild traumatic brain injury in juvenile mice correlates with heart-brain dysfunctions in adulthood. Acta physiologica (Oxford, England), 238(2), e13933. https://doi.org/10.1111/apha.13933

B. Annexe II

This result, I contributed PAI and US imaging to detect the multi-organs oxygen saturation and cardiac function assessment in MI murine model. Additionally, I contributed histology in pericytes immunofluorescence and quantification in publication:

David, H., Ughetto, A., Gaudard, P., Plawecki, M., Paiyabhroma, N., Zub, E., Colson, P., Richard, S., Marchi, N., & Sicard, P. (2021). Experimental Myocardial Infarction Elicits Time-Dependent Patterns of Vascular Hypoxia in Peripheral Organs and in the Brain. Frontiers in cardiovascular medicine, 7, 615507. https://doi.org/10.3389/fcvm.2020.615507

C. Annexe III

This result, I contributed US imaging to cardiac function assessment in doxorubicin toxicity effect in publication:

Lages, E. B., Fernandes, R. S., Andrade, M. M. S., Paiyabhroma, N., de Oliveira, R. B., Fernandes, C., Cassali, G. D., Sicard, P., Richard, S., Branco de Barros, A. L., & Ferreira, L. A. M. (2021). pH-sensitive doxorubicin-tocopherol succinate prodrug encapsulated in docosahexaenoic acid-based nanostructured lipid carriers: An effective strategy to improve pharmacokinetics and reduce toxic effects. Biomedicine & pharmacotherapy = Biomedecine & pharmacotherapie, 144, 112373. https://doi.org/10.1016/j.biopha.2021.112373

Résumé

Les traumatismes craniens légers (TCL) sont associés à un risque de développement de troubles neurologiques, mais aussi cardiovasculaires. L'évaluation diagnostique actuelle du TCL en imagerie (CT-scan, IRM) n'est pas systématique. Elle est réalisée uniquement après un examen neurologique perturbé et ne recherche que les conséquences anatomiques du TCL. La combinaison des rayonnements non invasifs et non ionisants de l'imagerie photoacoustique (PAI) et l'échographie haute résolution (US) permet d'obtenir des données anatomiques, moléculaires et fonctionnelles du cerveau et des organes périphériques. **L'objectif de notre travail a été de s'appuyer sur cette modalité d'imagerie pour évaluer les interactions cerveau-cœur dans un modèle préclinique de TCL juvénile sur le long terme.** Le TCL a été induit par un seul impact non invasif au 17ème jour après la naissance. Nous avons utilisé la PAI pour caractériser une hypoxie cérébrale transitoire 4h après le TCL. Le suivi pendant 6 mois, par échographie 2D et 4D, a permis de documenter le dévelopement d'une insuffisance cardiaque diastolique à fraction d'éjection préservée. Une épreuve d'effort à la dobutamine a révélé un dysfonctionnement cardiaque systolique associé à une diminution de la consommation d'oxygène du myocarde. Une corrélation entre l'hypoxie cérébrale aigue (pédiatrique) et différents index de dysfonction cardiaque chronique (au stade adulte) a été documentée. De plus, le niveau d'hypoxie 4h après le TCL est corrélé avec les changements de comportement de l'animal, notamment au niveau de l'apprentissage et des défauts de performance motrice à long terme. En conclusion, les techniques d'imagerie PAI en 2D et 4D ont révélé les conséquences délétères à long-terme au niveau comportemental et au niveau de la fonction cardiaque après TCL au stade pédiatrique. Notre étude permet d'envisager une amelioration de l'évaluation précoce du TCCm, avec un rayonnement non invasif et non ionisant, et une approche rapide.

Abstract

Mild traumatic brain injury (mTBI) is a silent epidemic worldwide that causes suffering from the long-term effects on behavior changes and the peripheral organs system, especially in the pediatric population. The current diagnostic assessment for mTBI has not covered those traces of the disease that do not appear when using CT-scan and MRI imaging techniques. Moreover, shades of evidence showed that TBI is associated with cardiac dysfunction, but the pathophysiology is still unclear. The combination of photoacoustic imaging (PAI) and high-resolution ultrasound (US) makes it possible to assess the oxygen saturation (sO2) of organs and to measure cardiac function accurately. **The objective of our work was to longitudinal assess and monitor brain-to-heart interactions with PAI and US imaging for measuring sO2 and cardiac function in a juvenile mTBI model.** The mTBI was induced by a single impact of closed-head injury. We introduced PAI to assess transient brain hypoxia. The two-and four-dimensional ultrasound (2DUS and 4DUS) detected progressively cardiac diastolic dysfunction with preserved ejection fraction. During dobutamine stress test the animals exhibited cardiac systolic dysfunction and impaired oxygen consumption of the myocardium. The correlations between brain hypoxia and cardiac dysfunction enlightened brain-heart interactions after mTBI. Moreover, animal status post-mTBI correlated with behavior changes in learning and motor performance defects in the long term. In conclusion, PAI, 2D, and 4D imaging techniques revealed that mTBI in the juvenile model leads to transient brain hypoxia, eliciting cardiac dysfunction and behavior alterations in the long term. This study gives a new promise to improve early assessment for mTBI with non-invasive, non-ionizing radiation and a rapid approach.

Keywords: Mild traumatic brain injury, pediatric, juvenile, hypoxia, cardiac dysfunction, photoacoustic imaging, and ultrasound.